The role of osteopontin in macrophage-mediated inflammation

Susan Amanda Lund

A dissertation
submitted in partial fulfillment of the
requirements for the degree of

Doctor of Philosophy

University of Washington

2012

Marta Scatena, Chair
Cecilia M. Giachelli
James D. Bryers

Program Authorized to Offer Degree:
Department of Bioengineering

University of Washington

Abstract

The role of osteopontin in macrophage-mediated inflammation

Susan Amanda Lund

Co-chairs of the Supervisory Committee:
Professor Cecilia M. Giachelli
Research Associate Professor Marta Scatena
Department of Bioengineering

Osteopontin (OPN) is highly expressed by macrophages and plays a key role in the pathology of several chronic inflammatory diseases. Macrophages are central players in chronic inflammation and OPN orchestrates macrophage function at multiple levels by mediating adhesion, migration, and survival. However, the molecular mechanisms by which OPN regulates macrophage biology are not well understood. Insights into these mechanisms could allow for the creation of therapeutics designed to selectively target OPN function in inflammatory diseases.

We explored the role of osteopontin in macrophage-mediated inflammation and defined the OPN functional domains and cell surface receptors mediating this process. OPN interacts with integrins via two main functional domains: the RGD motif that binds to α_V-containing integrins and the SLAYGLR sequence that binds to integrins $\alpha_4\beta_1$ and $\alpha_9\beta_1$. In chemotaxis studies, we

found that migration to OPN was mediated via integrins α_4 and α_9 *in vitro*. We also evaluated the relative contributions of the RGD and SLAYGLR domains of OPN to leukocyte accumulation in an *in vivo* model of acute inflammation. For these studies we created chimeric mice expressing mutated forms of OPN in macrophages. We found that the SLAYGLR domain of OPN mediates macrophage accumulation in response to thioglycollate-elicited peritonitis. Together, these data suggest that the SLAYGLR domain of OPN interacts with integrins α_4 and α_9 to regulate macrophage migration and accumulation.

We also determined the effect of OPN on macrophage activation state. Contrary to previous reports, we show that OPN does not affect macrophage activation in terms of pro-inflammatory cytokine expression or cell surface receptor expression. We also found that primary macrophages from wild type and OPN-null mice did not differ in their ability to be polarized to either the M1 or M2 macrophage activation state. Finally, OPN could not induce NF-κB signaling in macrophages, further evidence that OPN does not regulate macrophage activation. Overall, these studies indicate that while OPN does not affect macrophage activation, it does promote macrophage migration and accumulation. Consequently, specifically targeting the interactions between the SLAYGLR domain of OPN and integrins α_4 and α_9 could be used therapeutically to reduce macrophage-mediated inflammation.

Table of Contents

List of Figures

List of Tables

List of Abbreviations

AngII	angiotensin II
ApoE	apolipoprotein E
Arg	arginase
BAEC	bovine aortic endothelial cell
BMDM	bone marrow derived macrophage
BMT	bone marrow transplant
BSA	bovine serum albumin
CDI	1,1'-carbonyldiiamidazole
DC	dendritic cell
EC	endothelial cell
ECM	extracellular matrix
EDTA	ethylenediaminetetraacetic acid
ELISA	enzyme-linked immunosorbent assay
FBGC	foreign body giant cell
FBS	fetal bovine serum
GFAV	gluteraldehyde fixed aortic valve
H&E	hematoxylin and eosin
HPF	high powered field
HRP	horseradish peroxidase
IL-1RII	IL-1 type II decoy receptor
iNOS	inducible nitric oxide synthase

LDL	low density lipoprotein
LDLR	low density lipoprotein receptor
LPS	lipopolysaccharide
M-CSF	macrophage-colony stimulating factor (CSF-1)
MGP	matrix gla protein
MMP	matrix metalloproteinase
MR	mannose receptor
OPN	osteopontin
PBMC	peripheral blood mononuclear cell
PBS	phosphate buffered saline
PE	phycoerythrin
pHEMA	poly(2-hydroxyethyl methacrylate)
PTM	post-translational modification
PVA	polyvinyl alcohol
rhOPN	recombinant human OPN
rmOPN	recombinant murine OPN
RNI	reactive nitrogen intermediates
ROI	reactive oxygen intermediates
SD	standard deviation
SEM	standard error of the mean
SMC	smooth muscle cell
SR	scavenger receptor
VCAM-1	vascular cell adhesion protein 1

VLDL	very low density lipoprotein
WT	wild type

Chapter 1

Background

1.1 Significance

OPN is a multifunctional molecule that plays an important role in both normal physiological processes and in pathological disease states. One of the main physiological roles of OPN is the regulation of biomineralization (1). OPN is a potent inhibitor of mineralization, prevents ectopic calcification, and is an inducible inhibitor of vascular calcification (2, 3). Due to its ability to inhibit calcification, OPN is being considered as a potential therapeutic for the treatment of pathological mineralization in cardiovascular settings. However, growing evidence suggests that OPN is required for macrophage function in chronic inflammation. Clinically, OPN plasma levels are correlated with chronic inflammatory diseases such as Crohn's disease (4), cancer (5), and autoimmune disorders including lupus (6), multiple sclerosis (7), and rheumatoid arthritis (8). Thus, although OPN's anti-calcific properties make it attractive as a potential therapeutic, its role in inflammation may limit its clinical usefulness. Understanding the structure/function relationship governing the properties of OPN could lead to the creation of therapies designed to specifically target OPN's anti-calcific and pro-inflammatory functions separately.

1.2 Osteopontin (OPN) biology

OPN is a phosphorylated glycoprotein that mediates diverse biological functions. As a matricellular protein, OPN exists both as a soluble cytokine and as an extracellular matrix

component. OPN was originally isolated from bone, but was later found to have a wider distribution (9). In adults, OPN expression is normally restricted to the bone, kidney, epithelial linings, and bodily fluids including milk, blood, and urine (10). In contrast to its limited distribution in normal tissue, OPN is strikingly upregulated in response to inflammation and tissue remodeling where it is localized in and around immune cells (11, 12).

1.3 OPN structure

The pleiotropic nature of OPN may reflect the various isoforms and post-translational modifications of OPN and the diversity of cell types which it can interact with. OPN interacts with integrins via two major functional domains (Figure 1.1). While the OPN protein is poorly conserved among species (63% human to mouse), its functional domains are conserved. The adhesive RGD domain mediates interactions via $\alpha_V\beta_1$, $\alpha_V\beta_3$, $\alpha_V\beta_5$, $\alpha_V\beta_6$, $\alpha_8\beta_1$, and $\alpha_5\beta_1$ integrins (13-16). Immediately C-terminal to the RGD motif is the SVVYGLR (SLAYGLR in mouse) domain that mediates interactions with $\alpha_4\beta_1$, $\alpha_9\beta_1$, and $\alpha_4\beta_7$ integrins (17-19). Additionally, a second binding site for integrin $\alpha_4\beta_1$ has been described in human OPN, although this domain is not well conserved among species (20).

In addition to interacting with integrins, OPN has also been reported to interact with the hyaluronic acid receptor, CD44 (21). While OPN does not bind to the standard isoform, CD44H, it can bind to some CD44 splice variants, notably v6 and v7 (22, 23). However, the precise domain of OPN that interacts with CD44 has not been identified.

OPN is subject to extensive post-translational modification which can alter its bioactivity. Phosphorylation of OPN is dependent on cell type with phosphorylation levels varying depending on the tissue type. Normal rat kidney cells can secrete both phosphorylated and non-phosphorylated forms, indicating regulated control of phosphorylation (24). In some cases OPN function is tightly controlled by phosphorylation state. Calcification of smooth muscle cells *in vitro* is inhibited by native OPN, but dephosphorylated or recombinant bacterially-derived OPN has no effect on calcification (25). In contrast, the adhesive activity of OPN is not dependent on post-translational modifications as bacterially-produced OPN supports cell adhesion in a wide variety of cell types (26, 27). Bacterially-derived OPN is also chemotactic for certain cell types including smooth muscle cells and endothelial cells (28-30)

The bioactivity of OPN can be further regulated by proteolytic processing. OPN is a substrate for thrombin and the matrix metalloproteinases, MMP-2 (gelatinase A), MMP-3 (stromelysin-1), MMP-7 (matrilysin), and MMP-9 (gelatinase B) (31-33). More recently it has been demonstrated that OPN is a novel substrate for plasmin and cathepsin D (34). Proteolytic processing may represent a way to locally regulate the function of OPN as the properties of the cleaved form differ from those of the intact molecule. Of particular interest rather than mediating degradation and inactivating OPN-mediated functions, proteolytic processing of OPN can increase the biological activity of the molecule (35). There are a few studies to date suggesting that OPN fragments play a functional role *in vivo*. Enhanced production of the thrombin-cleaved form of OPN is found in the synovial fluid of patients with rheumatoid arthritis (36) and the cryptic SLAYGLR motif was found to play an essential role in the pathogenesis of the disease in both a murine and a primate model of rheumatoid arthritis (37, 38).

OPN can interact directly with extracellular matrix proteins including fibronectin (39) and collagen type I (40, 41). OPN is also subject to sulfation (42), glycosylation (43), and transglutamination (44).

An intracellular form of OPN (iOPN) has been reported to be expressed in a subset of dendritic cells (plasmacytoid DCs) (45). In this cell type, OPN is generated due to translation initiation downstream of the usual start site, generating a truncated iOPN form that lacks the N-terminal signal sequence and consequently localizes to the cytoplasm. Others have found that iOPN may associate with the intracellular domain of CD44 and with the ezrin/radixin/moesin (ERM) protein ezrin (46). iOPN in this context may modulate cytoskeletal rearrangements important for macrophage migration and osteoclast fusion (47).

1.4 OPN and macrophage-mediated inflammation

Chronic inflammation is associated with the persistence of macrophages at the site of inflammation. Functionally, OPN plays a key role in macrophage biology by regulating macrophage adhesion, migration, survival, and pro-inflammatory cytokine production. OPN is not expressed by circulating monocytes, but is dramatically upregulated during macrophage differentiation and constitutes one of the major macrophage products (48). OPN expression is induced in macrophages by several inflammatory cytokines including TNF-α, IL-1β, IL-6, and other factors including angiotensin-II, high glucose, oxidized LDL, and phorbol-ester (49-51).

OPN functions in the earliest aspects of inflammation by promoting macrophage recruitment to the site of inflammation. Several studies have established OPN as a potent macrophage

chemoattractant (51-54). Deficits in macrophage accumulation have been observed in OPN-null mice when challenged with acute and chronic inflammatory conditions including atherosclerosis (55), delayed-type hypersensitivity (56), granulomatous disease (57), thioglycollate elicited peritonitis (51), and biomaterial implantation (2, 58). Together, these studies suggest that OPN may be particularly important in promoting migration and retention of macrophages at sites of inflammation.

In vitro, OPN-null macrophages exhibit reduced basal migration and impaired migration toward MCP-1, despite the fact that wild type and OPN-null macrophages express comparable levels of CCR-2, the MCP-1 receptor (51). Macrophages deficient in OPN are also more susceptible to apoptosis (59). Recently, we have shown that OPN protects macrophages from apoptosis via an α_4 integrin-initiated pathway. Together with impaired migration, macrophage apoptosis may further contribute to the impaired macrophage accumulation observed in OPN-null mice in response to acute and chronic inflammatory stimuli.

Altogether, these data suggest that OPN may be particularly important in promoting recruitment and retention of macrophages at sites of acute and chronic inflammation by regulating multiple macrophage functions. Additionally, these studies emphasize the importance of macrophage-derived OPN in the regulation of OPN's functions, suggesting that macrophages are both a source and a target of OPN.

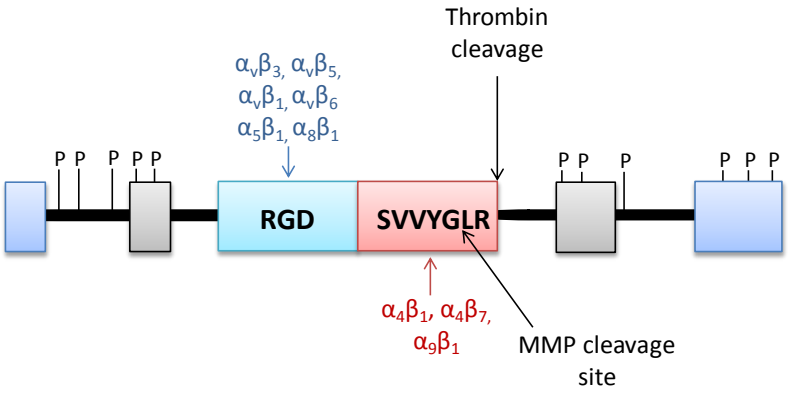

Figure 1.1: OPN structural features.
OPN interacts with integrins via the RGD and SVVYGLR (SLAYGLR in mouse) functional domains. OPN is also subject to proteolytic cleavage by thrombin and MMPs. Phosphorylation sites are shown in black (P) and calcium binding sites are in gray. Other matrix binding sites are shown in blue boxes.

Chapter 2

Defining the role of OPN in macrophage activation

2.1 Abstract

In this chapter the role of osteopontin in macrophage activation was explored. OPN has been reported to stimulate IL-12 secretion from macrophages and inhibit IL-10 production thereby skewing the immune system toward Th1 type responses. Consequently, we hypothesized that OPN could promote an M1 pro-inflammatory macrophage activation phenotype. To this end, we developed a panel of markers to differentiate M1 and M2 macrophages via flow cytometry. Using this system, we then assessed the effect of OPN on macrophage phenotype. In contrast to previous reports, OPN did not affect macrophage activation in terms of cell surface receptor expression and cytokine production in bone marrow derived macrophages or thioglycollate elicited peritoneal macrophages. Both soluble and immobilized forms of OPN were tested for their ability to promote macrophage activation and neither form was to found influence macrophage phenotype. Further, we determined that primary macrophages from wild type and OPN-null mice did not differ in their ability to be polarized to either the M1 or M2 macrophage activation state. Finally, we show that OPN does not stimulate NF-κB signaling in the macrophage cell line, RAW264.7.

2.2 Introduction

OPN has been implicated in regulating multiple functions of macrophage biology including migration, survival, and cytokine production (60). While OPN is not expressed in circulating monocytes, its expression is strikingly upregulated during monocyte to macrophage differentiation and it constitutes one of the major macrophage products (48). OPN is frequently identified as being expressed by macrophages in pathological disease states where its expression is associated with inflammation (11, 61-63). The role of OPN in macrophages may underlie its physiological role in many pathological disease states. In this chapter, we define the role of OPN in macrophage activation.

2.2.1 M1/M2 macrophage activation

Upon exposure to cytokines or microbial products macrophages become polarized to distinct activation states. Stimulation with IFN-γ and LPS drives macrophages towards a classically activated phenotype, while treatment with IL-4 produces alternatively activated macrophages (64). Mirroring the Th_1/Th_2 nomenclature of T-helper lymphocytes, classical and alternatively activated macrophages are often referred to as M1 and M2 macrophages, respectively. Polarized macrophages differ in terms of receptor expression, cytokine and chemokine production, and effector function (65, 66). M1 macrophages are characterized by increased production of pro-inflammatory cytokines, upregulation of opsonic receptors, and increased generation of reactive oxygen and nitrogen intermediaries (67). In contrast, M2 macrophage activation induces increased expression of non-opsonic receptors such as the macrophage mannose receptor and scavenger receptors, as well as increased production of arginase (68-70). Generally, M1

macrophages are associated with inflammation where they are thought to propagate the immune response, while M2 macrophages are implicated in resolving inflammation and promoting tissue remodeling (71). Figure 2.1 summarizes differences in gene expression between M1 and M2 macrophages. While M1 and M2 macrophages are generally referred to as distinct activation states, it should be noted that *in vivo* macrophages are exposed to a milieu of cytokines and polarizing signals, which likely results in a spectrum of macrophage activation (72).

2.2.2 OPN and macrophage activation

OPN has been previously reported to induce IL-12p70 production in resident peritoneal macrophages, in a time course similar to LPS stimulation, while inhibiting IL-10 production (73, 74). Later work showed that OPN's ability to stimulate IL-12 production is dependent on phosphorylation and mediated via integrin β_3 and RGD (75). Interestingly, IL-12 production was mediated via an N-terminal OPN fragment, while IL-10 inhibition occurred via a C-terminal fragment of OPN. *In vivo*, in atherosclerosis-prone ApoE-/- mice, OPN deficiency resulted in reduced aortic IFN-γ and IL-12p40 expression and increased levels of IL-10 in response to angiotensin II (Ang II) stimulation (51). *In vivo*, OPN-null mice display impaired Th1 responses to the intracellular bacterium *Listeria monocytogenes* and the viral pathogen HSV1 (herpes simples virus type 1), both of which depend on the induction of IL-12 for protection (73). Taken together these data suggest that OPN's ability to modulate cytokine production in macrophages may regulate the Th_1-Th_2 bias of the adaptive immune system. Given OPN's important role in macrophage function, we hypothesized that OPN could promote an M1 macrophage activation phenotype.

2.3 Materials and Methods

2.3.1 Production of recombinant OPN

Recombinant histidine-tagged wild type human OPN was expressed in *Escherichia coli* (*E. coli*) as a full-length fusion protein and was purified as previously described with the following exception; a high salt wash (50 mM NaH_2PO_4, 0.9 M NaCl, 10 mM imidazole, 10% glycerol, pH 6.0) was included prior to protein elution (76). Endotoxin was removed from *E. coli*-derived OPN by passing the purified protein solution over a Hi-Trap Q HP anion exchange column (GE Healthcare). Endotoxin levels were determined using the Pyrogen® Plus Gel Clot LAL assay (0.06 EU/ml sensitivity, Lonza) following the manufacturer's directions. Endotoxin levels were less than 0.04 EU/μg protein. Protein concentration was determined using the Micro BCA assay (Pierce) following the manufacturer's directions. Purity levels of the recombinant OPN protein was assayed by SDS-PAGE and Western blotting using a polyclonal goat anti-OPN antibody (OP-199) (28). OPN bioactivity was assessed by the ability to support adhesion of bovine aortic endothelial cells (BAECs) as previously described (29).

2.3.2 Cell culture

2.3.2.1 Mice

OPN-null mice were generated on a C57Bl/6 background as previously described (77). Wild type (WT) mice on the C57Bl/6 background were bred in house or were purchased from The Jackson Laboratory. All animal experiments were approved by the University of Washington Institutional Animal Care and Use Committee (IACUC) and followed federal guidelines for the use and care of laboratory animals.

2.3.2.2 Bone marrow derived macrophages

For the generation of primary bone marrow derived macrophages (BMDMs), femora were harvested from wild type (WT) and OPN-null (OPN-/-) mice. Bone marrow cells were thoroughly dispersed and were expanded in macrophage expansion media (50% RPMI, 30% L929-conditioned media, and 20% fetal bovine serum (FBS)). Cells were fed on Day 4 and mature macrophages were harvested on Day 7 for assays.

2.3.2.3 Thioglycollate elicited peritoneal macrophages

Thioglycollate elicited peritoneal macrophages from C57Bl/6 mice were elicited by intraperitoneal injection of 1 ml of 3% thioglycollate medium (BD Biosciences, cat #221199). 72 hours after injection, thioglycollate elicited peritoneal macrophages were harvested by peritoneal lavage with ice-cold PBS/5 mM EDTA.

2.3.3 Preparation of immobilized OPN surfaces

2.3.3.1 Spin-coating of poly(HEMA) on glass coverslips

pHEMA spin-coated glass coverslips were produced as previously described (78). Round glass coverslips (12 mm diameter) were cleaned by sonicating sequentially in methylene chloride, acetone, and then methanol, for 5 minutes per solvent. Clean coverslips were then baked overnight at 60°C. The next day, coverslips were coated with a 2.5% ethyl methacrylate/silane solution by pipetting 10 ul of the solution onto a coverslip while spinning at 4000 rpm for 20 seconds. Coverslips were baked at 60°C overnight. Coverslips were soaked in 2 changes of

ethyl acetate for 1 hour per solvent change, followed by rinsing in methanol for 10 minutes. Coverslips were then spin-coated with 2.5% polyHEMA dissolved in methanol.

2.3.3.2 poly(HEMA) activation using 1,1'carbonyldiiamidazole (CDI)

CDI chemistry was used to activate hydroxyl groups on poly(HEMA) spin-coated coverslips. Coverslips were rinsed three times with 1,4'-dioxane and placed in a 50 mM CDI solution in 1,4'-dioxane for 2.5 hours at 50°C to produce an active intermediate carbamate at the hydroxyl groups on the pHEMA surface. Samples were then washed and sonicated three times in dioxane to remove any unreacted CDI. pHEMA samples were then rinsed three times in sterile PBS and incubated in OPN diluted in 0.1M sodium carbonate/bicarbonate buffer (pH 9.3) overnight at 4°C. The next day, samples were rinsed with PBS to remove unbound OPN. The final product was OPN immobilized via primary amines to the hydroxyl groups on the pHEMA surface with a carbonyl spacer introduced by the CDI chemistry (79).

2.3.3.3 Quantification of immobilized OPN by radiolabeling

The amount of OPN immobilized on spin-coated pHEMA disks was determined using I-125 radiolabeled OPN. Recombinant OPN was radio-iodinated with I-125 using Iodobeads (Pierce) following the manufacturer's instructions. Radiolabeled OPN was passed over two consecutive Econo-Pac10 DG columns (BioRad) to remove unbound I-125. Solutions of OPN were prepared and spiked with radiolabeled OPN. OPN was immobilized on pHEMA disks as described above using radiolabeled OPN and radioactivity was measured.

2.3.4 Macrophage activation experiments

WT and OPN-null BMDMs were stimulated with IFN-γ (20 ng/ml, Abcam, Cambridge, MA) and LPS (100 ng/ml, Sigma) to produce M1 macrophages, or with IL-4 (60 ng/ml, R&D Systems) to produce M2 macrophages. Serum-free RPMI supplemented with pen/strep was used for stimulations. Unstimulated macrophages incubated in serum-free RPMI were used as a control. Cells were stimulated for 24 hours. For the analysis of cell surface markers (mannose receptor, CD86, and IL-1RII) cells were harvested after 24 hours of stimulation and stained for flow cytometry. For the analysis of IL-1RII expression, cells were incubated with the broad spectrum MMP inhibitor, GM6001. For analysis of IL-12p40 production, BMDMs were treated with Brefeldin A (GolgiPlug, BD Biosciences) at 0.5 μg/ml in RPMI/10% FBS for the final 5 hours of stimulation. For flow cytometric analysis of intracellular molecules (iNOS, IL-12p40) cells were harvested, fixed and permeabilized with Cytofix/Cytoperm™ (BD Bioscience) according to the manufacturer's directions.

2.3.5 Flow cytometric analysis of M1/M2 macrophage activation markers

IL-12p40 (clone C17.8, Santa Cruz Biotech, CA), CD86 (clone PO3.1, eBioscience, San Diego, CA), and iNOS (ab15323, Abcam) were used as markers of M1 macrophage activation, while mannose receptor (AF2535, R&D Systems) and IL-1 type II decoy receptor (clone 4E2, BD Bioscience, San Jose, CA) were used as M2 markers. Antibody dilutions for flow cytometry experiments are shown in Table 2.1. PE-conjugated secondary antibodies ($F(ab')_2$ fragment, Jackson ImmunoResearch) were used for detection at a 1:200 dilution. For antibody staining of cell surface markers (CD86, MR, IL-1RII) all incubations were carried out in FACS staining buffer (PBS/1.0% FBS/0.1% sodium azide) and cells were fixed with 4% paraformaldehyde

prior to analysis. For staining of intracellular markers (iNOS, IL-12p40) all incubations were performed in 1X BD Perm/Wash™ Buffer (BD Bioscience) and cells were resuspended in FACS staining buffer for analysis. Cells were analyzed on a BD FACscan flow cytometer and data was analyzed using FlowJo software.

2.3.6 IL-12p70 production from resident peritoneal macrophages

Resident peritoneal macrophages were harvested from WT C57Bl/6 mice by peritoneal lavage with PBS (without Ca^{2+} or Mg^{2+}). Cells were treated with ACK buffer (0.15 M NH_4Cl, 1 mM $KHCO_3$, 0.1 mM Na_2EDTA, pH 7.2-7.4) to lyse red blood cells. Cells were plated in non-tissue culture treated 48-well plates in DMEM/10% FBS and allowed to adhere for 2 hours. Adherent cells were stimulated with IFN-γ (20 ng/ml) and LPS (100 ng/ml), or recombinant mammalian-derived murine OPN (R&D Systems) in serum-free DMEM. Conditioned mediim was collected after 24 or 48 hours of stimulation. IL-12p70 concentration in conditioned media was determined using the mouse IL-12p70 Ready-Set-Go!® ELISA (eBioscience, cat #88-7121).

2.3.7 NF-κB activation in RAW 264.7 cells

Activation of NF-κB signaling by OPN was assayed using a luciferase reporter construct in RAW264.7 cells. RAW 264.7 cells (0.7×10^4 cells/well) in DMEM/10% FBS were plated in a 48-well tissue culture-treated plate. The next day, cells were transiently transfected with 0.2 μg pBIIX-LUC-NF-κB reporter construct (80) with 1.5 μl Lipofectamine 2000 (Invitrogen) in serum-free OPTI-MEM. The pBIIX-LUC-NF-κB construct contains the *fos* gene core promoter fused to two NF-κB sites derived from the Igκ promoter driving the luciferase gene. Cells were co-transfected with an equal amount (0.2 μg) of a pRL Renilla luciferase construct (Promega) as

a control for transfection efficiency. After 6 hours, transfection media was replaced with serum-free DMEM and cells were allowed to recover overnight. The following day, transfected cells were treated with 5 nM or 100 nM rmOPN (NSO-derived, R&D Systems) in serum-free DMEM. LPS (100 ng/ml) was used as a positive control for NF-κB activation. After 6 hours, cells were lysed with Passive Lysis Buffer (Promega) and firefly and *Renilla* luciferase were measured using the Promega Dual-Luciferase® Reporter Assay System following the manufacturer's directions. Firefly luciferase was normalized to *Renilla* luciferase.

2.4 Results and Discussion

2.4.1 M1/M2 macrophage marker development

To determine the effect of OPN on macrophage activation, we first developed a system to identify M1 and M2 macrophages by flow cytometry. Flow cytometry was chosen as it provides rapid, quantitative, and detailed analysis of macrophage subpopulations while allowing for simultaneous measurement of multiple cellular parameters. As shown in Figure 2.2, stimulation with IFN-γ + LPS to drive macrophages toward the M1 pathway resulted in significant upregulation of iNOS, CD86, and IL-12p40. Consequently, for future studies these markers were selected for identification of M1 macrophages.

On the other end of the spectrum, stimulation with IL-4 resulted in increased expression of the macrophage mannose receptor (MR) and the IL-1 type II decoy receptor (IL-1RII) compared to unstimulated cells (Figure 2.2). These receptors were chosen as markers of M2 macrophage activation.

2.4.2 Immobilized OPN does not affect macrophage activation

Having established a system to identify M1/M2 macrophages via flow cytometry, we then investigated the effect of OPN on macrophage activation. Prior studies in our lab demonstrated that immobilized OPN could stimulate pro-inflammatory cytokine production in the macrophage-like cell line, RAW264.7. We sought to determine if this effect could be recapitulated in primary murine macrophages. For these studies OPN was immobilized on spin-coated poly(2-hydroxyethyl methacrylate) [(pHEMA)] disks using CDI chemistry. pHEMA was used due to its relatively low protein adsorption and cell adhesion, as well as the abundance of hydroxyl functional groups allowing for the bioconjugation of proteins (81). BMDMs were plated on OPN surfaces or on control surfaces that had been activated with CDI (CDI control) in serum-free RPMI for 24 hours. As a positive control for M1 macrophage activation, BMDMs were stimulated with IFN-γ + LPS, and macrophages were stimulated with IL-4 as a control for M2 macrophages. After 24 hours of stimulation IL-12p40 production was determined by flow cytometry. As shown in Figure 2.3, treatment with IFN-γ + LPS resulted in a significant increase in IL-12p40 production compared to unstimulated macrophages. However, immobilized OPN surfaces failed to induce IL-12p40 production in BMDMs. We also found that immobilized OPN surfaces failed to increase expression of the other M1 markers assayed, iNOS and CD86 (data not shown).

To determine if this effect was specific to cell source we also explored whether immobilized OPN surfaces could stimulate M1 macrophage activation in thioglycollate elicited peritoneal macrophages. However, we found that immobilized OPN also failed to induce production of IL-12p40 in peritoneal macrophages as well (data not shown).

2.4.3 Verification of OPN immobilization by radiolabeling

To confirm that OPN had been successfully immobilized on our pHEMA surfaces, radiolabeling experiments were performed. Binding of OPN to pHEMA surfaces was dose dependent over the range of concentrations tested. At the highest concentration tested (100 μg/ml) the quantity of OPN bound was 70 ng/cm^2 confirming successful immobilization of OPN to our spin-coated pHEMA surfaces.

2.4.4 Soluble OPN does not affect pro-inflammatory cytokine production

In addition to being a part of the extracellular matrix, OPN also exists as a soluble cytokine. Consequently, we tested whether soluble, exogenous OPN could stimulate macrophages to the M1 macrophage phenotype. However, we found that treatment with recombinant bacterially-derived human OPN did not stimulate IL-12p40 production, even at doses as high as 500 nM (Figure 2.5). Similar results were obtained for the other M1 markers analyzed, iNOS and CD86 (data not shown). To account for the possibility that post-translational modifications of OPN are necessary for macrophage activation, recombinant murine mammalian-derived OPN was also included as a control. However, this OPN form also failed to induce IL-12 production as well (Figure 2.5). A time course study was also performed and IL-12 production was assayed after 24, 36, 48, and 72 hours of stimulation with OPN. Prolonged stimulation with OPN did not result in increased production of IL-12p40 compared to untreated macrophages (data not shown).

To determine if these effects were specific to bone marrow derived macrophages, studies were performed using resident peritoneal macrophages. Resident peritoneal macrophages were

stimulated with IFN-γ + LPS or recombinant mammalian-derived murine OPN in serum-free DMEM. Conditioned medium was collected after 24 or 48 hours of treatment and IL-12p70 levels were determined by ELISA. As expected, stimulation with IFN-γ + LPS induced IL-12p70 secretion from resident peritoneal macrophages. However, treatment with OPN did not induce IL-12p70, even at concentrations as high as 100 nM (Figure 2.6).

2.4.5 OPN deficiency does not affect macrophage phenotype

We then questioned whether OPN deficiency affects the ability of macrophages to respond to signals polarizing macrophages to either the M1 or M2 phenotype. WT and OPN-null BMDMs were stimulated with IFN-γ + LPS to activate macrophages toward the M1 pathway or with IL-4 to produce M2 macrophages. As seen in Figure 2.7, OPN deficiency did not alter the production of IL-12p40 from BMDMs or mannose receptor expression (Figure 2.8). Furthermore, OPN deficiency did not affect the other markers of macrophage activation tested (data not shown). These results indicate that OPN does not affect macrophage activation phenotype.

2.4.6 OPN does not activate NF-κB in macrophages

Finally, we determined the effect of OPN on NF-κB signaling in macrophages. The transcription factor NF-κB is a key regulator of inflammation and OPN has been shown to stimulate NF-κB signaling in other cell types. In endothelial cells, OPN induces NF-κB signaling through integrin $\alpha_V\beta_3$ to promote cell survival (80). To determine if OPN activates NF-κB signaling in macrophages, the monocyte-macrophage cell line, RAW264.7, was transiently transfected with a NF-κB luciferase reporter construct. This construct contains two NF-κB consensus binding sites in the promoter. RAW264.7 cells were chosen for these experiments due to their ease of

transfection as compared to primary macrophages. Transfected RAW264.7 cells were stimulated with rmOPN for 6 hours and cell lysates were collected and luciferase was assayed. As expected, stimulation with LPS, a known activator of NF-κB signaling, resulted in a three-fold induction of the reporter construct compared to unstimulated control cells (Fig 2.9). In contrast, stimulation with either 5 nM or 100 nM OPN did not result in increased luciferase expression. Taken together, these results indicate that OPN does not affect macrophage activation.

2.5 Discussion

While we were unable to show a role for OPN in macrophage activation, there are several possible explanations for the discrepancies between our results and those previously published. First, endotoxin contamination could be responsible for inducing pro-inflammatory cytokine production in macrophages in previous reports. In this regard, a study by Konno et al., found that commercially available preparations of both recombinant and native OPN contain variable levels of endotoxin contamination (82). In this study, it was further shown that the ability of OPN to induce pro-inflammatory cytokine production in human peripheral blood mononuclear cells (PBMCs) was due to contaminating endotoxin. Given the exquisite sensitivity of macrophages to endotoxin, even low levels of contamination can result in macrophage activation. In our experiments we found that endotoxin levels as low as 0.36 EU/ml (equivalent to ~0.036 ng/ml endotoxin) were sufficient to induce IL-12p40 production in BMDMs. Given the relatively high concentrations of OPN used in some previously published works (83), endotoxin contamination could play a confounding role.

Additionally, the discrepancies between our results and those previously published could be due to differences in the source of OPN used for experiments. For our studies, we used commercially available recombinant OPN produced from NSO (myeloma) cells, while previous studies have used native OPN derived from bone cell cultures or the osteoblastic MC3T3E1 cell line (73, 75). Post-translational modifications (PTMs) of OPN vary between sources, and PTMs have been shown to tightly control OPN's bioactivity in some cases. Calcification of smooth muscle cells *in vitro* is inhibited by native OPN, but dephosphorylated or recombinant bacterially produced OPN has no effect on calcification (25). In contrast, the adhesive activity of OPN is not dependent on post-translational modifications, since bacterially-derived OPN has been shown to support cell adhesion in a wide variety of cell types (26, 27).

Additionally, in the literature, controversy exists over whether OPN affects macrophage activation. Several other labs have been unable to repeat the finding that OPN stimulates IL-12 in macrophages *in vitro*. Abel et al., found that recombinant OPN produced in insect cells was unable induce IL-12p40 or inhibit LPS-induced IL-10 production from resident or thioglycollate elicited peritoneal macrophages (84). Additionally, studies by Potter et al., demonstrated that recombinant OPN had no effect on IL-12p40 or IL-10 production from bone marrow derived macrophages or splenic macrophages (85).

Finally, we do not dispute that OPN plays a role in shaping Th1 type immune responses *in vivo*. OPN-induced pro-inflammatory cytokine production from macrophages may require co-stimulation. O'Regan et al. demonstrated T-cell dependent IL-12 production from PBMCs, but found that in PBMCs alone OPN could not stimulate IL-12 production (86). Further, *in vivo*,

other cell types could contribute to IL-12 production as well. In atherosclerosis-prone ApoE-/- mice, OPN deficiency results in reduced aortic IFN-γ and IL-12p40 expression and increased levels of IL-10 in response to Ang II stimulation (51). While this could be due to macrophage cytokine production, dendritic cells also produce IL-12. In this regard, dendritic cell (DC) accumulation in atherosclerotic lesions has recently been demonstrated (87) and OPN has been shown to stimulate IL-12p70 production in DCs, inducing enhanced IFN-γ production by T-cells (88). OPN-null DCs have impaired migration toward chemotactic gradients of cytokines and chemokines, including TNF-α and CCL19, and decreased migratory capacity *in vivo* (89). Taken together these results suggests that OPN regulation of Th_1 cytokines seen in the angiotensin II-accelerated model of atherosclerosis could be due to IL-12 production by dendritic cells, not macrophages.

2.6 Conclusions

In this chapter we developed a system for identifying M1 and M2 macrophages by flow cytometry. We then utilized this system to explore the role of OPN in macrophage activation. Contrary to previous reports we found that OPN does not play a role in macrophage activation *in vitro*. Stimulation with immobilized OPN or soluble OPN did not induce pro-inflammatory cytokine production from macrophages or alter cell surface receptor expression. Further, we found no differences between WT and OPN-null macrophages in their ability to be stimulated to either the M1 or M2 macrophage activation phenotype. To account for possible differences between macrophages obtained from different sources, studies were carried out with both bone marrow derived macrophages and peritoneal macrophages. Finally, we show that OPN does not activate NF-κB signaling in macrophages.

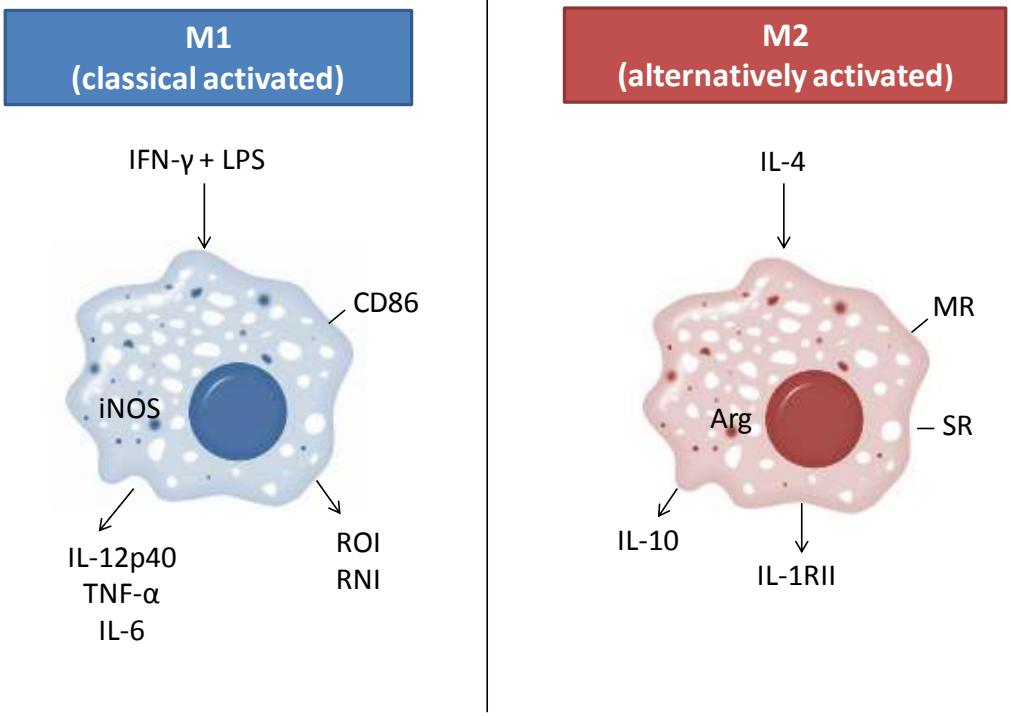

Figure 2.1: A simplified view of M1/M2 macrophage activation.
Macrophages become activated and acquire different functional properties upon exposure to external stimuli. Exposure to IFN-γ and LPS polarizes macrophages toward the M1 phenotype, while stimulation with IL-4 produces M2 macrophages. M1 macrophages are characterized by increased production of pro-inflammatory cytokines, upregulation of opsonic receptors, and increased production of reactive oxygen and nitrogen species. At the other end of the spectrum, M2 macrophages have increased production of IL-10, scavenger receptors, and arginase. Abbreviations: Arg, arginase; iNOS, inducible nitric oxide synthase; MR, mannose receptor; SR, scavenger receptor; ROI, reactive oxygen intermediates; RNI, reactive nitrogen intermediates.

Antibody	Manufacturer	Cat. #	Clonality	Isotype	Final Concentration (µg per 100 µl)
CD86	eBioscience	14-0861	monoclonal	rat IgG2b	0.5
IL-1RII	BD PharMingen	554448	monoclonal	rat IgG2a	0.5
MR	R&D Systems	AF2535	polyclonal	goat IgG	0.5
IL-12p40	Santa Cruz	sc-57258	monoclonal	rat IgG2a	0.5
iNOS	Abcam	ab15323	polyclonal	rabbit IgG	0.5

Table 2.1: Antibodies used for M1/M2 macrophage identification by flow cytometry. Primary antibodies tested as markers for M1 or M2 macrophage activation. Abbreviations: IL-1RII, IL-1 type II decoy receptor; MR, mannose receptor

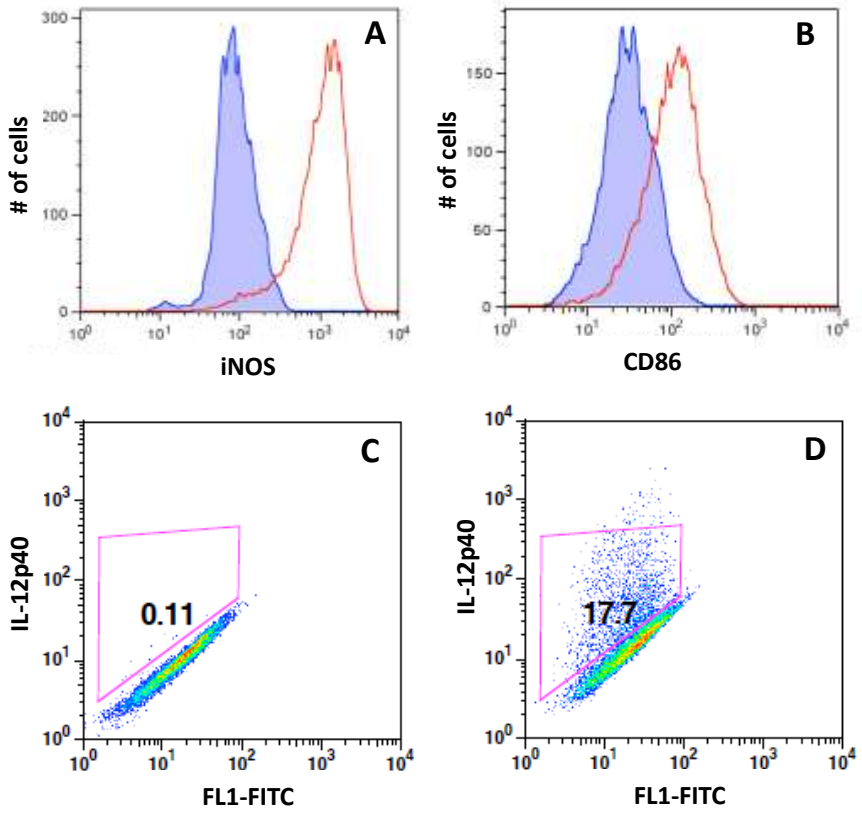

Figure 2.2: M1 markers of macrophage activation.
(**A and B**) BMDMs were stimulated with IFN-γ + LPS (red histograms) to produce M1 macrophages. Unstimulated macrophages (blue histograms) were used as a control. After 24 hours of stimulation, BMDMs were stained for iNOS **(A)** or CD86 **(B)** and analyzed by flow cytometry. (**C and D**) BMDMs were also analyzed for IL-12p40 production by flow cytometry Unstimulated macrophages are shown in **(C)** and cells treated with IFN-γ + LPS are shown in **(D)**.

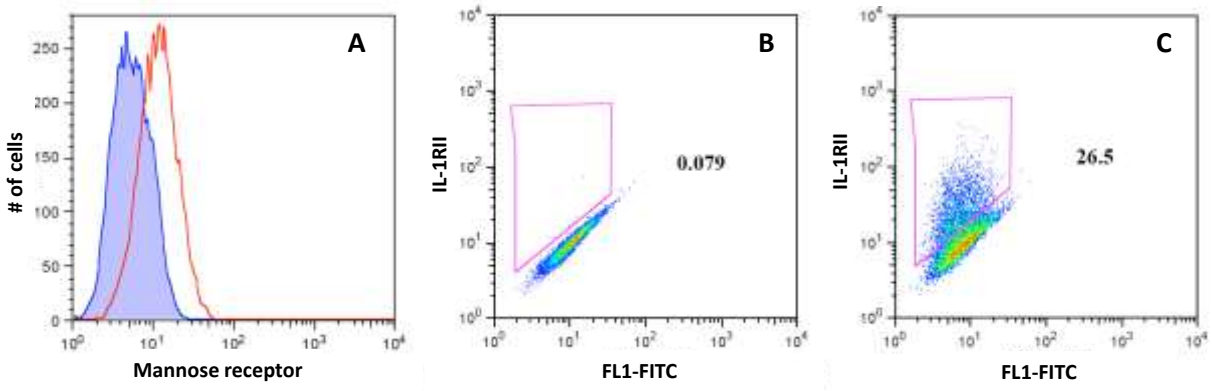

Figure 2.3: M2 markers of macrophage activation.
(**A**) BMDMs were stimulated with IL-4 (red histogram) for 24 hours to produce M2 macrophages and were stained mannose receptor and analyzed by flow cytometry. Unactivated macrophages (blue filled histogram) were included as a control. (**B and C**) Untreated (**B**) and IL-4 treated (**C**) macrophages were also stained for IL-1RII and analyzed by flow cytometry.

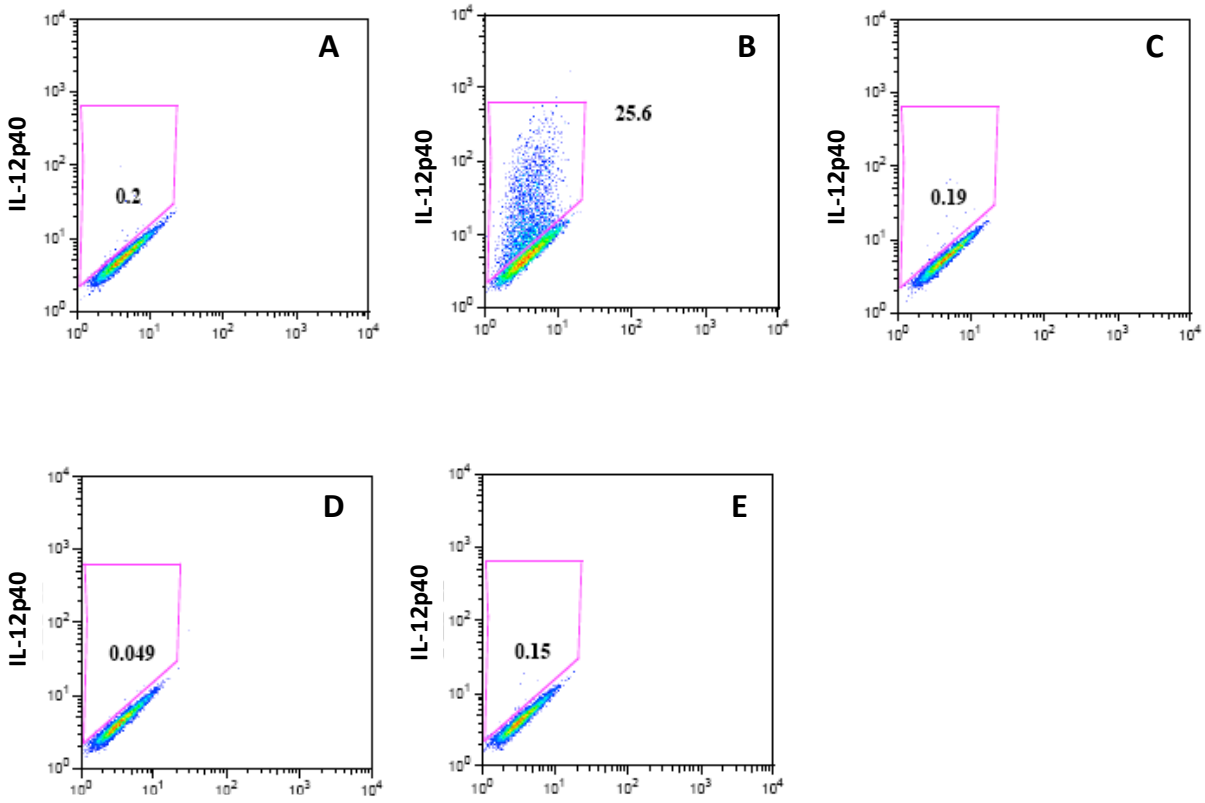

Figure 2.4: Immobilized OPN does not stimulate IL-12p40 production.
BMDMs were stimulated for 24 hours with media alone (**A**), IFN-γ + LPS (**B**), IL-4 (**C**), or plated on immobilized OPN surfaces (**D**) or on CDI-activated control surfaces (**E**). Macrophages were treated with Brefeldin A for the last 6 hours of stimulation and IL-12p40 expression was analyzed by flow cytometry.

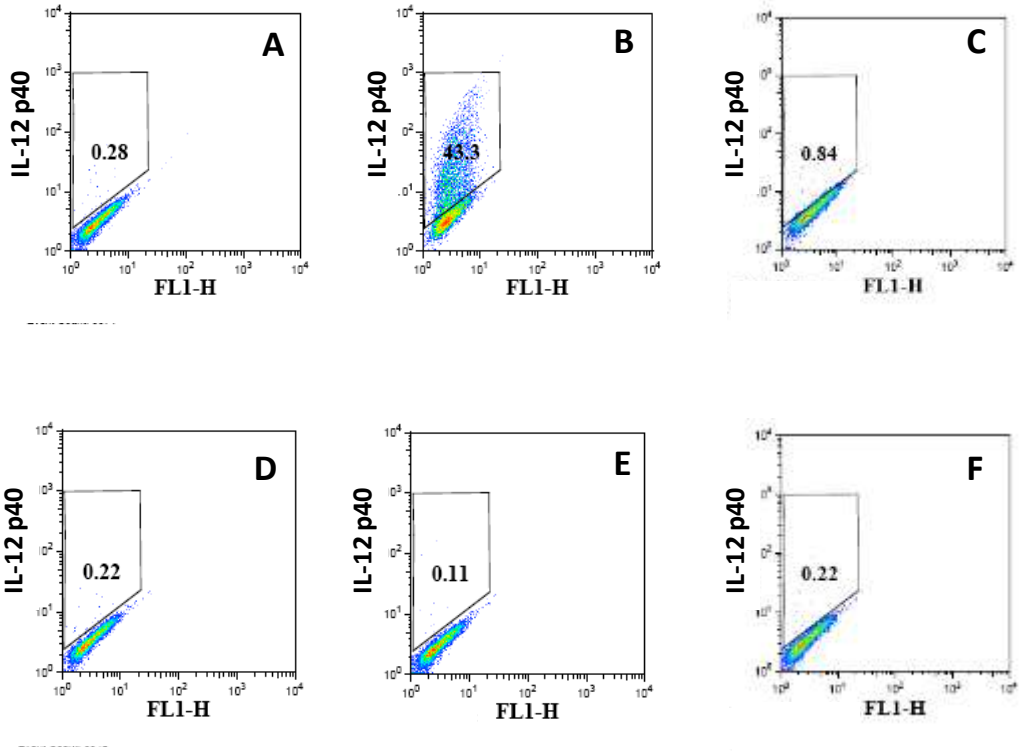

Figure 2.5: Exogenous OPN does not affect pro-inflammatory cytokine production. BMDMs were stimulated for 24 hours with media alone (**A**), IFN-γ + LPS (**B**), recombinant mammalian OPN (**C**), or recombinant bacterially-derived OPN at a concentration of 100 nM (**D**), 250 nM (**E**), or 500 nM (**F**). Macrophages were treated with Brefeldin A for the final 6 hours of stimulation, and IL-12p40 production was analyzed by flow cytometry.

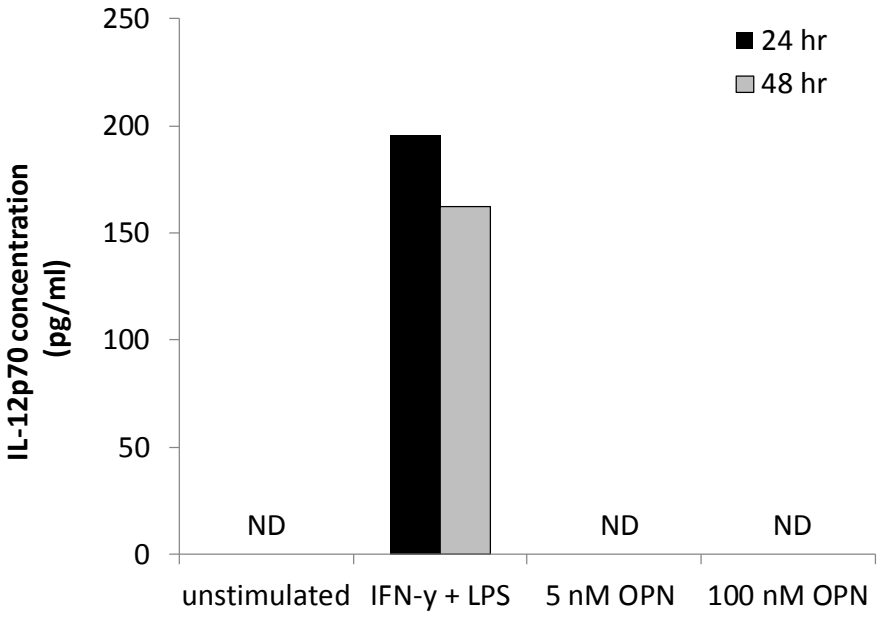

Figure 2.6: OPN does not induce IL-12p70 in resident peritoneal macrophages.
Resident peritoneal macrophages were stimulated with IFN-γ + LPS, 5 nM rmOPN, or 100 nM rmOPN, and the concentration of IL-12p70 was assayed after 24 hours (black bars) or 48 hours (gray bars). ND: not detectable.

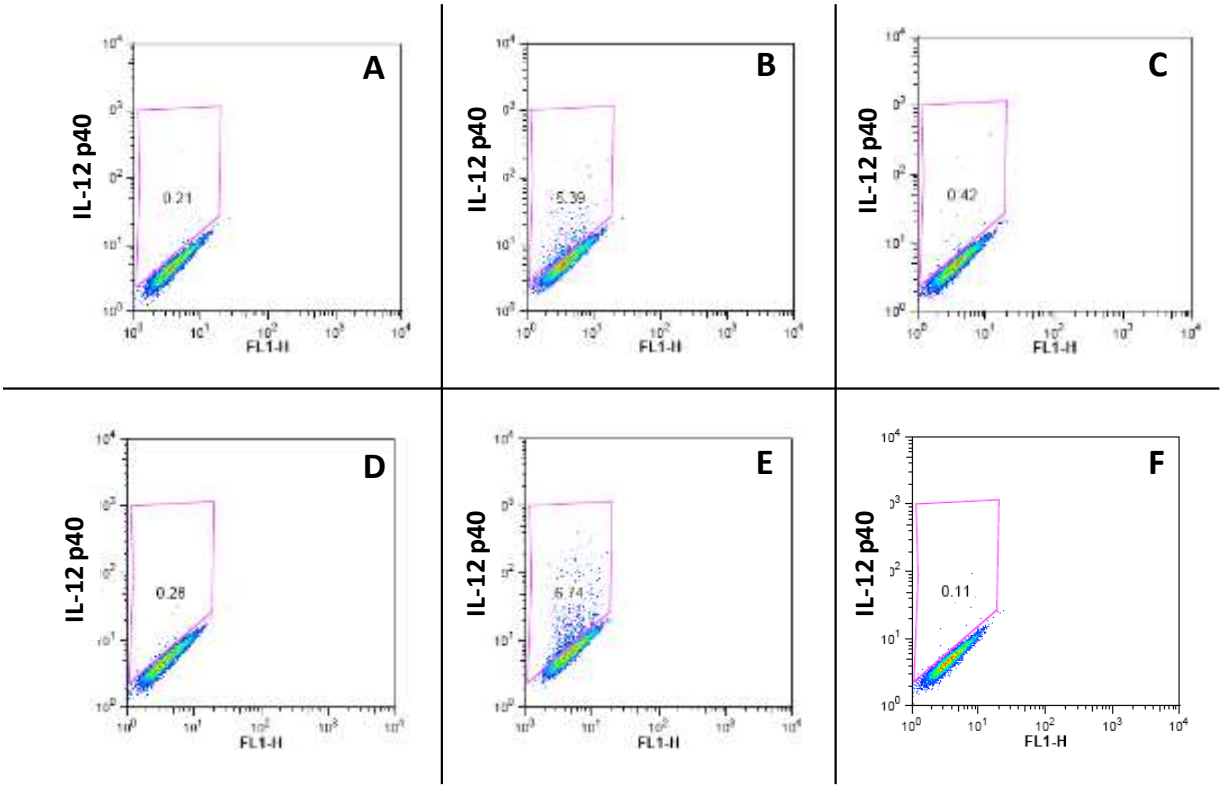

Figure 2.7: OPN deficiency does not affect macrophage activation phenotype.
BMDMs from wild type mice were stimulated with media alone (**A**), LPS + IFN-γ (**B**), or IL-4 (**C**) for 24 hours and IL-12p40 production was analyzed by flow cytometry. OPN-null macrophages were also treated with media alone (**D**), LPS + IFN-γ (**E**), or IL-4 (**F**) and IL-12p40 was analyzed.

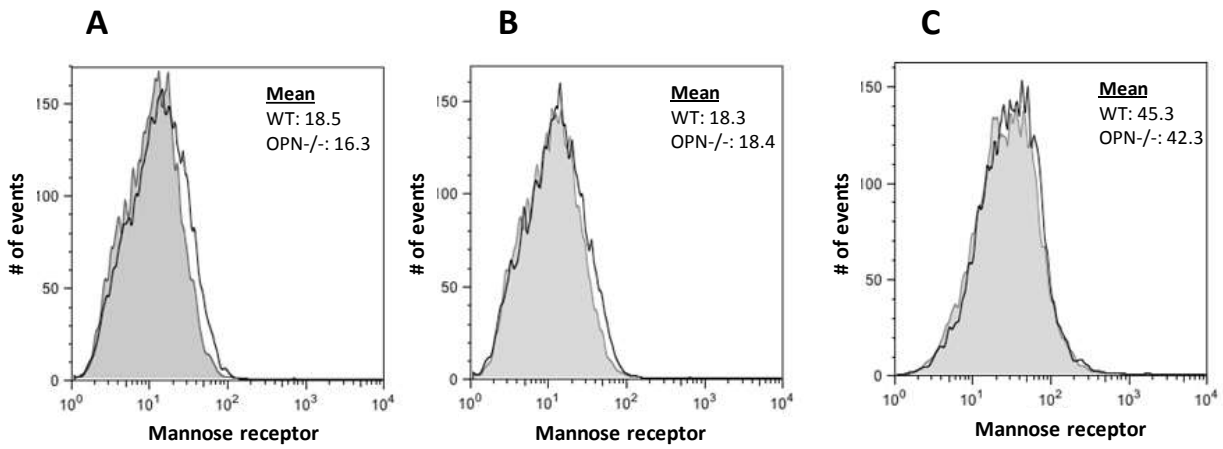

Figure 2.8: OPN deficiency does not affect mannose receptor expression.
WT and OPN-/- macrophages stimulated with media alone (**A**), IFN-γ + LPS (**B**), or IL-4 (**C**) for 24 hours and were analyzed for mannose receptor expression. Open histograms (black) represent WT macrophages and filled histograms (gray) represent OPN-/- macrophages.

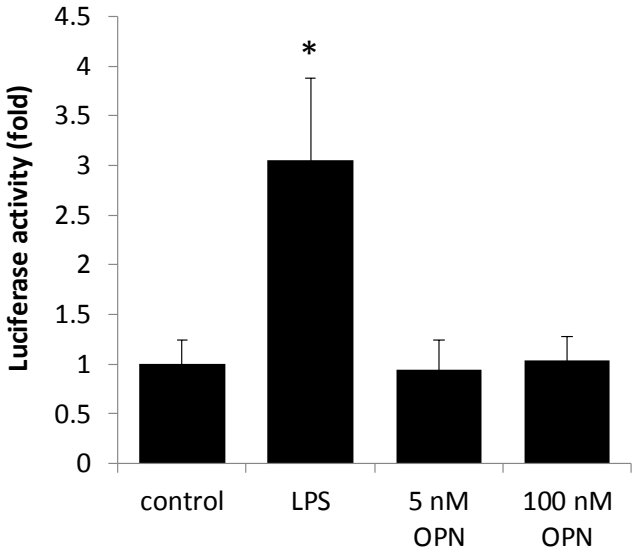

Figure 2.9: OPN does not induce NF-κB signaling in macrophages.
RAW264.7 cells were transiently transfected with a NF-κB reporter construct. Cells were co-transfected with a *Renilla* reporter construct to control for transfection efficiency. Transfected RAW264.7 cells were stimulated with LPS (100 ng/ml) or rmOPN for 6 hours. Cell lysates were collected and luciferase was measured. Data presented as mean ± SD. * p=0.001 vs unstimulated control cells.

Chapter 3

OPN promotes macrophage migration via integrins α_4 and α_9

3.1 Abstract

OPN is a potent macrophage chemoattractant, both *in vivo* and *in vitro*, and OPN expression is strikingly upregulated at sites of inflammation. Despite abundant evidence that OPN is critical for macrophage migration, little is known about the signaling pathways and cell surface receptors mediating these effects. In this chapter, we assessed integrin expression on primary BMDMs via flow cytometry and found that BMDMs express abundant levels of integrin α_4 with low levels of integrin α_V and α_9. We then define the integrins mediating macrophage migration to OPN. In a Transwell macrophage migration assay, we show that OPN induces macrophage migration via interactions with integrins α_4 and α_9 with little contribution of integrin from α_V. Finally, we observed that mammalian-derived OPN is chemotactic for macrophages, but bacterially-derived OPN is not, suggesting that post-translational modifications of OPN are necessary for macrophage migration

3.2 Introduction

3.2.1 Macrophage migration

Migration of leukocytes to sites of inflammation is crucial for the development of innate and adaptive immune responses. Cell migration is a highly orchestrated process that involves spatial and temporal integration of multiple steps (90). While cell migration is a complex process that varies among cell types, the cycle of cell migration can be described via five general steps: (1) cell polarization; (2) protrusion of the leading edge driven by actin polymerization; (3) integrin mediated adhesion of the protrusion to the ECM to generate necessary traction; (4) forward translocation of the cell body via actomyosin contraction; and (5) de-adhesion of the trailing edge of the cell.

Migration of macrophages is mediated by adhesion receptors that link the cell to extracellular matrix ligands, thereby providing the signals and forces necessary for migration. Many adhesion receptors participate in macrophage migration, including the integrin family. Integrins are heterodimeric transmembrane receptors that consist of one α and one β chain. Integrins possess a large extracellular domain that binds to ECM ligands and a short cytoplasmic domain. While integrins themselves lack catalytic activity, they are able to signal through interaction with adaptor molecules (91). Additionally, integrin binding to ligands can lead to confirmation changes and integrin clustering (92). This in turn initiates intracellular signals that regulate organization of the cytoskeleton and generates cell polarity necessary for migration (93).

3.2.2 OPN and macrophage migration

OPN is a potent macrophage chemoattractant *in vitro* (47, 59) and *in vivo* (53, 94) and expression of OPN is strikingly upregulated at sites of inflammation where it is localized in and around immune cells. *In vivo* studies suggest that OPN recruits macrophages to sites of inflammation in a variety of pathological conditions including atherosclerosis (56), rheumatoid arthritis (37, 38), granulomatous disease (57), and biomaterial implantation (58, 95).

In vitro, OPN-null macrophages have a selective defect in their ability to respond to chemotactic gradients. Macrophages deficient in OPN migrate normally to M-CSF (CSF-1), which signals through a tyrosine kinase receptor (Zhu 2004). However, OPN-null macrophages are impaired in their ability to migrate to MCP-1 and fMLP, which signal through G-protein coupled receptors (47, 96). Interestingly, this defect in migration to MCP-1 is not due to a decrease in expression of the MCP-1 receptor, CCR2, as studies show that OPN-null and WT macrophages express similar levels of this receptor (51). Additionally, OPN-null macrophages are more compact and extend fewer processes than WT macrophages (47). Plating of OPN-null macrophages on an OPN substratum was found to increase the formation of cell processes and modestly restored migration to MCP-1 (97). Thus, while it is well established that OPN promotes macrophage migration, the integrin receptors and intracellular signaling pathways that mediate this effect remain unknown.

3.2.3 OPN and integrins

OPN interacts with integrins via two main functional domains (see Figure 1.1), that are conserved among species. The adhesive RGD domain mediates interactions via $\alpha_V\beta_1$, $\alpha_V\beta_3$, $\alpha_V\beta_5$, $\alpha_V\beta_6$, $\alpha_8\beta_1$, and $\alpha_5\beta_1$ integrins (13-16). Immediately C-terminal to the RGD motif is the SVVYGLR (SLAYGLR in mouse) domain that mediates interactions with $\alpha_4\beta_1$, $\alpha_9\beta_1$, and $\alpha_4\beta_7$ integrins (17-19). Additionally, a second binding site for integrin $\alpha_4\beta_1$ has been described in human OPN, although this sequenced is not well conserved among species (20).

In this chapter we determine the integrin receptors responsible for macrophage migration to OPN and utilize flow cytometry to determine OPN receptor expression on primary BMDMs.

3.3 Materials and Methods

3.3.1 Cell culture

BMDMs were isolated from WT C57Bl/6 mice as described in Chapter 2.

3.3.2 Transwell macrophage migration assay

Macrophage migration assays were performed with WT BMDMs using 24-well Transwell inserts with 8 µm pore size polycarbonate membranes (6.5 mm insert, Costar, Corning, Lowell, MA). 2 x 10^5 BMDMs in RPMI containing 0.4% FBS were added to the upper chamber and incubated for 1 hour at 37°C to allow cells to attach. Chemoattractant media containing macrophage-colony stimulating factor (M-CSF, 1.32 nM, R&D Systems), recombinant human OPN (rhOPN bacterial, 5 µg/ml, bacterially derived), recombinant mammalian-derived human

OPN (rhOPN, 5 μg/ml, NSO-derived, R&D Systems), or recombinant mammalian-derived murine OPN (rmOPN, 5 μg/ml, NSO-derived, R&D Systems) in RPMI/0.4% FBS was then added to the lower chamber and cells were allowed to migrate for 8 hours. Non-migrating cells were removed from the upper surface of the insert using a cotton tipped applicator. Cells that had migrated to the lower surface of the insert were fixed with methanol and stained with May-Grunwald Giemsa stain (Sigma, St. Louis, MO) according to the manufacturer's directions. Migrating cells were manually counted per high-powered field (HPF). Five HPFs were counted per Transwell insert.

3.3.3 BAEC migration experiments

Transwell migration assays were performed as previously described (29). Briefly, polycarbonate Transwell inserts (8 μm, 6.5 mm insert) were coated with 1 μg/ml fibronectin in PBS overnight at 4°C. The next day filters were air dried. 5×10^4 bovine aortic endothelial cells in DMEM containing 200 μg/ml BSA were added to the upper chamber. Chemoattractant media containing recombinant human OPN (rhOPN bacterial, 50 nM, bacterially-derived as described in Chapter 2), or recombinant mammalian-derived OPN (rhOPN, 50 nM, NSO-derived, R&D Systems) in DMEM/200 μg/ml BSA was then added to the lower chamber and cells were allowed to migrate for 5 hours. Migration was assessed in the same manner previously described for BMDM migration assays.

3.3.4 Antibody blocking migration studies

To assess which integrins participate with OPN in macrophage chemotaxis, a series of antibodies known to bind and block selective integrins were used in the migration assays above. For these

blocking experiments, BMDMs were pre-incubated with neutralizing antibody to integrin α_4 (LEAF purified anti-mouse CD49d antibody (clone R1-2), BioLegend, San Diego, CA), integrin α_V (LEAF purified anti-mouse CD51 antibody ((clone RMV-7), BioLegend), non-immune rat IgG isotype control (BioLegend), or non-immune Armenian Hamster IgG isotype control (BioLegend) for 15 minutes at room temperature prior to plating and assessing migration to rmOPN. Armenian hamster anti-mouse integrin α_9 antibody (clone 55A2C) was a kind gift from Toshimistu Uede, Hokkaido Univeristy, Japan (98). 2×10^5 BMDMs in RPMI/0.4% FBS were added to the upper chamber and incubated for 1 hour at 37°C to allow cells to attach. Chemoattractant media containing mammalian recombinant murine OPN (rmOPN, 4 μg/ml, NSO-derived, R&D Systems) in RPMI/0.4% FBS was added to the lower chamber and migration was assessed as for previous assays.

3.3.5 Peptide blocking migration experiments

For migration experiments with blocking peptides, BMDMs were pre-incubated with cyclo(-RGDfK) peptide (Anaspec, San Jose, CA) or cyclo(-RADfK) control peptide (Anaspec) for 15 minutes at room temperature prior to plating. Migration to rmOPN was assessed as in antibody blocking experiments above.

3.3.6 Flow cytometric analysis of BMDM integrin expression

Integrin expression on BMDMs was tested by labeling WT BMDMs with rat anti-mouse α_4 integrin antibody (2.5 μg/ml, LEAF Purified anti-mouse CD49d antibody (clone R1-1), BioLegend), goat anti-mouse α_9 integrin antibody (5 μg/ml, R&D Systems), or rat anti-mouse α_v integrin antibody (2.5 μg/ml, LEAF Purified anti-mouse CD51 antibody (clone RMV-7),

BioLegend), followed by PE-donkey anti-rat or PE-donkey anti-goat antibody at a 1:200 dilution ($F(ab')_2$ fragment, Jackson Immunoresearch). Bone marrow was used as a positive control for integrin α_V staining. Bone marrow was isolated from the femur of a WT C57Bl6 mouse. Whole bone marrow was treated with ACK buffer (0.15 M NH_4Cl, 1 mM $KHCO_3$, 0.1 mM Na_2EDTA, pH 7.2-7.4) for 3 minutes at room temperature to lyse red blood cells prior to staining. Mouse smooth muscle cells were used as a positive control for integrin α_9 expression.

3.3.7 Statistics

One-way ANOVA with Tukey's post-hoc was used for comparison among multiple groups.

3.4 Results

3.4.1 BMDMs express primarily α_4 integrin

First, we determined the integrin expression profile on BMDMs via flow cytometry. BMDMs were stained with antibodies against integrin α_4, α_9, and α_V, the main OPN receptors. A high percentage of BMDMs expressed integrin α_4 (52.0 ± 13.0 %), with lower expression levels of integrin α_9 (11.0 ±3.6%), and relatively few cells expressed integrin α_V (4.5 ± 0.9%). Figure 3.1 shows representative flow cytometry data for integrin expression on BMDMs.

3.4.2 Post-translationally modified, but not bacterially-derived OPN, is chemotactic for murine BMDMs.

We then began studies to determine the functional domains of OPN responsible for macrophage migration to OPN by assessing migration to recombinant OPN structural mutants. As a pilot study we assessed the ability of our recombinant *E.coli*-derived OPN to promote macrophage

migration in a Transwell assay system. As seen in Figure 3.2, recombinant bacterially-derived human OPN (rhOPN bacterial, which lacks post-translational modifications was unable to induce macrophage migration. However, post-translationally modified recombinant mammalian-derived murine OPN (rmOPN) or human OPN (rhOPN) was chemotactic for macrophages. Similar migration was seen in response to either human or murine mammalian-derived OPN, suggesting that a species specific difference in amino acid sequence between human and murine OPN did not contribute to the difference in macrophage migration to bacterially-derived rhOPN. While the OPN protein is poorly conserved among species (63% human to mouse homology), the major functional domains are conserved. The bioactivity of bacterially-derived rhOPN was confirmed by its ability to induce migration of bovine aortic endothelial cells (BAECs) (29). Bacterially-derived rhOPN induced BAEC chemotaxis at similar levels to mammalian-derived OPN (Figure 3.2). Together these results indicate that post-translational modifications are necessary for OPN-mediated macrophage chemotaxis.

3.4.3 OPN promotes macrophage migration via α_4 and α_9 integrin

Results above indicate that it would not be feasible to use bacterially-derived OPN structural mutants to determine the OPN functional domains mediating macrophage migration. Thus, antibody blocking studies with WT BMDMs were employed to determine the receptors through which post-translationally modified OPN induces macrophage migration. BMDMs were pre-incubated with neutralizing antibodies against integrin α_4 or α_9 prior to plating on Transwell inserts and assessing migration to OPN. Neutralizing antibody against integrin α_4 or integrin α_9 completely inhibited migration to OPN, indicating that a α_4 and α_9 integrin-dependent pathway play a central role in OPN-induced migration in macrophages (Figure 3.3).

We then assessed the role of the RGD domain in macrophage migration to OPN. BMDMs were pre-incubated with either cyclo-RGD peptide or the control cyclo-RAD peptide prior to plating on Transwell inserts. Pre-incubation with RGD peptide did not affect macrophage migration to OPN compared to the RAD control peptide (Figure 3.4). Higher concentrations of RGD peptide (up to 500 uM) were assessed, but at this concentration the RAD peptide non-specifically inhibited macrophage migration (data not shown).

To further rule out possibility of the RGD domain mediating macrophage migration to OPN, we assessed the effects of an integrin α_V blocking antibody. As shown in Figure 3.5, pre-incubation of macrophages with an integrin α_V neutralizing antibody had no effect on macrophage migration to OPN even at doses as high as 10 μg/ml.

3.5 Discussion

In this chapter, we show that OPN-induced migration in macrophages is mediated by integrin α_4, with no apparent involvement of integrin α_V. Integrin α_4 is one of the major leukocyte receptors involved in adhesion to endothelial VCAM-1, thus regulating trafficking (99). At a cellular level, α_4 integrin promotes cell migration that is dependent on its cytoplasmic domain interaction with several adaptor molecules and the activation of the small GTPase Rac1 pathway and subsequent actin polymerization (100). Therefore, it is not surprising that α_4 integrin also mediates OPN-directed macrophage migration. The role of integrin α_9 in modulating macrophage function is less clear, however, recent data indicates that α_9 mediates macrophage and dendritic cell regulation of Th17 responses (101). Our integrin α_4 and α_9 migration data

further substantiates OPN structure-function studies showing that inhibition of monocyte migration to OPN can be blocked by interfering with the SLAYGLR sequence of OPN which has been shown to interact with α_4 and α_9 integrins (37, 38).

To complement our macrophage migration experiments, we also assessed integrin expression on BMDMs via flow cytometry. BMDMs expressed abundant levels of integrin α_4 and much lower levels of α_9. Surprisingly, BMDMs expressed little integrin α_V. These results are in agreement with those of Shima et al. who showed that differentiation with M-CSF leads to increased expression of integrin α_4 on BMDMs (102). Additionally, a recent study shows that synovial macrophages from arthritic mice express high levels of integrin α_4 as well as some expression of integrin α_9 (98).

Additionally, we observed that macrophage migration to OPN requires post-translational modifications of the protein, as mammalian-derived OPN promoted macrophage chemotaxis, while bacterially-produced OPN did not. These results are distinct from those for endothelial cells in which both bacterially-derived and mammalian-derived OPN induce migration (29). In this regard, post-translational modifications may represent a mechanism to regulate the biological activity of OPN and the cells it targets. Indeed, in some cases, post-translational modifications of OPN have been shown to tightly regulate function. Studies by Razzouk et al., showed that phosphorylation of OPN is required for bone resorption by osteoclasts, but not for osteoclast adhesion (103). Phosphorylation of OPN is markedly heterogeneous. Despite the fact that OPN forms from different sources contain similar numbers of potential phosphorylation sites, actual phosphorylation levels vary greatly between OPN from different origins (104). A

comparison by Christensen et al. of OPN produced by two different sources highlights this difference: *ras*-transformed fibroblasts produced OPN containing only four phosphate groups, while osteoblast-produced OPN contained 21 phosphates (105). Differences in both the PTMs of OPN produced by various cell types and variations in target cell receptor repertoire may be important in determining OPN signaling, thereby modulating the response in a given cell type.

At this time it is unknown which post-translational modifications of OPN are necessary for macrophage migration. OPN is subject to extensive post-translational modifications including phosphorylation, glycosylation, sulfation, and transglutamination (42-44). Of these post-translational modifications, phosphorylation has been most extensively studied. Indeed, phosphorylation of OPN may be critical for macrophage migration, as phosphorylation of OPN is necessary for the haptotactic migration of osteoclasts, which share a common myeloid progenitor with macrophages (106).

3.6 Conclusions

OPN has long been known to be a potent macrophage chemoattractant and has been shown to mediate macrophage recruitment in numerous models of acute and chronic inflammation (61). However, the OPN functional domains and macrophage surface receptors mediating macrophage migration have remained unexplored. In this chapter, we utilized an *in vitro* Transwell migration assay system to show that OPN-mediated macrophage migration requires post-translational modifications, as mammalian-derived OPN was chemotactic for macrophages while bacterially-produced OPN was not. Further, using a Transwell migration assay and neutralizing antibodies, we demonstrate that OPN interacts with integrin α_4 and α_9 on macrophages to induce chemotaxis

to OPN. Surprisingly, neither neutralizing antibody against integrin α_V or cyclo-RGD peptide affected OPN-directed macrophage migration. Finally, we assayed integrin expression profile on bone marrow derived macrophages. BMDMs expressed primarily integrin α_4, with lower levels of α_9 and very little expression of α_V.

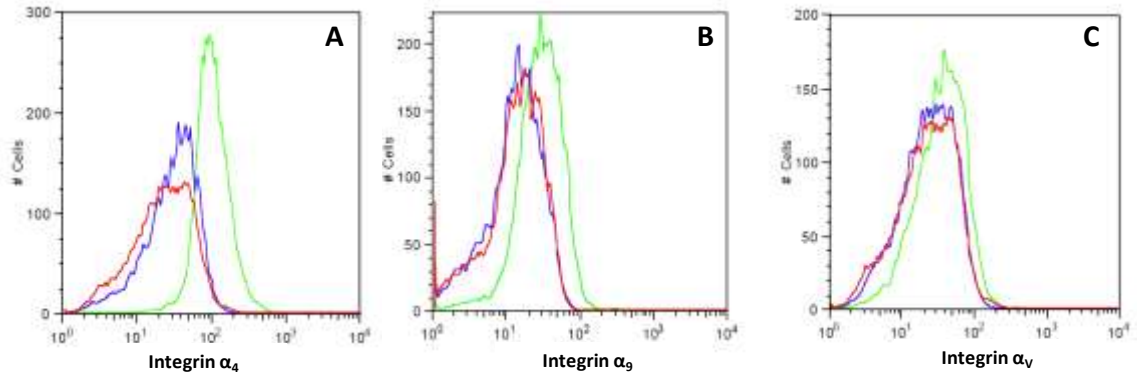

Figure 3.1: Bone marrow derived macrophages express primarily integrin α_4.
WT BMDMs were analyzed for integrin expression by flow cytometry. BMDMs were stained for integrin α_4 **(A)**, integrin α_V **(B)**, or integrin α_9 **(C)**. Blue histograms represented unstained cells, red histograms represent cells stained with isotype control antibody, and green histograms represent cells stained with antibodies against the specified integrin. Data is representative of 3-4 individual experiments.

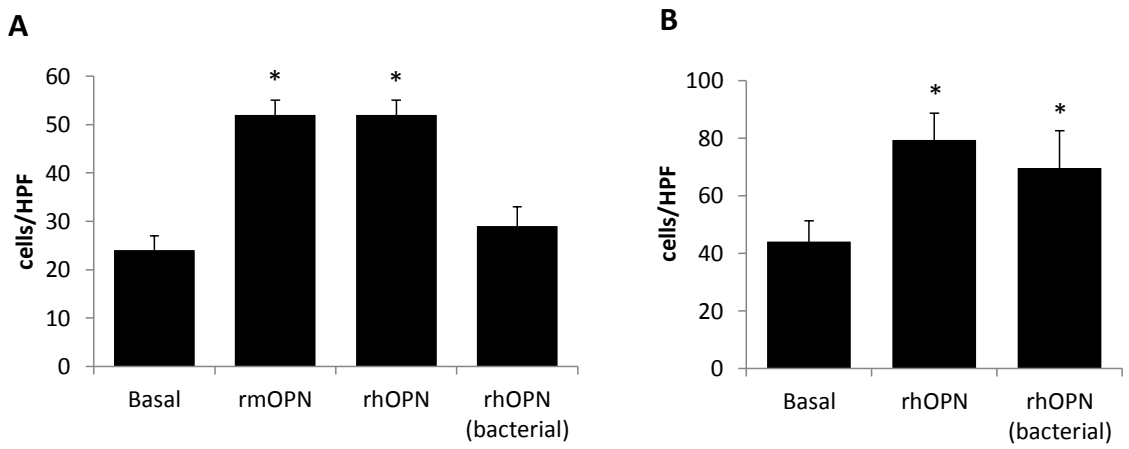

Figure 3.2: Post-translationally modified OPN is a potent macrophage chemoattractant. **(A)** Migration of WT BMDMs to OPN was determined using a Transwell migration assay. BMDMs were plated on 8 μm-pore size Transwell inserts and migration to recombinant mammalian-derived human OPN (rhOPN, 5 μg/ml), recombinant mammalian-derived mouse OPN (rmOPN, 5 μg/ml), and recombinant bacterially-derived OPN (rhOPN bacterial, 5 μg/ml) was determined. Data is expressed as cell number per high power field (HPF) ± SEM. **(B)** Migration of bovine aortic endothelial cells (BAECs) to OPN was determined. BAECs were plated on fibronectin-coated Transwell inserts and migration to recombinant mammalian-derived human OPN (rhOPN, 50 nM) and recombinant bacterially-derived human OPN (rhOPN bacterial, 50 nM) was determined. Data expressed as cells/HPF ± SD. *$p<0.05$ vs basal.

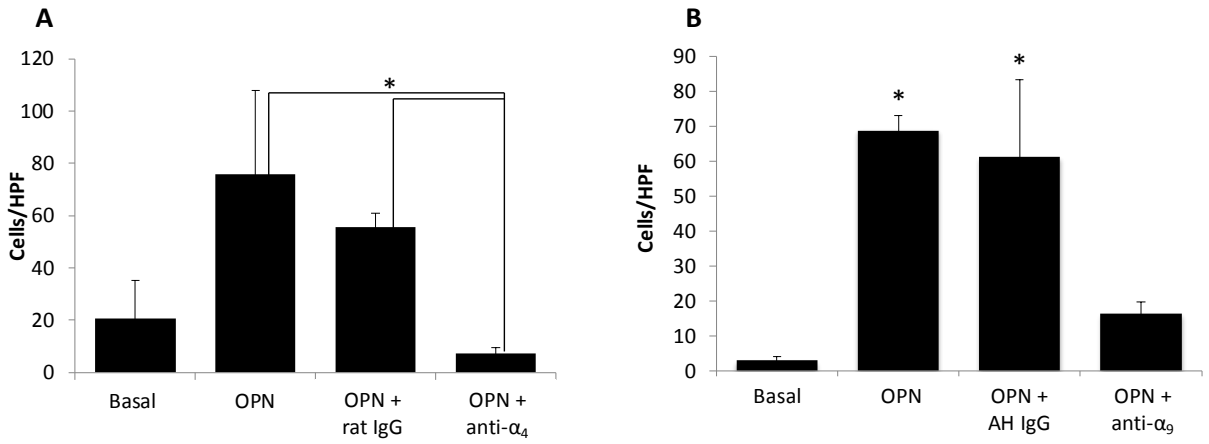

Figure 3.3: OPN promotes macrophage migration via integrin α_4 and α_9.
(A) WT BMDMs were pre-incubated with 1 μg/ml α_4 integrin neutralizing antibody or control rat IgG prior to assessing migration to OPN in a Transwell migration assay. Data expressed as cell number per high power field (HPF) ± SD of triplicate wells representative of three independent experiments. * $p < 0.05$. **(B)** BMDMs were pre-incubated with anti-integrin α_9 antibody or Armenian Hamster IgG isotype control (AH IgG) prior to assessing migration to OPN in a Transwell migration assay. Data expressed as cells/HPF ± SEM. *$p<0.05$ compared to basal and OPN + anti-α_9.

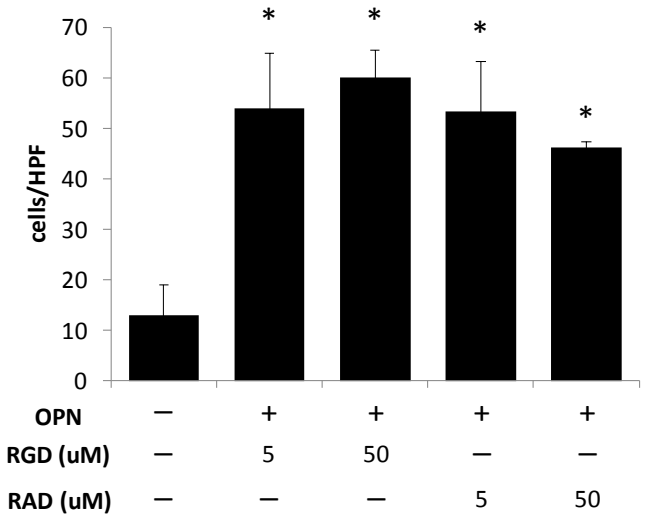

Figure 3.4: The RGD functional domain does not mediate macrophage migration to OPN. WT BMDMs were pre-incubated with cyclo-RGD peptide or cyclo-RAD control peptide prior to assessing migration to OPN in a Transwell migration assay. Data expressed as cell number per high power field (HPF) ± SD. *$p<0.05$ vs basal.

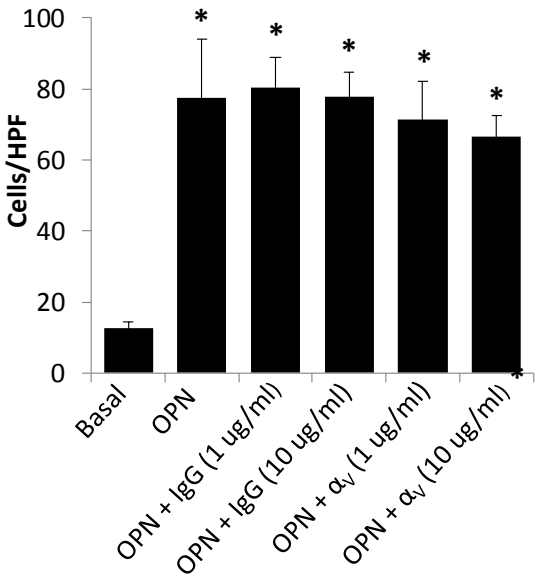

Figure 3.5: Integrin α_V does not mediate macrophage migration to OPN.
WT BMDMs were pre-incubated with 1 μg/ml α_V integrin neutralizing antibody or control rat IgG prior to assessing migration to OPN in a Transwell migration assay. Data are expressed as cell number per high power field (HPF) ± SD of triplicate wells. * $p < 0.05$ vs basal. Data from a single experiment only.

Chapter 4

The role of OPN functional domains in acute and chronic inflammation *in vivo*

4.1 Abstract

OPN is highly expressed by infiltrating leukocytes at sites of acute and chronic inflammation. Functional inhibition and genetic ablation of OPN in mice greatly impairs macrophage recruitment in several models of acute inflammation. Deficits in macrophage accumulation have also been noted in OPN-null mice when challenged with chronic inflammatory conditions, including atherosclerosis, delayed-type hypersensitivity, granulomatous disease, and biomaterial implantation. These data suggest that OPN may be particularly important in promoting migration and retention of macrophages at sites of acute and chronic inflammation. However, it is unknown which OPN functional domains mediate leukocyte accumulation in response to inflammation. In this chapter, we explore the relative contributions of the RGD and SLAYGLR functional domains of OPN in macrophage-mediated inflammation *in vivo*. To this end, we created chimeric mice expressing OPN structural mutants specifically from macrophages. In sterile thioglycollate-elicited peritonitis, a model of acute inflammation, we show that mutational inactivation of SLAYGLR domain results in decreased leukocyte accumulation due to reduced macrophage accumulation. Surprisingly, expression of OPN specifically from macrophages resulted in a striking increase in neutrophil accumulation in response to thioglycollate. Additionally, we tested the relative contributions of the RGD and SLAYGLR domains in the PVA sponge implantation model of chronic inflammation. In contrast to previous reports, we

found no differences in between WT and OPN-null mice in terms of macrophage accumulation in PVA sponge implants or the formation of foreign body giant cells. Consequently, mutational inactivation of the RGD or SLAYGLR domain had no effect on the host response to biomaterial implantation.

4.2 Introduction

4.2.1 OPN mediates macrophage recruitment in response to inflammation

In response to inflammation, the host responds with an orchestrated series of events. Neutrophils are rapidly recruited to sites of acute inflammation and dominate the initial influx of leukocytes (107). Later in inflammation, monocytes/macrophages replace neutrophils as the predominant cell type. Macrophages play a central role in the inflammatory response, releasing cytokines that control key events in the initiation, resolution, and repair processes (108). In chronic inflammation the sustained recruitment of monocytes/macrophages has been associated with disease, emphasizing the importance of understanding mechanisms involved in macrophage recruitment.

OPN plays a pivotal role in the development of immune responses. OPN is strikingly upregulated at sites of inflammation where it is localized in and around immune cells. In many inflammation models the formation of granulation tissue and the intensity of the inflammatory reaction are reduced in the absence of OPN (61). However, the OPN functional domains mediating macrophage recruitment remains unexplored. OPN interacts with integrins via two main functional domains: the RGD and the SLAYGLR domain. The RGD domain mediates interactions with α_v-containing integrins, including $\alpha_v\beta_3$, $\alpha_v\beta_5$, $\alpha_v\beta_1$, $\alpha_v\beta_6$ as well as $\alpha_8\beta_1$, and $\alpha_5\beta_1$

(13-16). Immediately C-terminal to the RGD domain is the SLAYGLR domain, which facilitates binding to $\alpha_4\beta_1$, $\alpha_4\beta_7$, $\alpha_9\beta_1$ (17-19). Studies investigating the chronic inflammatory response associated with atherosclerosis suggest that integrin α_4 is important for early macrophage accumulation in atherosclerotic lesions (109). Furthermore, work presented in the previous chapter indicates that OPN interacts with macrophages via integrins α_4 and α_9 to promote macrophage migration. Unpublished data from our lab demonstrated that OPN promotes macrophage survival, also via an integrin α_4 mediated pathway. Consequently, we hypothesized that OPN interacts with macrophages via the SLAYGLR functional domain to promote macrophage accumulation in acute and chronic inflammation *in vivo*.

4.2.2 Thioglycollate elicited peritonitis

In this chapter, we utilize sterile thioglycollate elicited peritonitis as a model of acute inflammation. Administration of thioglycollate produces time-dependent leukocyte accumulation in the peritoneal cavity, which follows the typical profile of an acute inflammatory response (110). At steady state, resident peritoneal macrophages are present in the peritoneum (111). Following the injection of thioglycollate, resident macrophages disappear by adhering to the peritoneal lining in a process termed the macrophage disappearance reaction (112). Simultaneously, neutrophils accumulate in the cavity followed by the subsequent appearance of macrophages (113). Macrophages reach maximum numbers at 72 hours and remain at this level for at least 96 hours post-thioglycollate elicitation (114). OPN plays a pivotal role in orchestrating the inflammatory response to thioglycollate as OPN-null mice display reduced leukocyte accumulation in the peritoneal cavity following the injection of thioglycollate (51). Thioglycollate elicited peritoneal macrophages also have decreased viability as measured by

Annexin V staining and caspase-3 activation. Further, co-injection of recombinant OPN at the time of thioglycollate elicitation was able to rescue OPN-null leukocytes from apoptosis.

4.2.3 The foreign body response

To determine the role of the RGD and SLAYGLR functional domains in chronic inflammation, we used biomaterial implantation as an experimental model of chronic inflammation. The foreign body reaction to implanted biomaterials begins almost immediately following implantation of foreign materials with the non-specific adsorption of proteins to the biomaterial surface (115). Following blood-biomaterial interactions, platelets release growth factors that stimulate inflammatory cell infiltration (116). Neutrophils are the first cells to arrive at the implant, followed shortly by macrophages. Neutrophils predominate during the first few days of the inflammatory response, but these cells are short lived and monocytes/macrophages eventually become the predominant cell type (117). The recruitment of macrophages to the implant site promotes the production of additional chemoattractants, thereby amplifying the response. Macrophages unsuccessfully attempt to phagocytose the implant and fuse to form multinucleated foreign body giant cells (118). In the final stage of the foreign body reaction, a fibrotic response occurs in which fibroblasts proliferate and deposit collagen leading to the formation of a foreign body capsule isolating the implant from the surrounding tissue. Encapsulation generally occurs around 3-4 weeks post-implantation (119).

Previous studies in our lab showed that OPN plays a critical role in the foreign body response. When porous PVA sponges were implanted in wild type and OPN-null littermates, significantly fewer macrophages accumulated in and around the PVA sponges in OPN-null mice (58). Surprisingly, despite the deficit in macrophage recruitment, more foreign body giant cells

(FBGC) formed at the surface of implants in OPN-null mice. Further, *in vitro*, in a human FBGC formation assay, OPN inhibited macrophage fusion in a dose-dependent manner. Similar results were observed in studies in which glutaraldehyde-fixed porcine aortic valve leaflets (GFAV) were implanted in mice. A 50% decrease in macrophage accumulation was seen in GFAV implants in OPN-/- mice compared to WT controls (2). OPN's ability to inhibit FBGC formation is unique, as most other molecules studied increase, facilitate, or are required for macrophage fusion. In addition to OPN, the tetraspanins, CD9 and CD81, and the CD44 ligands, hyaluronic acid and chondroitin sulfates are known inhibit FBGC formation (120, 121).

4.3 Materials and Methods

4.3.1 Mice

OPN-null mice were generated on a C57Bl/6 background as previously described (77). Wild type C57Bl/6 mice were purchased from The Jackson Laboratory. Mice were age-matched for the thioglycollate-elicited peritonitis and PVA sponge implantation experiments. All animal experiments were approved by the University of Washington Animal Care and Use committee and followed federal guidelines for the use and care of laboratory animals.

4.3.2 CD68S-based retroviral constructs

All constructs were generated using standard molecular biology techniques and were confirmed by restriction digest analysis and DNA sequencing. Mutations in the RGD and SLAYGLR functional domains of OPN were generated in the retroviral expression plasmid pBMN-IRES-Puro-OPN (122) using the Stratagene QuikChange II XL site-directed mutagenesis kit following

the manufacturer's directions. The pBMN-IRES-Puro-OPN vector contains a 1097-bp fragment spanning the region of -18 to +1079 of mouse OPN cDNA (NM_009263). The primers used for mutagenesis were as follows: RGD→RAD, 5'-CCCAACGGCCGAGCTGATAGCTTGGCT-3', and SLAYGLR→SLAAGLR, 5'-GGCCGAGGTGATAGCTTGGCTGCTGGACTGAGGT-3'. Nucleotides changed relative to the sequence of wild-type OPN cDNA are underlined. For the RAD SLAAGLR double mutant, the SLAAGLR mutation was introduced and a subsequent round of site-directed mutagenesis was performed to introduce the RAD mutation.

To provide macrophage-specific expression, OPN cDNA fragments were cloned into the LZRS-CD68S-HA-EGFP vector (Figure 4.1) (123). This vector incorporates a 342-bp fragment of the 5' flanking region from the human CD68 gene in addition to the CD68 first intron to drive macrophage-specific transgene expression. OPN PCR fragments were generated with NotI sites and cloned into the LZRS-CD68S-HA-EGFP vector that was NotI to remove the HA-EGFP cDNA gene. The LZRS-CD68S-HA-EGFP vector was used as a vector control for *in vivo* studies.

4.3.3 Generation of chimeric mice

Bone marrow transduction and transplantation were performed as previously described (123). Briefly, plasmid DNA was used to transfect the ecotropic Phoenix packaging cell line using calcium phosphate-mediated transfection. High titer retroviral supernatant was produced by selection of transfection Phoenix cells in medium containing puromycin (2 μg/ml). Bone marrow cells were isolated from OPN-null donor mice that had been injected intraperitoneally with 300 ul of 5-fluorouracil (10 mg/ml) three days prior to bone marrow isolation. Bone

marrow cells were then cultured for 48 hours in complete stem cell medium (DMEM with 15% FBS and stem cell factor (100 ng/ml), IL-3 (10 ng/ml), and IL-6 (20 ng/ml)) to stimulate proliferation. Cells were then transduced for 48 hours using retroviral supernatants supplemented with 50 mM HEPES, 4 μg/ml polybrene, and stem-cell factor, IL-3, and IL-6 at the previously mentioned concentrations in fibronectin-coated dishes. Fibronectin-coated dishes were created by coating each well of a 6-well tissue culture plate with 1 ml of human plasma fibronectin (Gibco/Invitrogen, endotoxin-free) at 25 μg/ml in PBS overnight at 4°C. After transduction, cells were harvested and injected intravenously into OPN-null recipient mice. Male recipient mice were lethally irradiated 24 hours prior to transplantation with 10.5 Gy. Mice were housed for 4-6 weeks following transplantation to allow for reconstitution of monocytes/macrophages.

4.3.4 Thioglycollate-elicited peritonitis

Animals for the thioglycollate elicited peritonitis model were between 17-20 weeks of age. Mice were injected intraperitoneally with 1.0 ml of thioglycollate (3% solution, BD BBL, 221199) to induce thioglycollate-elicited peritonitis. After 72 hours, mice were euthanized by CO_2, and peritoneal leukocytes were harvested by peritoneal lavage. Peritoneal lavage was performed by injecting 5 ml of ice-cold PBS/5 mM EDTA intraperitoneally into mice, the abdomens were massaged, and the fluid was withdrawn. Up to 4.0 ml of fluid was recoverable. Peritoneal lavages containing red blood cell contamination were excluded from analysis. Lavage fluid was diluted in trypan blue and cell concentration was determined by manual counting using a hemocytometer. For analysis of cell composition, peritoneal leukocytes were analyzed by flow cytometry. Peritoneal leukocytes were labeled with PE-conjugated primary antibodies against

CD115 (macrophages, eBioscience 12-1152), CD3 (T cells, BD Biosciences, 555275), CD11b (BD Biosciences, 553311), B220 (B cells, BD Biosciences, 553089), Ly6G (neutrophils, BD Biosciences, 551461), rat IgG2b (isotype control, eBioscience, 12-4371), or rat IgG2a (isotype control, eBioscience, 12-4031). For staining, peritoneal leukocytes were washed 2x in FACS staining buffer (PBS/1% FBS/0.09% sodium azide) and 0.5 x 10^6 cells were resuspended in 100 ul FACS buffer with 1 µl BD Mouse Fc Block (rat anti-mouse CD16/CD32, BD Biosciences, 553142, 0.5 mg/ml). Cells were incubated at 4°C for 5 minutes to block FcγRII/III receptors. PE-conjugated primary antibodies (0.06 µg per tube) were then added directly to the pre-incubated cells in the presence of Mouse Fc Block and incubated on ice for 30 minutes. Cells were then washed 2x in FACS staining buffer and fixed in 4% paraformaldehyde for 20 minutes at 4°C. Following fixation, cells were washed 2x in FACS staining buffer and stored at 4°C until analysis. Cells were analyzed on a BD FACscan flow cytometer and data was analyzed with FloJo software.

4.3.4.1 OPN quantification in peritoneal lavage fluid

To quantify OPN levels, peritoneal lavage fluid was centrifuged to remove cells and lavage fluid was aliquoted and stored at -20°C until analysis. OPN concentration in peritoneal lavage fluid was determined using the Mouse Osteopontin DuoSet (R&D Systems, DY441) following the manufacturer's directions.

4.3.5 PVA sponge implantation

Porous PVA sponges (6 mm diameter, 1 mm thickness, PVA Unlimited) were implanted subcutaneously in the dorsa of mice. Prior to implantation, PVA sponges were ethylene oxide

sterilized and tested for endotoxin using the Pyrogent® Plus Gel Clot LAL assay (0.06 EU/ml sensitivity, Lonza) following the manufacturer's directions. All PVA sponges tested negative for endotoxin (<0.06 EU/ml endotoxin). Mice were anesthetized with isofluorane and a one-inch incision was made on the central dorsal surface. A small subcutaneous pocket was made on either side of the incision and one PVA sponge was inserted into each pocket. Two weeks after implantation, mice were euthanized and sponges were carefully explanted. Explanted sponges were fixed in modified methyl carnoys (3:1 methanol: acetic acid) for 4 hours and then transferred to 70% ethanol until processed. Each group consisted of 6 mice per OPN construct. This sample size was chosen based on power analysis of previously published data (Tsai 2005).

4.3.6 Histology and FBGC quantification

To ensure sections were taken from the same location in each implant, each sample was cross-sectioned at the centerline and embedded in paraffin with the interior facing down. 5 µm sections were cut and slides were baked at 60°C for 30 min. Sections were stained with hematoxylin and eosin using the progressive method of staining and analyzed by brightfield microscopy (Nikon E800 upright microscope, Nikon USA, Melville, NY). A total of 12 fields of view per sponge were chosen and giant cells per field were counted manually. FBGCs were defined as cells containing 3 or more nuclei.

4.3.7 Immunohistochemistry

Macrophages were detected using the monoclonal anti-murine pan macrophage antibody BM8, (F4/80, eBioscience) at 6 µg/ml. Normal rat IgG2a (eBioscience) was used as an isotype control to confirm specificity of staining. For immunohistochemical staining, slides were baked,

deparaffinized in xylene, and rehydrated to PBS. Slides were incubated in 0.3% hydrogen peroxide in methanol for 10 minutes to quench endogenous peroxidases. Slides were then washed in PBS and avidin and biotin blocking was carried out using an Avidin/Biotin Blocking Kit following the manufacturer's recommendations (Vector Laboratories). Slides were rinsed in PBS and incubated in 4% normal rabbit serum/0.25% BSA in PBS for 30 minutes. Sections were then incubated with primary antibody in 2% normal rabbit serum/0.25% BSA in PBS for 1 hour. Sections were washed and incubated with biotinylated rabbit anti-rat IgG secondary antibody (Vector Laboratories, #BA-4001, 0.5 mg/ml) at a 1:500 dilution in 2% normal rabbit serum/0.25% BSA in PBS for 30 minutes. Sections were washed again and incubated with a streptavidin-peroxidase complex (Vectastain ABC Kit, Vector Laboratories) for 30 min. Slides were developed for 2 minutes with SigmaFast DAB (Sigma). Slides were rinsed, dehydrated, and coverslipped with Permount (Fisher Scientific). In some cases slides were counter-stained with methyl green before dehydration. A total of 9 fields per view were imaged per sponge. The percent area that stained positively for BM8 was quantified using ImageJ analysis software.

4.3.8 Statistics

Unpaired two-tailed student's t-test was used for comparison between pairs. One-way ANOVA with Tukey's post-hoc was used for comparison among multiple groups.

4.4 Results

4.4.1 OPN deficiency results in decreased macrophage accumulation in response to acute inflammation

As a preliminary step, we confirmed and expanded on the finding of Bruemmer et al, that OPN deficiency results in decreased leukocyte accumulation in thioglycollate elicited peritonits. WT and OPN-null mice were injected intraperitoneally with thioglycollate and 72 hours later peritoneal exudates were harvested by peritoneal lavage and leukocyte accumulation was determined by manual counting. Peritoneal lavages from OPN-null mice contained significantly fewer cells compared to WT mice (Figure 4.2). In WT mice, leukocyte accumulation in response to thioglycollate was accompanied by a striking increase in OPN levels in the peritoneal lavage fluid. Lavage fluid from unelicited mice contained ~0.264 ng/ml OPN (n=2), while at 72 hours post-thioglycollate injection OPN levels had increased more than 600-fold, reaching 170 ± 144 ng/ml (n=5).

Next, the effect of OPN deficiency on the cellular composition of the peritoneal exudates was quantified. Peritoneal leukocytes were stained with cell surface markers and analyzed by flow cytometry. Cells were stained for CD11b, CD115 (macrophages), Ly6G (neutrophils), B220 (B-cells), or CD3 (T-cells). The reduction in peritoneal leukocytes seen in OPN-null animals was largely accounted for by a decrease in the number of macrophages with little change in the total number of T-cells, B-cells, or neutrophils (Figure 4.3A). In OPN-null mice the decrease in the number of macrophages resulted in an increase in the relative proportion of neutrophils and T-cells, such that the relative composition of peritoneal leukocytes was altered (Figure 4.3B).

4.4.2 Creation of chimeric mice expressing OPN structural mutants

Having established that OPN deficiency decreases macrophage accumulation in thioglycollate elicited peritonitis, we then explored the OPN functional domains mediating leukocyte recruitment in this model. For these studies, we focused on the effects of the two major OPN functional domains; the adhesive RGD domain and the SLAYGLR functional domain. To address the contributions of each domain to leukocyte accumulation, we created retroviral constructs expressing full-length wild type mouse OPN or OPN structural mutants in which the RGD, SLAYGLR, or both functional domains were inactivated (Figure 4.4). These constructs were cloned into a retroviral vector in which the gene of interest is under control of the CD68 promoter thereby restricting expression to macrophages (123). Key features of the macrophage-specific CD68S retroviral vector are shown in Figure 4.1. This retroviral vector has been shown to generate stable, therapeutically relevant levels of transgene expression for at least 16 weeks *in vivo* (123). Retroviral constructs were then used to transfect OPN-/- hematopoietic stem cells that were transplanted into OPN-null mice, thereby generating chimeric mice expressing OPN structural mutants. An outline of the retroviral transduction and bone marrow transplantation scheme is shown in Figure 4.5.

4.4.3 CD68S constructs provide high transgene expression

To determine transfection efficiency in our chimeric mice, peritoneal leukocytes from mice transplanted with a CD68S control vector expressing enhanced green fluorescent protein (eGFP) were analyzed for GFP expression by flow cytometry. A high percentage of peritoneal leukocytes were eGFP positive (51.4% ± 6.9%), indicating high transfection efficiency of

hematopoietic stem cells with little variation between mice. Figure 4.6 shows representative eGFP expression via flow cytometry.

4.4.4 Chimeric mice express high levels of OPN

We confirmed expression of OPN from our chimeric mice expressing OPN specifically from macrophages. Chimeric mice were injected with thioglycollate to induce leukocyte migration to the peritoneal cavity and 72 hours later peritoneal lavage fluid was harvested and OPN levels were analyzed by ELISA. As shown in Figure 4.7, the CD68S retroviral vector provided high levels of OPN expression in OPN-null chimeric mice transplanted with the CD68S retroviral vector encoding WT OPN. As a control, thioglyocllate elicited peritoneal lavage fluid was collected from WT mice and OPN levels were similar.

4.4.5 Mutational inactivation of the SLAYGLR domain results in decreased leukocyte accumulation in thioglycollate-elicited peritonitis

Having established that our chimeric mice expressed the OPN transgene, we then analyzed leukocyte accumulation in response to inflammatory stimuli. Animals were injected with thioglycollate intraperitoneally and 72 hours later peritoneal leukocytes were obtained by lavage. Peritoneal exudates from chimeric OPN-null mice expressing OPN from macrophages (OPN) tended to contain more cells than peritoneal exudates from mice expressing the eGFP control (eGFP), although this result was not statistically significant (Figure 4.8). Inactivation of the SLAYGLR functional domain (SLAAGLR) decreased cell recruitment in response to thioglycollate while mutation of the RGD domain (RAD) had no effect.

4.4.6 The SLAYGLR domain mediates macrophage accumulation in response to acute inflammatory stimuli

Next, to determine whether or not inactivation of the RGD or SLAYGLR functional domains affected the cellular composition of the peritoneal lavage fluid, peritoneal exudates were analyzed by flow cytometry. No differences in the total numbers of CD3- or B220-positive cells were observed between groups (Figure 4.10). However, peritoneal exudates from wild-type mice (WT) contained significantly high numbers of CD115-positive cells compared to OPN-null mice expressing the eGFP control (eGFP) (Figure 4.9). Reconstitution of OPN in macrophages in OPN-null mice (OPN) restored CD115-positive cells to the WT level. Mutational inactivation of the RGD domain had no effect on macrophage accumulation, while inactivation of the SLAYGLR domain resulted in reduced accumulation of CD115-positive cells.

Interestingly, expression of OPN specifically from macrophages resulted in a dramatic increase (4-fold) in the number of Ly6G-positive cells that accumulated in the peritoneal cavity, compared to WT mice and to OPN-null chimeric mice expressing the eGFP control vector. Mutational inactivation of the RGD domain had no effect, while inactivation of the SLAYGLR domain resulted in a slight, though non-significant reduction.

4.4.7 PVA sponge model

With the finding that the SLAYGLR domain of OPN mediates macrophage accumulation in response to acute inflammatory stimuli, we then asked whether mutation inactivation of the RGD or SLAYGLR domain would affect macrophage accumulation in a murine model of chronic inflammation. To this end, porous polyvinyl alcohol (PVA) sponges were implanted

subcutaneously in chimeric mice expressing OPN structural mutants. Implants were allowed to heal for two weeks and then were explanted, fixed, and sectioned for analysis. In all animals, a robust foreign body reaction was induced by PVA sponge implantation. The host response was characterized macrophage infiltration into the PVA sponge and formation of foreign body giant cells at the surface of the implant.

4.4.8 OPN deficiency does not affect macrophage recruitment at the implant site

We first examined the effect of the RGD and SLAYGLR functional domains of OPN on macrophage accumulation in response to PVA sponge implantation. PVA sponge sections were stained with the pan-macrophage antibody BM8, which detects the F4/80 antigen. Figure 4.11A shows representative macrophage accumulation in porous PVA sponges. In each section, a total of nine fields of view were imaged, with three random fields of view selected on the muscle side of the implant, three from the interior of the implant, and three on the skin side of the implant. The percent area stained positive for BM8 was quantified using ImageJ software. In contrast to previous reports, no difference was seen in macrophage accumulation between WT and OPN-null mice expressing the eGFP control vector (Figure 4.11B-D).

4.4.9 OPN deficiency does not affect foreign body giant formation at the implant site

We then determined if mutational inactivation of the RGD or SLAYGLR functional domains of OPN influenced the propensity of macrophages to form foreign body giant cells at the surface of implanted PVA sponges. Sections of implanted PVA sponges were stained with hematoxylin and eosin, and foreign body giant cells were manually counted in twelve total fields of view per section. FBGCs were defined as cells containing 3 or more nuclei. As shown in Figure 4.12A,

FBGCs formed in close association with the surface of the PVA sponge implant. In contrast to previously published data no difference was seen in FBGC formation between WT and OPN-/- mice expressing the eGFP vector control (Figure 4.12B-D). However, fewer FBGCs formed at the surface of the implant in the interior of the implant in mice expressing the SLAAGLR structural mutant compared to WT mice (Figure 4.12 C). Additionally, statistically fewer FBGCs were formed on the skin side surface of implants in mice expressing the RAD construct compared to either the WT OPN construct or the RAD/SLAAGLR double mutant (Figure 4.12D).

4.4.10 Neutrophil score

While quantifying FBGC formed at the surface of the implant, it was noted that there was some variability in the accumulation of neutrophils at the PVA sponge implant. Based on the increased number of neutrophils seen in the thioglycollate elicited peritonitis model in OPN-null mice expressing OPN specifically from macrophages we questions whether the increased neutrophils were associated PVA sponges implanted in chimeric mice expressing OPN. PVA sponge sections were scored from 1-4 for neutrophil infiltration by a blinded observer with 0 indicating no neutrophils present to 4 corresponding to higher neutrophil infiltration. As shown in Figure 4.13, there was no difference in neutrophil score between chimeric mice expressing the eGFP control vector and those expressing OPN.

4.5 Discussion

The work in this chapter corroborates and expands upon previous work defining the role of OPN in the thioglycollate elicited peritonitis model of acute inflammation. In confirmation with

previous reports, we show that OPN deficiency results in decreased leukocyte accumulation in the peritoneal cavity in response to acute inflammation. In contrast to Bruemmer et al. who concluded that this decrease in leukocyte accumulation was due to a general decrease in accumulation of all cell types rather than a difference in cellular composition, we show that this decrease is largely due to reduced macrophage accumulation. This difference is attributable to the difference in markers used to identify macrophages. Studies of the expression of surface receptors with monoclonal antibodies have shown that tissue macrophages are markedly heterogeneous (124). The heterogeneity of macrophages reflects the specialized functions of macrophages within a particular microenvironment. In the previous report, Mac-1 was used as a macrophage marker, whereas we used CD115, the M-CSF receptor to identify macrophages. Mac-1 is a complement receptor (CR3) consisting of CD11b and CD18 (also known as integrin $\alpha_M\beta_2$). While Mac-1 is commonly used as a macrophage marker, it is also expressed on neutrophils, natural killer cells, myeloid-derived dendritic cells, and B-1 cells in addition to macrophages (125-127). Bruemmer et al., found no differences in the percentage of Mac-1 positive cells between WT and OPN-null mice, and consistent with this we found no differences in the percentage of CD11b+ cells between genotypes. However, using the myeloid specific-CD115 marker, we found that OPN-null mice have a deficit in macrophage accumulation in response to acute inflammation. However, it should be noted that CD115 is expressed by dendritic cells in addition to monocytes and macrophages (128, 129). Due to the heterogenous nature of macrophages, identification of macrophages by a single marker remains a challenge.

There are several possible mechanisms by which OPN deficiency could reduce macrophage accumulation in response to thioglycollate elicitation. First, OPN deficiency could affect

production of monocytes, the precursors of macrophages. However, OPN-/- mice have normal levels of circulating monocytes (96), indicating decreased leukocyte accumulation is not due to impaired myelopoiesis. OPN has been shown to play a central role in regulating multiple aspects of macrophage biology. Studies by several labs have established OPN as a potent macrophage chemoattractant and recent reports indicate that OPN serves as a pro-survival factor for macrophages as well (59). Together these data indicate that decreased migration and increased apoptosis may account for the impaired macrophage accumulation seen in OPN-null animals challenged with inflammatory stimuli.

In addition to directly mediating macrophage accumulation through receptor-mediated chemotactic effects, OPN may also modulate migration by facilitating migration to other chemokines. In this regard, OPN has been show to facilitate migration of macrophages to fMLP and MCP-1 (53, 96, 97). Macrophages from OPN-/- mice are impaired in their ability to migrate to MCP-1, an important chemokine in recruitment of leukocytes to the peritoneal cavity in response to thioglycollate (51). Additionally, OPN stimulates MCP-1 production in monocytes, suggesting that a positive feedback loop leading to amplification of the inflammatory response may be disrupted in OPN-null mice (130). Studies by Henderson et al., indicate that MCP-1 expressed by resident peritoneal cells is critical for mediating early monocyte recruitment in murine peritonitis (131). Mice deficient in MCP-1, or its receptor, CCR2, display a deficit in macrophage accumulation to thioglycollate elicited peritonitis (132, 133). Similar to our results in OPN-null mice, the decrease in macrophage recruitment led to a relative increase in the percentage of lymphocytes and neutrophils.

In this chapter we also determined the OPN functional domains mediating macrophage accumulation in thioglycollate elicited peritonitis. Work presented in the previous chapter indicates that OPN promotes macrophage chemotaxis via integrins α_4 and α_9. Unpublished work in our lab also demonstrates that OPN promotes macrophage survival via an integrin α_4-dependent pathway. OPN interacts with integrins α_4 and α_9 via the SLAYGLR functional domain and consequently we hypothesized that the SLAYGLR domain of OPN mediates macrophage recruitment *in vivo*. To test this hypothesis, we generated chimeric mice in which the SLAYGLR domain, the RGD domain, or both were mutationally inactivated. We found that inactivation of the SLAYGLR domain results in decreased recruitment of macrophages in response to sterile inflammation. These results complement those of Yamamoto et al. demonstrating that a neutralizing antibody against the SLAYGLR domain could reduce inflammatory cell infiltration in an *in vivo* arthritis model (37). A similar approach was used to treat collagen-induced arthritis in non-human primates (38). Collectively, these data suggest that neutralization of the interaction between OPN and α_4/α_9 integrins may useful as a future therapeutic target to reduce leukocyte accumulation in inflammatory conditions.

Interestingly, we found that expression of OPN specifically from macrophages resulted in a striking increase in neutrophil accumulation in response to thioglycollate elicitation. While much is known about the role of OPN in macrophage biology, only recently has the function of OPN in neutrophils been explored. Although neutrophils express low levels of OPN (134), OPN is important for the recruitment and migration of neutrophils, as neutrophils from OPN-null mice display reduced chemotaxis toward fMLP *in vitro*, and *in vivo*, the accumulation of neutrophils in the peritoneal cavity in response to sodium periodate is impaired in OPN-null mice (134).

Recent studies indicate that a polymeric form of OPN interacts with $\alpha_9\beta_1$ on neutrophils and functions as a potent neutrophil chemoattractant (135).

Surprisingly, a role for OPN in the host response to biomaterial implantation, in terms of macrophage recruitment or foreign body giant cell formation was inconclusive. However, there are several possible reasons for this discrepancy. In the previously published study, mice were on a 129/SvJ x Black Swiss background, while we used OPN-null mice on the C57Bl/6 background. In some cases, the genetic background of the mouse strain can have a striking impact on the pathology of disease. In mice on the B6 background, IL-10 deficiency results in only a slight increase in susceptibility to inflammatory bowel disease, while in mice on the 129/SvEv or Balb/c background, it greatly increases susceptibility to the disease (136). Further, studies of inbred mice by Champy et al. demonstrated important metabolic, hematologic, and biochemical differences among strains of mice (137). This underlines the importance of using mice of a well-defined background for experimental purposes.

Further, in the chimeric mice used in our experiments, OPN expression is restricted to macrophages. While OPN is expressed at high levels by macrophages during inflammation, OPN expression is also associated with other cell types, including fibroblasts, during wound healing (138). Studies indicate that OPN derived from different cell sources differs in PTM status, resulting in variances in bioactivity (105). Additionally, in our experiments, OPN expression is under control of the CD68 promoter, and consequently OPN expression in these mice may not mimic the regulated temporal expression of OPN seen in WT animals.

Finally, the chimeric animals used in our *in vivo* studies underwent lethal irradiation prior to bone marrow transplantation, while our WT control mice were not irradiated. At this time, it is unknown if irradiation and bone marrow transplantation affect the foreign body response. Additional studies comparing WT control mice to WT mice that were lethally irradiated and transplanted with WT bone marrow would be necessary to determine if irradiation and transplantation significantly alter macrophage accumulation and FBGC formation in response to biomaterial implantation.

4.6 Conclusions

To examine the role of OPN in acute inflammation we analyzed leukocyte accumulation in response to intraperitoneal administration of thioglycollate, a sterile irritant, in WT and OPN-/- mice. Mice deficient in OPN has a significant decrease in the accumulation of peritoneal leukocytes in response to thioglycollate elicitation. This decrease in leukocyte accumulation was largely accounted for by a decrease in macrophage accumulation with little difference in the total number lymphocytes or neutrophils.

We then used retroviral transduction and stem cell transplantation technologies to create chimeric mice expressing OPN structural mutants in which the RGD, SLAYGLR, or both functional domains of OPN had been mutationally inactivated. In sterile thioglycollate elicited peritonitis, mutational inactivation of the SLAYGLR domain resulted in decreased leukocyte accumulation, which was attributable to reduced macrophage accumulation. Surprisingly, expression of OPN specifically from macrophages resulted in a striking increase in neutrophil accumulation in the peritoneal cavity in response to thioglycollate.

Finally, we tested the relative contributions of the RGD and SLAYGLR domain in the PVA sponge implantation model of chronic inflammation. In contrast to previous reports, no differences in between WT and OPN-null mice in terms of macrophage accumulation in PVA sponge implants or the formation of foreign body giant cells were observed.

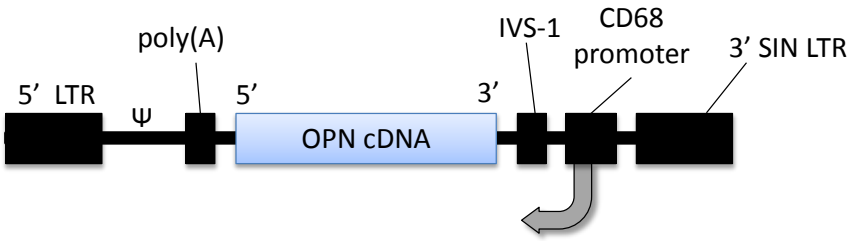

Figure 4.1: Features of the CD68S retroviral vector.
The macrophage-specific CD68S retroviral vector contains long terminal repeats (LTRs) and packaging signals (ψ) from the Moloney murine leukemia virus. The construct is self-inactivating (SIN) due to deletion of essential promoter and enhancer elements in the 3' LTR. Gene expression is driven by a 342-bp sequence 5' to the ATG initiation codon of the human CD68 gene, in addition to the CD68 first intron (IVS-1). The direction of transcription, as indicated by the arrow, is opposite that of the viral 5' LTR. The plasmid also contains a bovine growth hormone polyadenylation signal (poly(A)) to terminate RNA transcription. In addition, the vector has a puromycin resistance cassette and the Epstein-Barr virus nuclear antigen and origin of replication, which allows for production of high-titer recombinant retrovirus from packaging cells lines with episomal copies of the plasmid.

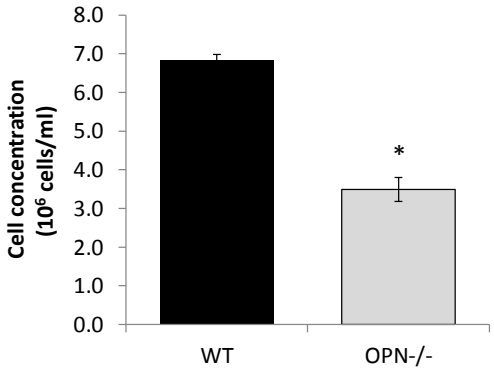

Figure 4.2: OPN deficiency results in decreased peritoneal leukocyte accumulation in response to thioglycollate elicitation.
WT and OPN-/- mice were injected intraperitoneally with thioglycollate and 72 hours later peritoneal leukocytes were collected by peritoneal lavage. Data expressed as mean ± SEM, *p<0.05 vs WT. n=5 for WT, n=7 for OPN-/-

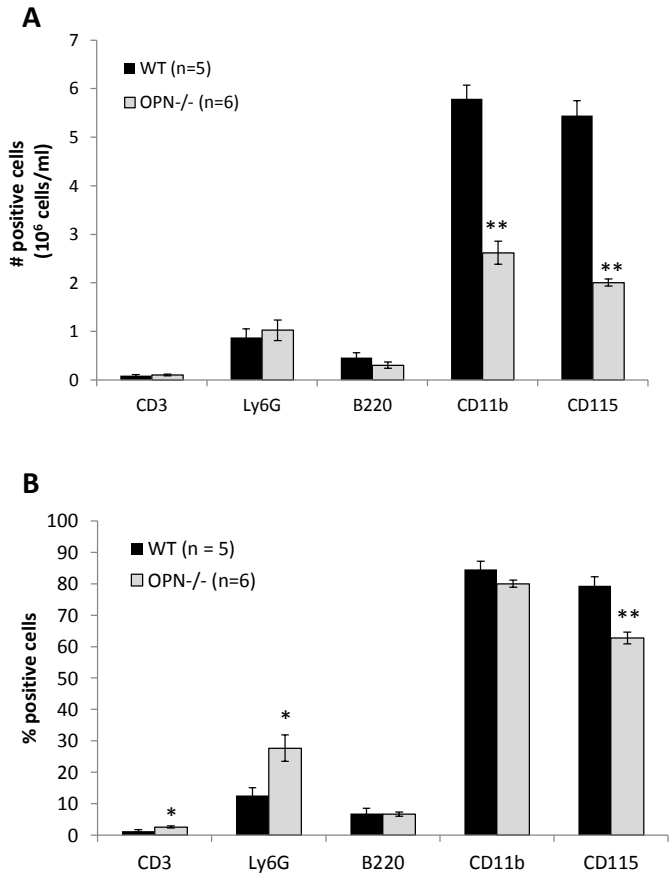

Figure 4.3: OPN deficiency alters peritoneal leukocyte composition in thioglycollate-elicited peritonitis.
Thioglycollate elicited peritoneal leukocytes from WT and OPN-/- mice were analyzed for cell composition by flow cytometry. Cells were stained for CD3, Ly6G, B220, CD11b, and CD115. **(A)** Quantification of peritoneal leukocytes. The total number of leukocytes recovered from individual mice was multiplied by the percentage of each cell type present. **(B)** Proportion of cells positive for each cell surface marker. Data presented as mean ± SEM, *p<0.05 vs WT, **p<0.001.

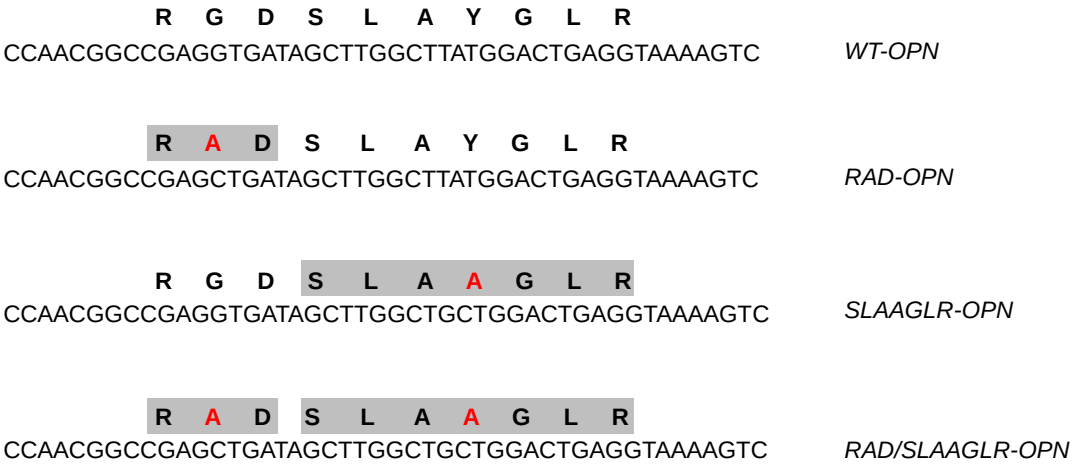

Figure 4.4: OPN structural mutants.
Retroviral constructs expressing OPN structural mutants were generated using site-directed mutagenesis. Red letters indicate amino acids mutated. Shaded areas represent the OPN structural domains inactivated by mutation.

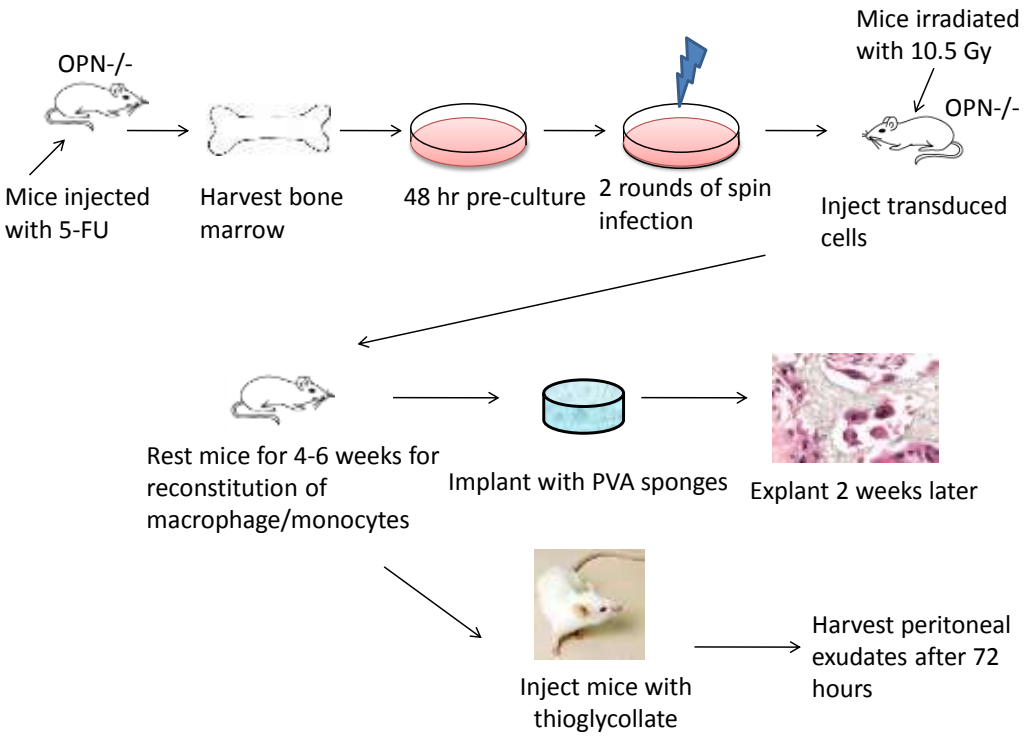

Figure 4.5: Retroviral transfection and bone marrow transplantation scheme.
To create chimeric OPN-/- mice expression OPN structural mutants specifically from macrophages, retroviral transfection and bone marrow transplantation techniques were used. OPN-/- donor mice were injected with 5-fluorouracil three days prior to harvest to increase the yield of stem cells. Bone marrow was then harvested from donor mice and treated with stem cell factor, IL-3 and IL-6 for 48 hours to stimulate proliferation. Cells were then transduced with 2 rounds of spin-transfection with retroviral constructs. OPN-/- recipient mice were lethally irradiated 24 hours prior to transplantation with 10.5 Gy . Donor cells were injected intravenously and mice were allowed to rest for 4-6 weeks to allow reconstitution of monocytes/macrophages. Chimeric animals were then used for either the thioglycollate elicited peritonitis model of acute inflammation or the PVA sponge implantation model of chronic inflammation.

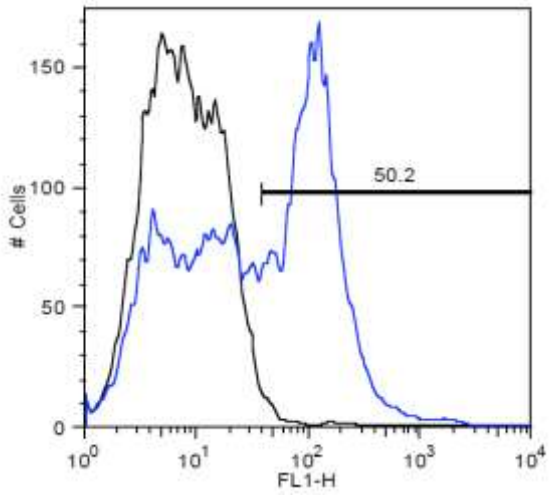

Figure 4.6: CD68S retroviral constructs provide high transgene expression *in vivo*.
FACS analysis of eGFP expression in thioglycollate elicited peritoneal leukocytes from chimeric mice expressing the CD68S eGFP control vector (blue histogram). The percentage of eGFP-positive cells was determined by using a gate set to exclude control cells from mice that had not been transplanted with a eGFP construct (black line). Histogram is from an individual animal that is representative of data from 6 mice.

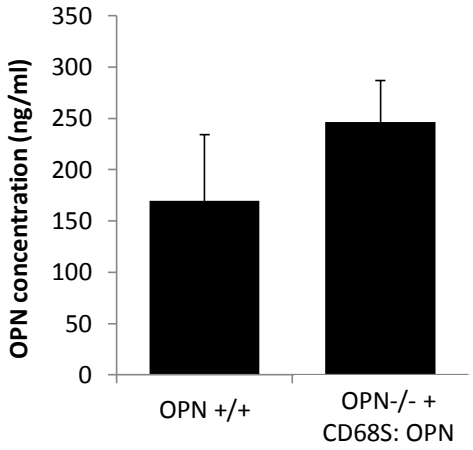

Figure 4.7: OPN expression from chimeric mice.
OPN levels in peritoneal lavage fluid from wild-type mice (OPN+/+) or OPN-/- mice that were transplanted with HSCs transduced with CD68S retroviral vector encoding WT OPN (OPN-/- + CD68S: OPN) was assessed by ELISA. Data expressed as mean ± SEM. n= 5 for OPN+/+, n=7 for CD68S:OPN.

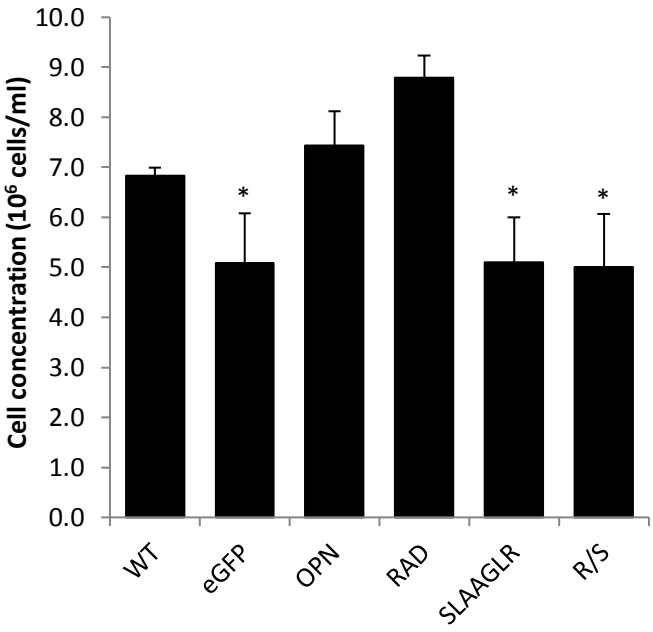

Figure 4.8: The SLAYGLR domain of OPN contributes to leukocyte accumulation in thioglycollate-elicited peritonitis.
Sterile peritonitis was elicited in OPN chimeric mice by the injection of thioglycollate intraperitoneally. After 72 hours peritoneal leukocytes were harvested by peritoneal lavage. Cell concentration was determined by manual counting with a hemocytometer. Cell accumulation was determined in wild type mice (WT) and OPN-null chimeric mice expressing OPN structural mutants from a CD68S macrophage-specific retroviral vector. To determine the relative contributions of OPN functional domains in acute inflammation, leukocyte accumulation was assessed in OPN-null chimeric mice in which the RGD domain (RAD), the SLAYGLR domain (SLAAGLR), or both (R/S) had been mutationally inactivated. OPN-null chimeric mice expressing eGFP (eGFP) or OPN (OPN) were included as controls. Data are expressed as mean ± SEM of between 5-7 individual animals. *$p<0.05$ vs RAD.

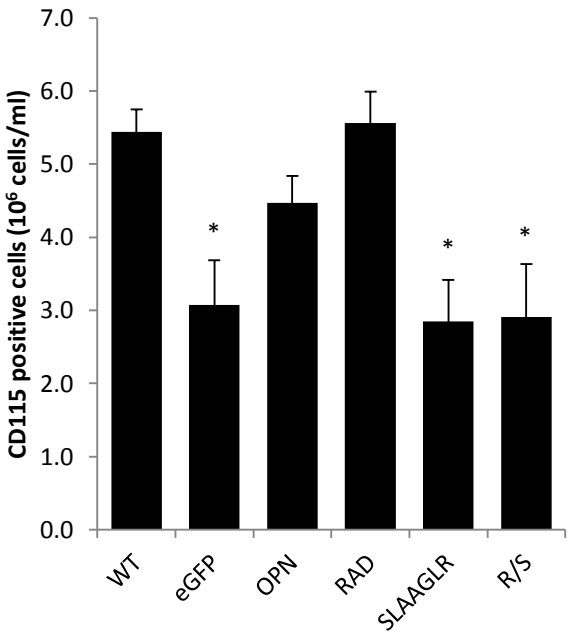

Figure 4.9: The SLAYGLR domain mediates macrophage recruitment in thioglycollate-elicited peritonitis.
The composition of cells recruited to the peritoneal cavity in response to thioglycollate elicitation was determined by flow cytometry by staining for CD115. The number of CD115 positive cells was determined in WT mice (WT) and OPN-null chimeric mice expressing eGFP (eGFP) or OPN (OPN) from a macrophage-specific retroviral vector. Additionally, leukocyte recruitment was assessed in chimeric mice in which the RGD domain (RAD), the SLAYGLR domain (SLAAGLR), or both (R/S) had been mutationally inactivated. Data are expressed as mean +/- SEM of between 5-7 individual animals. *$p<0.05$ versus WT.

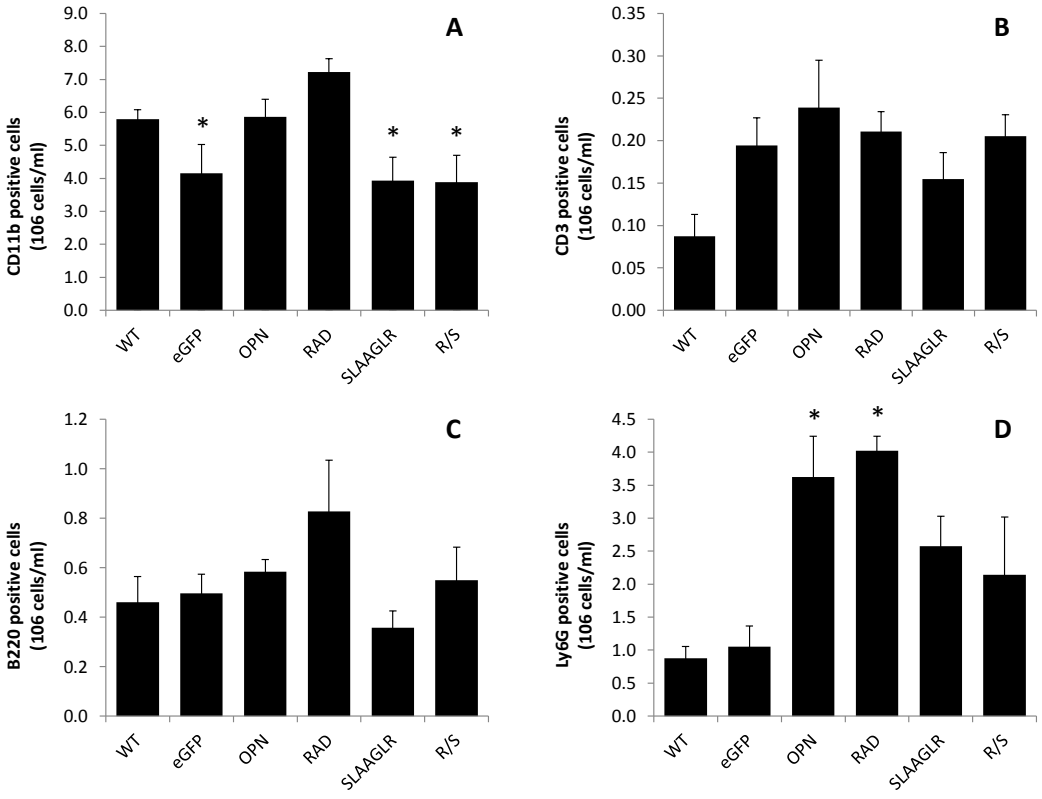

Figure 4.10: Leukocyte composition of peritoneal lavage fluids from chimeric mice expressing OPN structural mutants.
Thioglycollate elicited peritoneal leukocytes were analyzed for cell composition by flow cytometry from WT mice (WT) and OPN-null chimeric mice expressing eGFP (eGFP) or OPN (OPN) from a macrophage-specific retroviral vector. Leukocytes were also analyzed from chimeric mice in which the RGD domain (RAD), the SLAYGLR domain (SLAAGLR), or both (R/S) had been mutationally inactivated. Peritoneal leukocytes were stained for (A) CD11b, (B) CD3, (C) B220, and (D) Ly6G. Data are expressed as mean ± SEM of between 5-7 individual animals. For CD11b staining, *$p<0.05$ vs RAD. For Ly6G staining, *$p<0.05$ vs WT and eGFP.

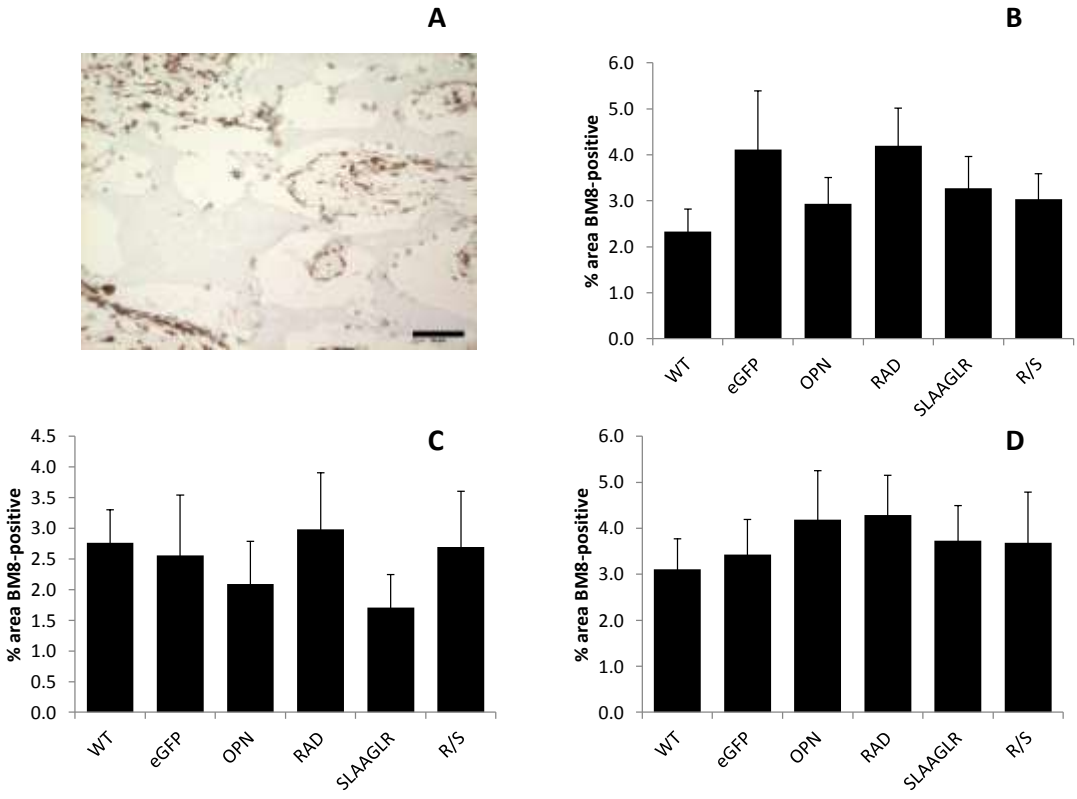

Figure 4.11: Quantification of macrophage accumulation in PVA sponges.
PVA sponges implanted subcutaneously in mice and were explanted 14 days later. Implants were stained with BM8 to determine macrophage accumulation. PVA sponges were implanted in WT mice (WT) and OPN-null chimeric mice expressing eGFP (eGFP) or OPN (OPN) from a macrophage-specific retroviral vector. Additionally, macrophage accumulation was assessed in chimeric mice in which the RGD domain (RAD), the SLAYGLR domain (SLAAGLR), or both (R/S) had been mutationally inactivated **(A)** Representative staining for BM8 in PVA sponge implants. Scale bar represents 20 μm. The percent area stained positive for BM8 was quantified in the **(B)** skin side, **(C)** interior, and **(D)** muscle side of the implant. Data presented as mean ± SEM. n= 6 mice.

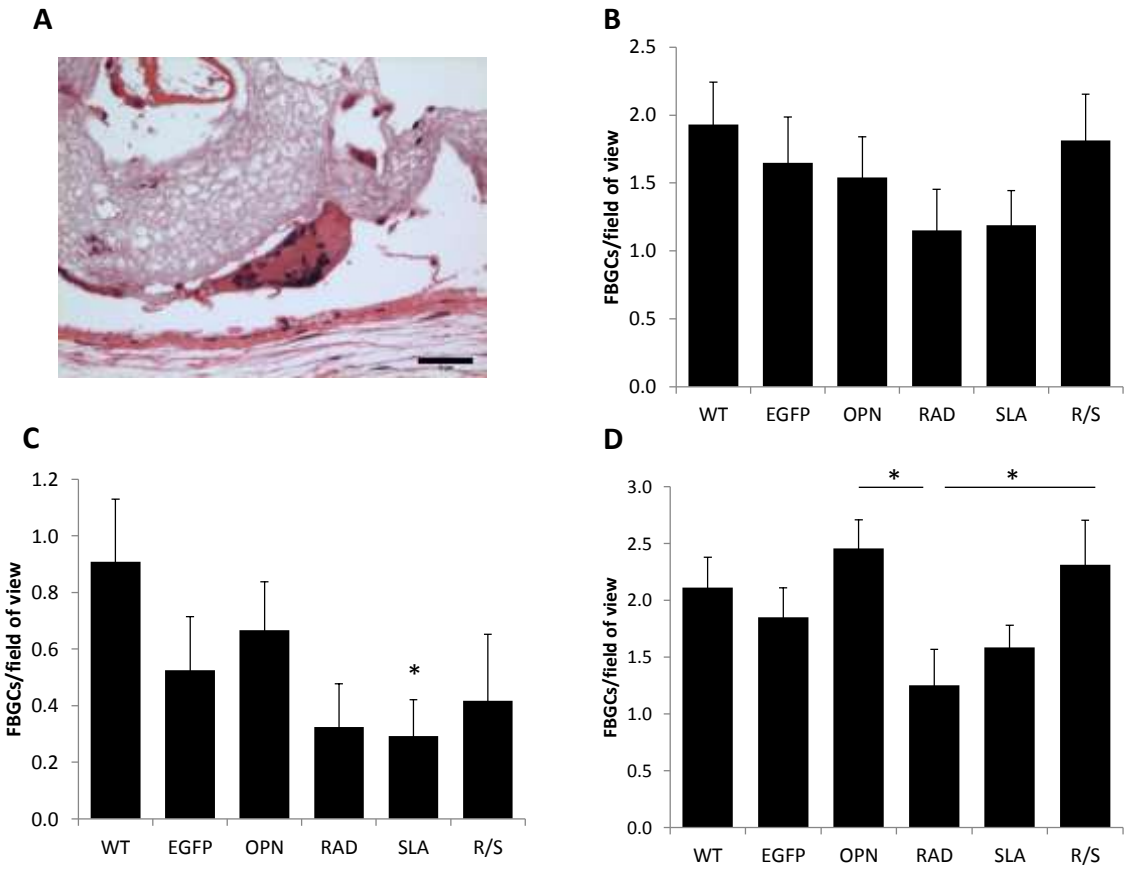

Figure 4.12: Quantification of foreign body giant cell formation in PVA sponges.
PVA sponges implanted subcutaneously in mice and were explanted 14 days later. Implants were stained with H&E and the number of foreign body giant cells (FBGC) per field of view were counted manually. FBGCs were defined as cells containing 3 or more nuclei. PVA sponges were implanted in WT mice (WT) and OPN-null chimeric mice expressing eGFP (eGFP) or OPN (OPN) from a macrophage-specific retroviral vector. Additionally, macrophage accumulation was assessed in chimeric mice in which the RGD domain (RAD), the SLAYGLR domain (SLA), or both (R/S) had been mutationally inactivated **(A)** Representative H&E staining of PVA sponge implants. Scale bar represents 10 μm. The number of FBGCs per field of view was quantified in the **(B)** skin side, **(C)** interior, and **(D)** muscle side of the implant. Data presented as mean ± SEM. n= 6 mice. In **(C)**, *p<0.05 vs WT.

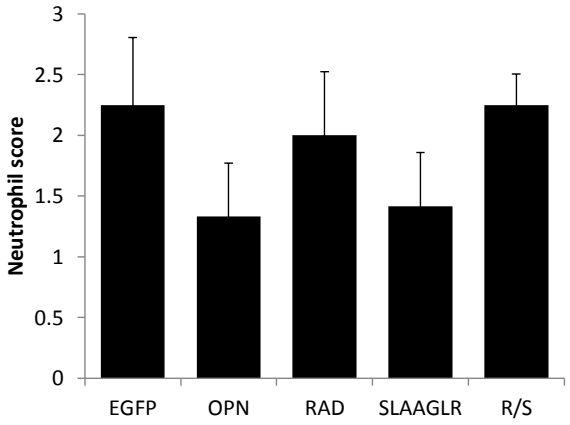

Figure 4.13: Neutrophil score in PVA sponge implants.
PVA sponges implanted subcutaneously in mice and were explanted 14 days later. Implants were stained with H&E and neutrophil infiltration was quantified by a blinded observer. the number of foreign body giant cells (FBGC) per field of view were counted manually. FBGCs were defined as cells containing 3 or more nuclei. PVA sponges were implanted in WT mice (WT) and OPN-null chimeric mice expressing eGFP (eGFP) or OPN (OPN) from a macrophage-specific retroviral vector. Additionally, macrophage accumulation was assessed in chimeric mice in which the RGD domain (RAD), the SLAYGLR domain (SLA), or both (R/S) had been mutationally inactivated **(A)** Representative H&E staining of PVA sponge implants. The number of FBGCs per field of view was quantified in the **(B)** skin side, **(C)** interior, and **(D)** muscle side of the implant. Data presented as mean ± SEM. n= 6 mice.

Chapter 5

OPN and atherosclerosis

5.1 Abstract

OPN is highly expressed in atherosclerotic lesions, in both humans and in animal models of atherosclerosis, and growing evidence suggests that OPN plays an essential role in the pathogenesis of atherosclerosis. OPN is expressed by several cell lineages in the vessel wall including macrophages, vascular smooth muscle cells, and endothelial cells. To determine the cell type responsible for OPN function in atherosclerosis, we created OPN chimeric mice on the atherosclerosis-prone ApoE-/- background using bone marrow transplantation. To determine if leukocyte-derived OPN is necessary for lesion formation, ApoE-/-OPN+/+ recipient mice were irradiated and transplanted with ApoE-/-OPN-/- bone marrow or ApoE-/-OPN+/+ marrow. Additionally, to determine if leukocyte-derived OPN alone is sufficient for lesion formation, ApoE-/-OPN-/- mice were transplanted with ApoE-/-OPN+/+ or ApoE-/-OPN-/- marrow. Bone marrow transplant mice were maintained on a normal chow diet and atherosclerotic lesion formation was analyzed at 30-34 weeks post-transplant. Morphometric analysis of the innominate artery showed no difference in lesion area between genotypes. However, mice with a systemic deficiency in OPN had decreased medial area compared to ApoE-/-OPN+/+ mice transplanted with either ApoE-/-OPN+/+ or ApoE-/-OPN-/- bone marrow. Finally, we analyzed calcification of the innominate artery by Alizarin Red staining and found that OPN-deficiency

resulted in an increase in calcification, although this result did not reach statistical significance due to the small sample size.

5.2 Introduction

5.2.1 Atherosclerosis

Atherosclerosis is a chronic, progressive disease, characterized by the accumulation of lipids in arteries and is one of the leading causes of death globally (139). The disease is initiated by infiltration of monocytes and lymphocytes into the activated endothelium (140). Endothelial dysfunction can be caused by diabetes, hyperlipidemia, hypertension, and other pre-existing pathological conditions (141-143). Monocytes then migrate into the intima, and uptake low-density lipoprotein (LDL) leading to the development of cholesterol-loaded foam cells that form early fatty streaks. Early lesions grow and recruit other cell types including smooth muscle cells (SMCs). SMCs proliferate within the lesion transforming the lesion into a fibro-fatty plaque. Later, lesions become more complex and are filled with SMCs, extensive extracellular matrix (ECM), cholesterol clefts, and a necrotic core. In advanced lesions, mineralization of matrix can occur and chondrocyte-like cells are associated with these mineral deposits. Calcification of advanced lesions is recognized as a major contributor to loss of arterial compliance. Common late stage complications of atherosclerosis include artery occlusion and plaque rupture.

5.2.2 Atherosclerosis as a chronic inflammatory disease

Inflammation and macrophage activation are integral to atherosclerotic development. Chronic inflammation associated with atherosclerosis plays a central role in plaque progression and subsequent complications. Consequently, identification of inflammatory pathways/molecules

involved in atherosclerosis could aid in the development of novel therapeutics designed to treat this disease.

5.2.3 OPN and atherosclerosis

OPN is highly expressed in atherosclerotic lesions and has been detected in both human lesions and in animal models of atherosclerosis (12, 144, 145). OPN is synthesized by cells of the macrophage/monocyte lineage and to a lesser extent by endothelial cells (ECs) and vascular SMCs. Recently, OPN has emerged as a potential biomarker of cardiovascular disease. Clinically, plasma OPN levels are associated with the presence and extent of coronary artery disease (146).

To date, several studies have investigated the contribution of OPN to the initiation and progression of atherosclerosis. In hyperlipidemic apolipoprotein E (ApoE)-null mice, Matsui et al., showed that OPN deficiency significantly reduces atherosclerotic lesion size in female ApoE-/-OPN-/- mice compared to ApoE-/-OPN+/+ mice after 36 weeks on a normal chow diet (Matsui). Interestingly, this phenomenon was sex-linked, as male mice showed no difference in lesion area. Similarly, studies in ApoE/LDLreceptor/OPN triple knockout mice showed that OPN deficiency resulted in decreased atherosclerotic lesion size and an increase in the number of apoptotic cells in lesions (147). Bone marrow transplantation studies in an angiotensin-II-accelerated model of atherosclerosis indicated that leukocyte-derived OPN contributes to OPN-mediated development of atherosclerosis (51). These studies suggest that OPN promotes macrophage accumulation and retention in atherosclerotic lesions, thus contributing to the chronicity of the disease.

In addition to regulating macrophage function, OPN also modulates other vascular cells associated with vascular pathology. OPN is re-expressed in SMCs associated with human restenotic lesions (148). Consistently, animal models have confirmed the role of OPN in promoting SMC migration and proliferation (28, 74). In addition, formation of the neointima is an injury response to damaged vessels and is thought to be an important first step in the progression of atherosclerosis. In rats, following arterial injury caused by balloon angioplasty, OPN expression is increased in neointimal SMCs indicating OPN may be important in the early process of neointimal formation (149). These studies indicate that during injury, OPN enhances the proliferation, migration, and accumulation of smooth muscle and endothelial cells involved in repair and remodeling processes of the vasculature.

In later stages of atherosclerosis, OPN also influences calcification. OPN is a potent inhibitor of mineralization, prevents ectopic calcification, and is an inducible inhibitor of vascular calcification (2). OPN binds hydroxyapatite and calcium ions thereby physically inhibiting crystal formation and growth *in vivo.* OPN appears to also be an important regulator of vascular calcification and is associated with mineralized deposition in humans (149). In mice, OPN levels are greatly elevated in the spontaneously mineralizing arteries of matrix gla protein (MGP)-null mice and it has been demonstrated that OPN is a major inducible inhibitor of arterial medial calcification in this system (3). Vascular calcification is now recognized as a marker of atherosclerotic plaque burden as well as a major contributor to loss of arterial compliance and increased pulse pressure seen with age, diabetes, and renal insufficiency. These findings suggest that OPN may be an important inhibitor of arterial mineral deposition under conditions of injury

and disease, and that strategies to replenish OPN might be useful to prevent or treat ectopic calcification, including vascular calcification.

OPN is expressed by multiple cell types in atherosclerotic lesions. This consequently limits efforts to dissect the relative contributions of leukocyte versus non-leukocyte derived OPN using global deletion or functional blockade of OPN. However, bone marrow transplantation provides a powerful tool to study the role of hematopoietic-derived OPN in the pathogenesis of atherosclerosis.

5.2.4 ApoE-/- mice as a murine model of atherosclerosis

For our studies, we used the hyperlipidemic ApoE-/-mice as a murine model of atherosclerosis. ApoE plays a critical role in lipoprotein metabolism and is required for clearance of very low density lipoprotein (VLDL). Wild type mice are resistant to atherosclerosis, but mice deficient in ApoE develop hyperlipidemia and extensive atherosclerotic lesions on a normal chow diet (150). Lesion development and composition in ApoE-/- mice is similar to that in humans (151). Early lesions feature initial fatty streaks comprised of macrophage-derived foam cells, and over time lesions become more complex with fibrous caps, a necrotic core, cholesterol clefts, and calcified depositions (152).

5.3 Materials and Methods

5.3.1 Bone marrow transplantation

Bone marrow transplants were performed in female ApoE-/-OPN+/+ and ApoE-/-OPN-/- recipient mice. Donor bone marrow cell suspensions were generated by flushing femurs and

tibias from either ApoE-/-OPN+/+ or ApoE-/-OPN-/- mice. Recipient mice were lethally irradiated 24 hours prior to transplantation with 10.5 Gy. Mice were then injected intravenously with 5 x 10^6 bone marrow cells. After transplantation, mice were placed on a normal chow diet for an additional 30-34 weeks.

ApoE-/-OPN+/+ recipient mice were transplanted at 11.5 weeks of age and were sacrificed at 45-46 weeks of age (33-34 weeks post-transplant). ApoE-/-OPN-/- recipient mice were transplanted at 11-14 weeks of age and were sacrificed at 40-44.5 weeks of age (29.5-34.5 weeks post-transplant).

All animal experiments were approved by the University of Washington Animal Care and Use committee and followed federal guidelines for the use and care of laboratory animals.

5.3.2 Tissue collection for analysis

Mice were sacrificed and perfusion-fixed via the left ventricle with 10 ml PBS containing 1 mM EDTA and 30 ml fixative (PBS, 4% paraformaldehyde, and 5% sucrose). The heart and aortic root were frozen and stored. The thoracic aorta and innominate (brachiocephalic) artery were embedded in paraffin to be used for lesion analysis.

5.3.3 Histology

The innominate artery was sectioned (5 um sections, 100 sections total). Slides were baked at 60°C for 30 minutes. Every 10^{th} slide was stained with hematoxylin and eosin (H&E). The area of the external elastic lamina, internal elastic lamina, and lumen was measured using ImageJ

software by a blinded observer. Lesion area was defined as the area of the internal elastic lamina minus lumen area. Percent lesion area was calculated as lesion area divided by the area of the internal elastic lamina. Medial area was defined as the area bound between the external elastic lamina and the internal elastic lamina. Sections adjacent to those stained with H&E were stained with 0.5% Alizarin Red pH 9.0 for 1 hour. Sections were destained in 0.1 M borate buffer pH 9.0 for 20 seconds. Slides were rinsed in distilled water, dehydrated, and coverslipped with Permount. The area positive for Alizarin Red staining was quantified by a blinded observer using manual thresholding with ImageJ software. The percent calcified area was calculated as the Alizarin Red positive stained area divided by the area of the external elastic lamina (external elastic lamina area was measured in the adjacent section).

5.3.4 Statistical analysis

One-way ANOVA with Tukey's post-hoc was used for comparison among multiple groups with equal variances. For comparison among groups with unequal variances, one-way ANOVA with Games-Howell post-hoc was used.

5.4 Results and Discussion

5.4.1 Generation of ApoE-/- bone marrow transplant (BMT) mice

In atherosclerotic lesions, OPN is expressed by several lineages of cells including monocytes/macrophages, SMCs and endothelial cells (144). ApoE-null mice deficient in OPN exhibit decreased atherosclerotic lesion size (51, 55, 147). To investigate the cell-specific contribution of leukocyte-derived OPN to the decrease in atherosclerotic lesion formation, we

performed bone marrow transplants in hyperlipidemic ApoE-null mice. To determine if leukocyte-derived OPN is necessary for lesion formation, ApoE-/-OPN+/+ recipient mice were irradiated and transplanted with ApoE-/-OPN-/- bone marrow or ApoE-/-OPN+/+ marrow. Additionally, to determine if leukocyte-derived OPN alone is sufficient for lesion formation, ApoE-/-OPN-/- mice were transplanted with ApoE-/-OPN+/+ or ApoE-/-OPN-/- marrow. An overview of the bone marrow transplantation scheme is shown in Figure 5.1. Transplanted mice were fed a normal chow diet. Mice were sacrificed at 40-46 weeks of age, perfusion fixed, and tissues were collected and fixed for further analysis. An overview of the experimental timeline is shown in Figure 5.2.

5.4.2 Analysis of lesion area in ApoE-/- BMT mice

Having generated our bone marrow transplant mice we then analyzed atherosclerotic lesion area in these animals. To enable robust quantification of atherosclerotic plaque size, we concentrated on the innominate (brachiocephalic) artery, as preliminary studies in our lab indicated differences in lesion size between ApoE-/-OPN+/+ and ApoE-/-OPN-/- mice at this site. To determine atherosclerotic lesion area, innominate arteries were fixed, embedded in paraffin, and sectioned (5 um sections, 100 sections per mouse). Every tenth section was stained with hematoxylin and eosin and analyzed for lesion area. Figure 5.3 shows a representative section stained with H&E. The area of the external elastic lamina, internal elastic lamina, and lumen were measured using Image J software, and the average lesion area of the innominate artery was calculated. As shown in Figure 5.4, there was no difference in lesion area between ApoE-null mice transplanted with either ApoE-/-OPN-/- bone marrow or ApoE-/-OPN+/+ marrow. Similarly, in ApoE-/-OPN-/- double knockout mice, reconstitution with ApoE-/-OPN+/+ had no

effect on lesion size or percent lesion area. However, we did find that mice deficient in OPN had decreased medial area compared to ApoE-/-OPN+/+ mice transplanted with either ApoE-/-OPN+/+ or ApoE-/-OPN-/- bone marrow (Figure 5.5). Reconstitution of leukocyte-derived OPN in ApoE-/-OPN-/- mice did not increase medial area. Together these data suggest that non-leukocyte derived OPN may be important in promoting medial thickening in atherosclerotic prone ApoE-null mice.

5.4.3 Quantification of calcification in ApoE-/- BMT mice

OPN has been shown to inhibit vascular calcification, so we next investigated the relative contribution of leukocyte-derived OPN in calcification. Sections of the innominate artery from ApoE-/- BMT mice were stained with Alizarin Red to detect calcification (Figure 5.6). As shown in Figure 5.7, ApoE-/-OPN-/- BMT mice had an increase in calcification compared to ApoE-/-OPN+/+ BMT mice, although this difference did not meet statistical significance due to the limited sample size.

5.5 Discussion

Previously, Bruemmer et al., reported leukocyte-derived OPN to play a role in the progression of atherogenesis (51). However, in those studies mice were transplanted at a younger age (8 weeks vs. 11-14 weeks in our study). Additionally, their study utilized the AngII-accelerated model of atherosclerosis, in which lesion development occurs over a short 4 week time period. These data suggest that OPN deficiency is sufficient to abrogate the inflammatory response generated by AngII infusion, but OPN deficiency alone is not sufficient to affect the slower-progressing

atherosclerosis in uninfused ApoE-/- mice where hypercholesterolemia is the main cause of atherosclerosis.

While we were unable to show a role for OPN in lesion size, we did find that mice deficient in OPN had decreased medial area compared to ApoE-/-OPN+/+ mice transplanted with either ApoE-/-OPN+/+ or ApoE-/-OPN-/- bone marrow. Reconstitution of leukocyte-derived OPN in ApoE-/-OPN-/- mice did not increase medial area, suggesting that SMC and or EC-derived OPN play a role in medial thickening. These results are in agreement with previous studies showing OPN increases medial thickening. In OPN transgenic mice in which OPN was overexpressed globally via the cytomegalovirus enhancer/chicken β-actin promoter resulted in a 73% increase in aortic medial thickness compared to WT mice (74). Also, in ApoE/LDLR/OPN triple knockout mice a decrease in medial area was seen in female mice after 34 weeks on a normal chow diet compared to ApoE-/-LDLR-/- mice (147).

We also show a trend towards increased calcification of the innominate artery of ApoE-/-OPN-/- BMT mice compared to ApoE-/-OPN+/+ BMT mice. However, this result did not reach statistical significance due to the small sample size. Using data from this study, we performed power analysis and determined that a sample size of 20 mice per treatment group would be necessary to detect statistical significance.

5.6 Conclusions

In this chapter we used bone marrow transplantation to assess the role of leukocyte-derived OPN in the progression of atherosclerosis. ApoE-/-OPN+/+ mice were transplanted with either ApoE-

/-OPN-/- or ApoE-/-OPN+/+ bone marrow to assess if leukocyte-derived OPN is necessary for lesion formation. In addition, to determine if OPN expression from leukocytes alone is sufficient for lesion formation, ApoE-/-OPN-/- mice were transplanted with ApoE-/-OPN+/+ or ApoE-/-OPN-/- marrow. Atherosclerotic lesion area, medial thickness, and calcification were assessed in the innominate arteries of bone marrow transplant mice via histology. No difference was found between genotypes in terms of lesion area. However, mice deficient in OPN had decreased medial area compared to ApoE-/-OPN+/+ mice transplanted with either ApoE-/-OPN+/+ or ApoE-/-OPN-/- bone marrow. In terms of calcification, ApoE-/- mice deficient in OPN had a trend toward increased calcified area compared to ApoE-/-OPN+/+ recipient mice.

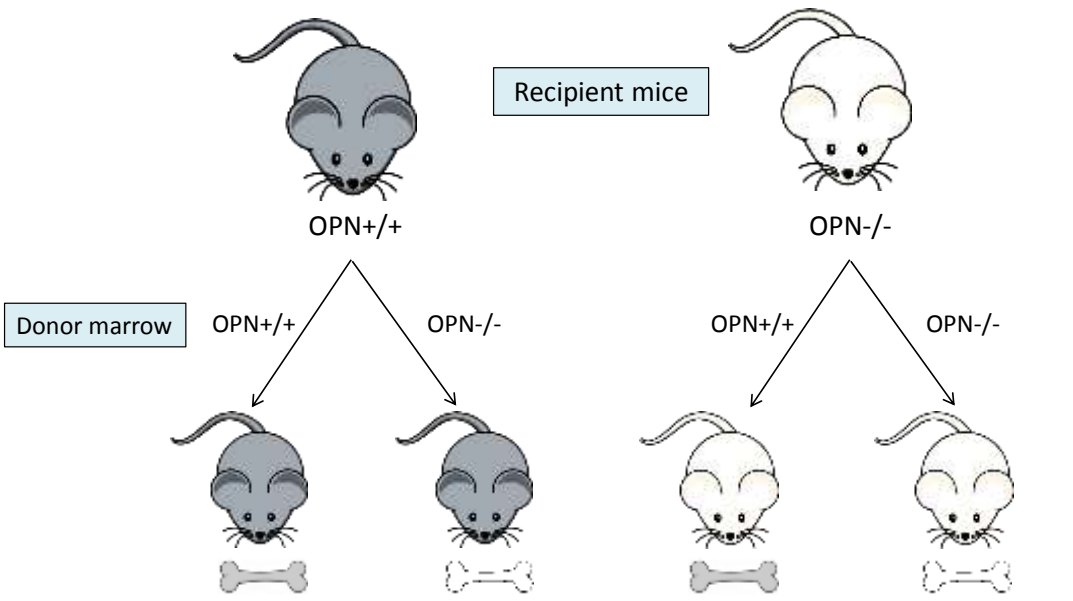

Host genotype	+/+	+/+	-/-	-/-
Marrow genotype	+/+	-/-	+/+	-/-

Figure 5.1: Overview of bone marrow transplantation scheme in ApoE-null mice.
To investigate the cell-specific contribution of leukocyte-derived OPN to atherosclerotic lesion progression, bone marrow transplantation was performed in hyperlipidemic ApoE-null mice. To determine if leukocyte-derived OPN is necessary for lesion formation, ApoE-/-OPN+/+ recipient mice were irradiated and transplanted with ApoE-/-OPN-/- bone marrow or ApoE-/-OPN+/+ marrow. Additionally, to determine if leukocyte-derived OPN alone is sufficient for lesion formation, ApoE-/-OPN-/- mice were transplanted with ApoE-/-OPN+/+ or ApoE-/-OPN-/- marrow.

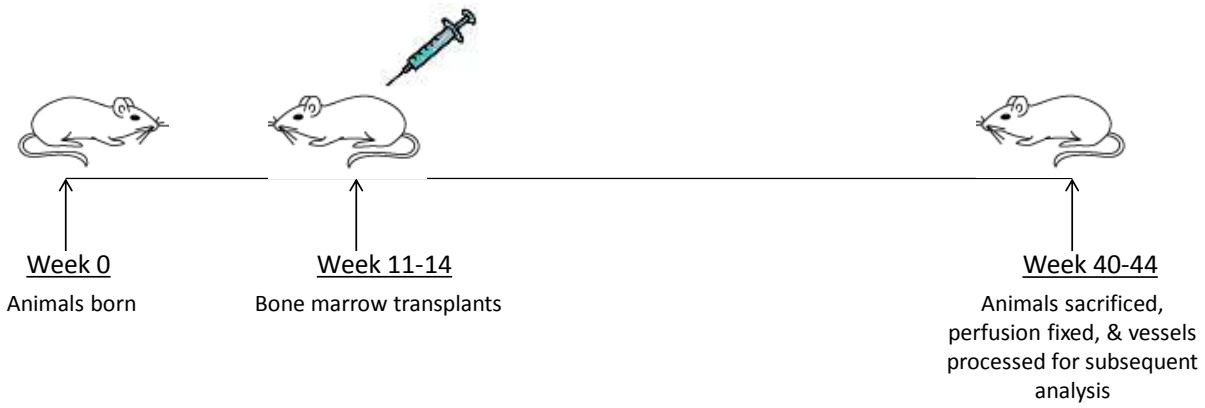

Figure 5.2: Overview of experiment timeline.
Bone marrow transplants were performed in ApoE-/- mice at 11-14 weeks of age. Animals were placed on a normal chow diet and were sacrificed at 40-44.5 weeks of age (29.5-34.5 weeks post-transplant).

Figure 5.3: Representative H&E image of the innominate artery from ApoE-/- BMT mice. Representative image of the innominate artery in an ApoE-/- mouse stained with hematoxylin and eosin. Scale bar represents 100 µm.

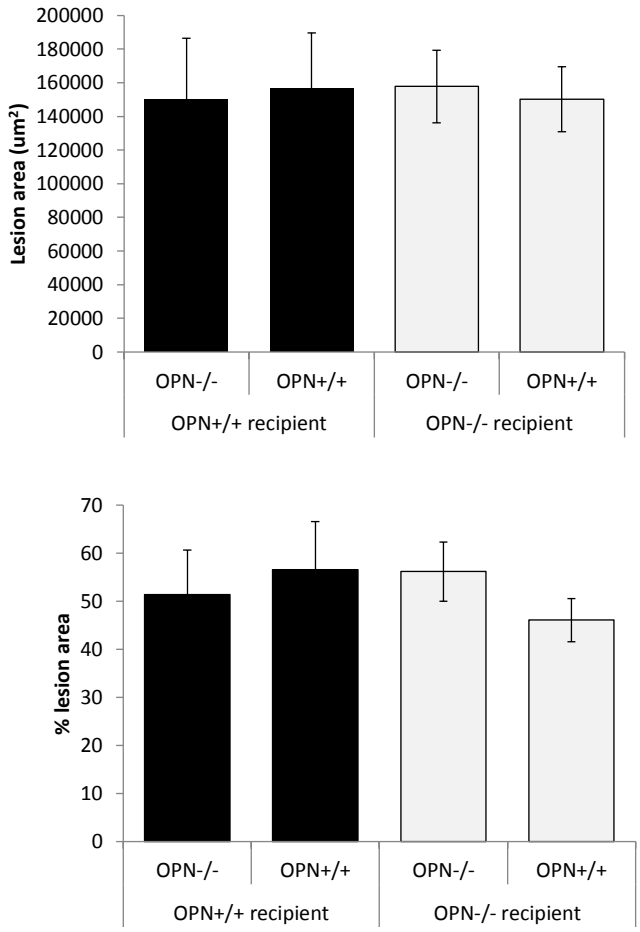

Figure 5.4: Quantification of lesion area in ApoE-/- BMT mice.
Lesion area was quantified in H&E stained sections of the innominate artery. Lesion area was quantified in ApoE-/-OPN+/+ mice (black bars) and ApoE-/-OPN-/- (gray bars) transplanted with ApoE-/-OPN+/+ or ApoE-/-OPN-/- bone marrow. Bone marrow genotype is indicated on the x-axis. The full length of the innominate artery was sectioned and every tenth slide was analyzed. Data presented as mean ± SEM.

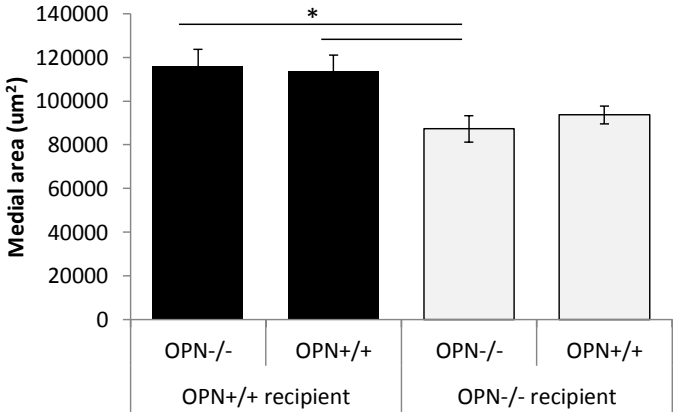

Figure 5.5: Quantification of medial area in ApoE-/- BMT mice.
Medial area was quantified in H&E stained sections of the innominate artery. Medial area was quantified in ApoE-/-OPN+/+ mice (black bars) and ApoE-/-OPN-/- (gray bars) transplanted with ApoE-/-OPN+/+ or ApoE-/-OPN-/- bone marrow. Bone marrow genotype is indicated on the x-axis. The full length of the innominate artery was sectioned and every tenth slide was analyzed. Data presented as mean ± SEM. *$p<0.05$.

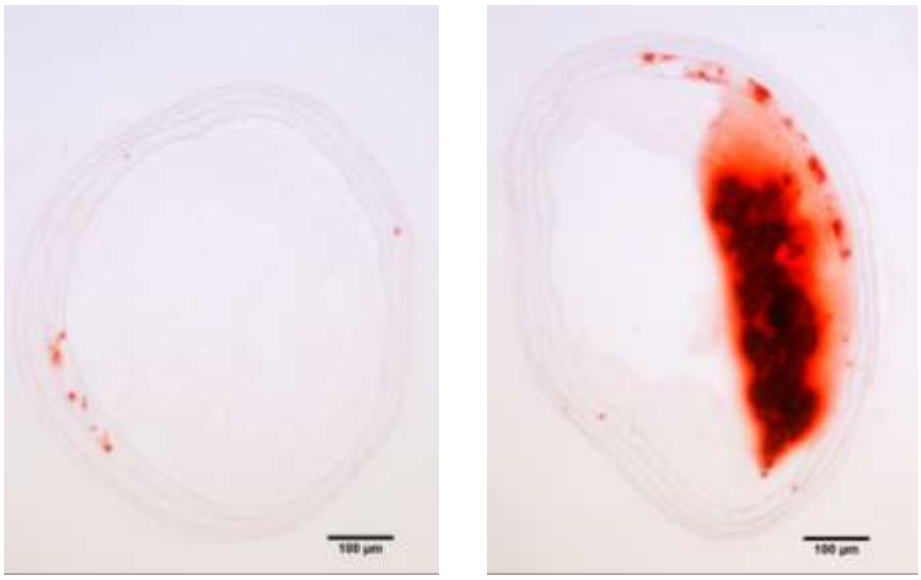

Figure 5.6: Representative Alizarin Red staining of the innominate artery.
Representative images of the innominate artery in an ApoE-/- mouse stained with Alizarin Red to detect calcification. Lesion on the left shows a low degree of calcification, while lesion on the right is highly calcified. Scale bars represent 100 μm.

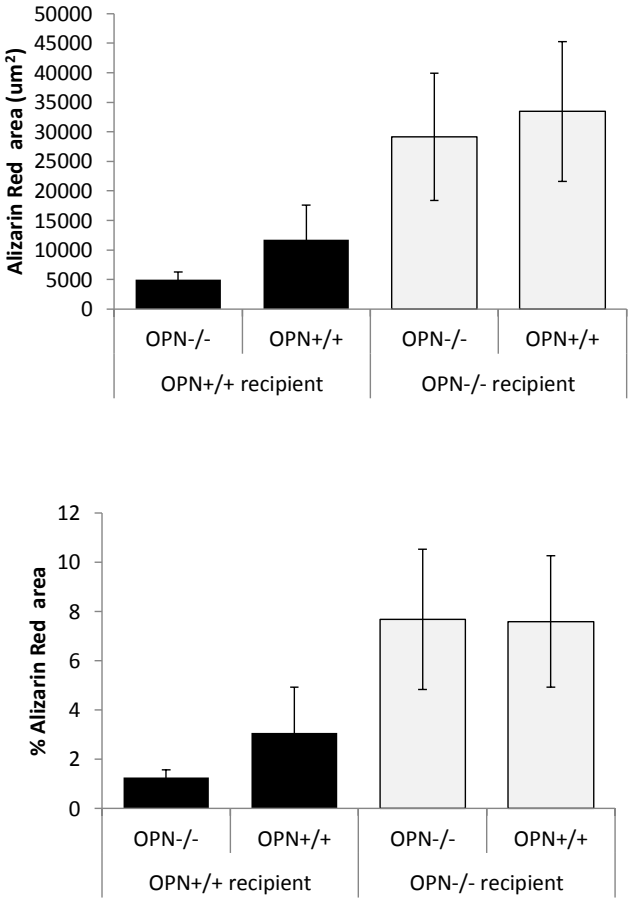

Figure 5.7: Quantification of calcification in ApoE-/- BMT mice.
Calcified area was quantified in Alizarin Red stained sections of the innominate artery. Alizarin Red-positive area was quantified in ApoE-/-OPN+/+ mice (black bars) and ApoE-/-OPN-/- (gray bars) transplanted with ApoE-/-OPN+/+ or ApoE-/-OPN-/- bone marrow. Bone marrow genotype is indicated on the x-axis. The full length of the innominate artery was sectioned and every tenth slide was analyzed. Data presented as mean ± SEM.

Chapter 6

Overall conclusions

In this work we explore the role of osteopontin in macrophage-mediated inflammation and define the OPN functional domains and cell surface receptors mediating these effects. We began our studies by determining the effect of OPN on macrophage activation state. Contrary to previous reports we showed that OPN does not affect macrophage activation in terms of pro-inflammatory cytokine expression or cell surface receptor expression. We also found that primary macrophages from wild type and OPN-null mice did not differ in their ability to be polarized to either the M1 or M2 macrophage activation state. Finally, OPN could not induce NF-κB activation in macrophages, further evidence that OPN does not regulate macrophage activation.

In an *in vitro* Transwell migration assay, we established that macrophage migration to OPN is induced via interaction with integrins α_4 and α_9. We then determined the OPN functional domains responsible for macrophage accumulation in response to acute inflammation *in vivo*. For these studies we created chimeric mice expressing mutated forms of OPN in macrophages. We found that mutational inactivation of the SLAYGLR resulted in decreased leukocyte accumulation in response to thioglycollate-elicited peritonitis. This decrease in leukocyte accumulation was accounted for mainly due to a decrease in macrophage accumulation. Together, these data suggest that the SLAYGLR domain of OPN interacts with integrins α_4 and α_9 to regulate macrophage migration and accumulation.

OPN is a multifunctional molecule that regulates both normal physiological processes as well as pathological disease states. The work in this dissertation provides an increased understanding of the structure/function relationship governing the pro-inflammatory properties of OPN. Such information could aid in the design of specific therapeutics aimed at targeting inflammatory diseases selectively.

Chapter 7

Future studies

The work presented in this dissertation begins to define structure/function relationships governing OPN's properties *in vivo*. Several directions for future studies are suggested below.

7.1 Examination of the function of OPN proteolytic fragments *in vivo.*

In this work, we explored the role of full-length OPN in macrophage biology. However, the role of OPN proteolytic fragments in the regulation of macrophage function still remains largely unexplored. OPN is substrate for multiple proteases including thrombin, cathepsin D, plasmin, and matrix metalloproteinases (31, 34). Interestingly, rather than mediating degradation and inactivating OPN-mediated functions, proteolytic processing of OPN can increase the biological activity of the molecule (35). Consequently, proteolytic processing may represent a way to locally regulate the function of OPN. OPN and MMPs are co-localized during wound healing, suggesting there may be a role for proteolyzed forms of OPN *in vivo* (153). Future studies that specifically address the role of OPN fragments in acute and chronic inflammation are greatly needed.

7.2 Determining the role of the SLAYGLR domain in pathological disease states

In these studies, we determined the relative contributions of the RGD and SLAYGLR functional domains of OPN in the thioglycollate elicited peritonitis model of acute inflammation. In this model of inflammation we found that the SLAYGLR domain mediated macrophage

accumulation in response to inflammatory stimuli. OPN promotes the pathogenesis of several inflammatory diseases including atherosclerosis, rheumatoid arthritis, and Crohn's disease. Whether the SLAYGLR domain mediates leukocyte recruitment in these pathological diseases states remains to be determined.

Literature Citations

1. Giachelli, C.M., Speer, M.Y., Li, X., Rajachar, R.M., and Yang, H. 2005. Regulation of vascular calcification: roles of phosphate and osteopontin. *Circ Res* 96:717-722.
2. Steitz, S.A., Speer, M.Y., McKee, M.D., Liaw, L., Almeida, M., Yang, H., and Giachelli, C.M. 2002. Osteopontin inhibits mineral deposition and promotes regression of ectopic calcification. *Am J Pathol* 161:2035-2046.
3. Speer, M.Y., McKee, M.D., Guldberg, R.E., Liaw, L., Yang, H.Y., Tung, E., Karsenty, G., and Giachelli, C.M. 2002. Inactivation of the osteopontin gene enhances vascular calcification of matrix Gla protein-deficient mice: evidence for osteopontin as an inducible inhibitor of vascular calcification in vivo. *J Exp Med* 196:1047-1055.
4. Agnholt, J., Kelsen, J., Schack, L., Hvas, C.L., Dahlerup, J.F., and Sorensen, E.S. 2007. Osteopontin, a protein with cytokine-like properties, is associated with inflammation in Crohn's disease. *Scand J Immunol* 65:453-460.
5. El-Tanani, M.K., Campbell, F.C., Kurisetty, V., Jin, D., McCann, M., and Rudland, P.S. 2006. The regulation and role of osteopontin in malignant transformation and cancer. *Cytokine Growth Factor Rev* 17:463-474.
6. Kariuki, S.N., Moore, J.G., Kirou, K.A., Crow, M.K., Utset, T.O., and Niewold, T.B. 2009. Age- and gender-specific modulation of serum osteopontin and interferon-alpha by osteopontin genotype in systemic lupus erythematosus. *Genes Immun*.
7. Comabella, M., Pericot, I., Goertsches, R., Nos, C., Castillo, M., Blas Navarro, J., Rio, J., and Montalban, X. 2005. Plasma osteopontin levels in multiple sclerosis. *J Neuroimmunol* 158:231-239.

8. Sennels, H., Sorensen, S., Ostergaard, M., Knudsen, L., Hansen, M., Skjodt, H., Peters, N., Colic, A., Grau, K., and Jacobsen, S. 2008. Circulating levels of osteopontin, osteoprotegerin, total soluble receptor activator of nuclear factor-kappa B ligand, and high-sensitivity C-reactive protein in patients with active rheumatoid arthritis randomized to etanercept alone or in combination with methotrexate. *Scand J Rheumatol* 37:241-247.

9. Brown, L.F., Berse, B., Van de Water, L., Papadopoulos-Sergiou, A., Perruzzi, C.A., Manseau, E.J., Dvorak, H.F., and Senger, D.R. 1992. Expression and distribution of osteopontin in human tissues: widespread association with luminal epithelial surfaces. *Mol Biol Cell* 3:1169-1180.

10. Chen, J., Singh, K., Mukherjee, B.B., and Sodek, J. 1993. Developmental expression of osteopontin (OPN) mRNA in rat tissues: evidence for a role for OPN in bone formation and resorption. *Matrix* 13:113-123.

11. Liaw, L., Birk, D.E., Ballas, C.B., Whitsitt, J.S., Davidson, J.M., and Hogan, B.L. 1998. Altered wound healing in mice lacking a functional osteopontin gene (spp1). *J Clin Invest* 101:1468-1478.

12. O'Brien, E.R., Garvin, M.R., Stewart, D.K., Hinohara, T., Simpson, J.B., Schwartz, S.M., and Giachelli, C.M. 1994. Osteopontin is synthesized by macrophage, smooth muscle, and endothelial cells in primary and restenotic human coronary atherosclerotic plaques. *Arterioscler Thromb* 14:1648-1656.

13. Liaw, L., Skinner, M.P., Raines, E.W., Ross, R., Cheresh, D.A., Schwartz, S.M., and Giachelli, C.M. 1995. The adhesive and migratory effects of osteopontin are mediated via distinct cell surface integrins. Role of alpha v beta 3 in smooth muscle cell migration to osteopontin in vitro. *J Clin Invest* 95:713-724.

14. Yokosaki, Y., Tanaka, K., Higashikawa, F., Yamashita, K., and Eboshida, A. 2005. Distinct structural requirements for binding of the integrins alphavbeta6, alphavbeta3, alphavbeta5, alpha5beta1 and alpha9beta1 to osteopontin. *Matrix Biol* 24:418-427.

15. Denda, S., Reichardt, L., and Muller, U. 1998. Identification of osteopontin as a novel ligand for the integrin alpha8 beta1 and potential role for this integrin-ligand interaction in kidney morphogenesis. *Molecular biology of the cell* 9:1425-1435.

16. Hu, D.D., Lin, E.C., Kovach, N.L., Hoyer, J.R., and Smith, J.W. 1995. A biochemical characterization of the binding of osteopontin to integrins alpha v beta 1 and alpha v beta 5. *J Biol Chem* 270:26232-26238.

17. Yokosaki, Y., Matsuura, N., Sasaki, T., Murakami, I., Schneider, H., Higashiyama, S., Saitoh, Y., Yamakido, M., Taooka, Y., and Sheppard, D. 1999. The integrin alpha(9)beta(1) binds to a novel recognition sequence (SVVYGLR) in the thrombin-cleaved amino-terminal fragment of osteopontin. *J Biol Chem* 274:36328-36334.

18. Ito, K., Kon, S., Nakayama, Y., Kurotaki, D., Saito, Y., Kanayama, M., Kimura, C., Diao, H., Morimoto, J., Matsui, Y., et al. 2009. The differential amino acid requirement within osteopontin in alpha4 and alpha9 integrin-mediated cell binding and migration. *Matrix Biol* 28:11-19.

19. Green, P.M., Ludbrook, S.B., Miller, D.D., Horgan, C.M., and Barry, S.T. 2001. Structural elements of the osteopontin SVVYGLR motif important for the interaction with alpha(4) integrins. *FEBS Lett* 503:75-79.

20. Bayless, K.J., and Davis, G.E. 2001. Identification of dual alpha 4beta1 integrin binding sites within a 38 amino acid domain in the N-terminal thrombin fragment of human osteopontin. *J Biol Chem* 276:13483-13489.

21. Weber, G.F., Ashkar, S., Glimcher, M.J., and Cantor, H. 1996. Receptor-ligand interaction between CD44 and osteopontin (Eta-1). *Science* 271:509-512.

22. Smith, L.L., Greenfield, B.W., Aruffo, A., and Giachelli, C.M. 1999. CD44 is not an adhesive receptor for osteopontin. *J Cell Biochem* 73:20-30.

23. Katagiri, Y.U., Sleeman, J., Fujii, H., Herrlich, P., Hotta, H., Tanaka, K., Chikuma, S., Yagita, H., Okumura, K., Murakami, M., et al. 1999. CD44 variants but not CD44s cooperate with beta1-containing integrins to permit cells to bind to osteopontin independently of arginine-glycine-aspartic acid, thereby stimulating cell motility and chemotaxis. *Cancer Res* 59:219-226.

24. Singh, K., DeVouge, M.W., and Mukherjee, B.B. 1990. Physiological properties and differential glycosylation of phosphorylated and nonphosphorylated forms of osteopontin secreted by normal rat kidney cells. *J Biol Chem* 265:18696-18701.

25. Jono, S., Peinado, C., and Giachelli, C.M. 2000. Phosphorylation of osteopontin is required for inhibition of vascular smooth muscle cell calcification. *J Biol Chem* 275:20197-20203.

26. Gao, Y.A., Agnihotri, R., Vary, C.P., and Liaw, L. 2004. Expression and characterization of recombinant osteopontin peptides representing matrix metalloproteinase proteolytic fragments. *Matrix Biol* 23:457-466.

27. Xuan, J., Hota, C., and Chambers, A. 1994. Recombinant GST-human osteopontin fusion protein i...[J Cell Biochem. 1994] - PubMed Result. *Journal of Cellular Biochemistry* 54:247-255.

28. Liaw, L., Almeida, M., Hart, C.E., Schwartz, S.M., and Giachelli, C.M. 1994. Osteopontin promotes vascular cell adhesion and spreading and is chemotactic for smooth muscle cells in vitro. *Circ Res* 74:214-224.

29. Liaw, L., Lindner, V., Schwartz, S.M., Chambers, A.F., and Giachelli, C.M. 1995. Osteopontin and beta 3 integrin are coordinately expressed in regenerating endothelium in vivo and stimulate Arg-Gly-Asp-dependent endothelial migration in vitro. *Circ Res* 77:665-672.

30. Smith, L.L., and Giachelli, C.M. 1998. Structural requirements for alpha 9 beta 1-mediated adhesion and migration to thrombin-cleaved osteopontin. *Exp Cell Res* 242:351-360.

31. Agnihotri, R., Crawford, H.C., Haro, H., Matrisian, L.M., Havrda, M.C., and Liaw, L. 2001. Osteopontin, a novel substrate for matrix metalloproteinase-3 (stromelysin-1) and matrix metalloproteinase-7 (matrilysin). *J Biol Chem* 276:28261-28267.

32. Dean, R.A., and Overall, C.M. 2007. Proteomics discovery of metalloproteinase substrates in the cellular context by iTRAQ labeling reveals a diverse MMP-2 substrate degradome. *Mol Cell Proteomics* 6:611-623.

33. Takafuji, V., Forgues, M., Unsworth, E., Goldsmith, P., and Wang, X.W. 2007. An osteopontin fragment is essential for tumor cell invasion in hepatocellular carcinoma. *Oncogene* 26:6361-6371.

34. Christensen, B., Schack, L., Kläning, E., and Sørensen, E.S. 2010. Osteopontin is cleaved at multiple sites close to its integrin-binding motifs in milk and is a novel substrate for plasmin and cathepsin D. *J Biol Chem* 285:7929-7937.

35. O'Regan, A.W., Chupp, G.L., Lowry, J.A., Goetschkes, M., Mulligan, N., and Berman, J.S. 1999. Osteopontin is associated with T cells in sarcoid granulomas and has T cell adhesive and cytokine-like properties in vitro. *J Immunol* 162:1024-1031.

36. Ohshima, S., Yamaguchi, N., Nishioka, K., Mima, T., Ishii, T., Umeshita-Sasai, M., Kobayashi, H., Shimizu, M., Katada, Y., Wakitani, S., et al. 2002. Enhanced local production of osteopontin in rheumatoid joints. *J Rheumatol* 29:2061-2067.

37. Yamamoto, N., Sakai, F., Kon, S., Morimoto, J., Kimura, C., Yamazaki, H., Okazaki, I., Seki, N., Fujii, T., and Uede, T. 2003. Essential role of the cryptic epitope SLAYGLR within osteopontin in a murine model of rheumatoid arthritis. *J Clin Invest* 112:181-188.

38. Yamamoto, N., Nakashima, T., Torikai, M., Naruse, T., Morimoto, J., Kon, S., Sakai, F., and Uede, T. 2007. Successful treatment of collagen-induced arthritis in non-human primates by chimeric anti-osteopontin antibody. *Int Immunopharmacol* 7:1460-1470.

39. Mukherjee, B.B., Nemir, M., Beninati, S., Cordella-Miele, E., Singh, K., Chackalaparampil, I., Shanmugam, V., DeVouge, M.W., and Mukherjee, A.B. 1995. Interaction of osteopontin with fibronectin and other extracellular matrix molecules. *Ann N Y Acad Sci* 760:201-212.

40. Chen, Y., Bal, B.S., and Gorski, J.P. 1992. Calcium and collagen binding properties of osteopontin, bone sialoprotein, and bone acidic glycoprotein-75 from bone. *J Biol Chem* 267:24871-24878.

41. Martin, S.M., Schwartz, J.L., Giachelli, C.M., and Ratner, B.D. 2004. Enhancing the biological activity of immobilized osteopontin using a type-1 collagen affinity coating. *J Biomed Mater Res A* 70:10-19.

42. Nagata, T., Todescan, R., Goldberg, H.A., Zhang, Q., and Sodek, J. 1989. Sulphation of secreted phosphoprotein I (SPPI, osteopontin) is associated with mineralized tissue formation. *Biochem Biophys Res Commun* 165:234-240.

43. Sorensen, E.S., and Petersen, T.E. 1995. Phosphorylation, glycosylation, and transglutaminase sites in bovine osteopontin. *Ann N Y Acad Sci* 760:363-366.

44. Beninati, S., Senger, D.R., Cordella-Miele, E., Mukherjee, A.B., Chackalaparampil, I., Shanmugam, V., Singh, K., and Mukherjee, B.B. 1994. Osteopontin: its transglutaminase-catalyzed posttranslational modifications and cross-linking to fibronectin. *J Biochem* 115:675-682.

45. Shinohara, M.L., Kim, H.J., Kim, J.H., Garcia, V.A., and Cantor, H. 2008. Alternative translation of osteopontin generates intracellular and secreted isoforms that mediate distinct biological activities in dendritic cells. *Proc Natl Acad Sci U S A* 105:7235-7239.

46. Zohar, R., Suzuki, N., Suzuki, K., Arora, P., Glogauer, M., McCulloch, C.A., and Sodek, J. 2000. Intracellular osteopontin is an integral component of the CD44-ERM complex involved in cell migration. *J Cell Physiol* 184:118-130.

47. Zhu, B., Suzuki, K., Goldberg, H.A., Rittling, S.R., Denhardt, D.T., McCulloch, C.A., and Sodek, J. 2004. Osteopontin modulates CD44-dependent chemotaxis of peritoneal macrophages through G-protein-coupled receptors: evidence of a role for an intracellular form of osteopontin. *J Cell Physiol* 198:155-167.

48. Krause, S.W., Rehli, M., Kreutz, M., Schwarzfischer, L., Paulauskis, J.D., and Andreesen, R. 1996. Differential screening identifies genetic markers of monocyte to macrophage maturation. *J Leukoc Biol* 60:540-545.

49. Nakamachi, T., Nomiyama, T., Gizard, F., Heywood, E.B., Jones, K.L., Zhao, Y., Fuentes, L., Takebayashi, K., Aso, Y., Staels, B., et al. 2007. PPARalpha agonists suppress osteopontin expression in macrophages and decrease plasma levels in patients with type 2 diabetes. *Diabetes* 56:1662-1670.

50. Ogawa, D., Stone, J.F., Takata, Y., Blaschke, F., Chu, V.H., Towler, D.A., Law, R.E., Hsueh, W.A., and Bruemmer, D. 2005. Liver x receptor agonists inhibit cytokine-induced osteopontin expression in macrophages through interference with activator protein-1 signaling pathways. *Circ Res* 96:e59-67.

51. Bruemmer, D., Collins, A.R., Noh, G., Wang, W., Territo, M., Arias-Magallona, S., Fishbein, M.C., Blaschke, F., Kintscher, U., Graf, K., et al. 2003. Angiotensin II-accelerated atherosclerosis and aneurysm formation is attenuated in osteopontin-deficient mice. *J Clin Invest* 112:1318-1331.

52. Persy, V., Verhulst, A., Ysebaert, D., De Greef, K., and De Broe, M. 2003. Reduced postischemic macrophage infiltration and i...[Kidney Int. 2003] - PubMed Result. *Kidney International* 63:543-553.

53. Giachelli, C.M., Lombardi, D., Johnson, R.J., Murry, C.E., and Almeida, M. 1998. Evidence for a role of osteopontin in macrophage infiltration in response to pathological stimuli in vivo. *Am J Pathol* 152:353-358.

54. Panzer, U., Thaiss, F., Zahner, G., Barth, P., Reszka, M., Reinking, R., Wolf, G., Helmchen, U., and Stahl, R. 2001. Monocyte chemoattractant protein-1 and osteopontin...[Kidney Int. 2001] - PubMed Result. *Kidney International* 59:1762-1769.

55. Matsui, Y., Rittling, S.R., Okamoto, H., Inobe, M., Jia, N., Shimizu, T., Akino, M., Sugawara, T., Morimoto, J., Kimura, C., et al. 2003. Osteopontin deficiency attenuates

atherosclerosis in female apolipoprotein E-deficient mice. *Arterioscler Thromb Vasc Biol* 23:1029-1034.

56. Yu, X.Q., Nikolic-Paterson, D.J., Mu, W., Giachelli, C.M., Atkins, R.C., Johnson, R.J., and Lan, H.Y. 1998. A functional role for osteopontin in experimental crescentic glomerulonephritis in the rat. *Proc Assoc Am Physicians* 110:50-64.

57. Nau, G.J., Liaw, L., Chupp, G.L., Berman, J.S., Hogan, B.L., and Young, R.A. 1999. Attenuated host resistance against Mycobacterium bovis BCG infection in mice lacking osteopontin. *Infect Immun* 67:4223-4230.

58. Tsai, A.T., Rice, J., Scatena, M., Liaw, L., Ratner, B.D., and Giachelli, C.M. 2005. The role of osteopontin in foreign body giant cell formation. *Biomaterials* 26:5835-5843.

59. Nystrom, T., Duner, P., and Hultgardh-Nilsson, A. 2007. A constitutive endogenous osteopontin production is important for macrophage function and differentiation. *Exp Cell Res* 313:1149-1160.

60. Scatena, M., Liaw, L., and Giachelli, C.M. 2007. Osteopontin: a multifunctional molecule regulating chronic inflammation and vascular disease. *Arterioscler Thromb Vasc Biol* 27:2302-2309.

61. Rittling, S.R. 2011. Osteopontin in macrophage function. *Expert Rev Mol Med* 13:e15.

62. O'Brien, E.R., Garvin, M.R., Stewart, D.K., Hinohara, T., Simpson, J.B., Schwartz, S.M., and Giachelli, C.M. 1994. Osteopontin is synthesized by macrophage, smooth muscle, and endothelial cells in primary and restenotic human coronary atherosclerotic plaques. *Arterioscler Thromb* 14:1648-1656.

63. Murry, C.E., Giachelli, C.M., Schwartz, S.M., and Vracko, R. 1994. Macrophages express osteopontin during repair of myocardial necrosis. *Am J Pathol* 145:1450-1462.

64. Mosser, D.M. 2003. The many faces of macrophage activation. *J Leukoc Biol* 73:209-212.

65. Biswas, S.K., Chittezhath, M., Shalova, I.N., and Lim, J.Y. 2012. Macrophage polarization and plasticity in health and disease. *Immunol Res*.

66. Mantovani, A., Sica, A., and Locati, M. 2007. New vistas on macrophage differentiation and activation. *Eur J Immunol* 37:14-16.

67. Mantovani, A., Sica, A., Sozzani, S., Allavena, P., Vecchi, A., and Locati, M. 2004. The chemokine system in diverse forms of macrophage activation and polarization. *Trends in Immunology* 25:677-686.

68. Van Ginderachter, J.A., Movahedi, K., Hassanzadeh Ghassabeh, G., Meerschaut, S., Beschin, A., Raes, G., and De Baetselier, P. 2006. Classical and alternative activation of mononuclear phagocytes: picking the best of both worlds for tumor promotion. *Immunobiology* 211:487-501.

69. Gordon, S., and Martinez, F.O. 2010. Alternative activation of macrophages: mechanism and functions. *Immunity* 32:593-604.

70. Gordon, S. 2003. Alternative activation of macrophages. *Nat Rev Immunol* 3:23-35.

71. Sica, A., and Mantovani, A. 2012. Macrophage plasticity and polarization: in vivo veritas. *J Clin Invest* 122:787-795.

72. Mosser, D.M., and Edwards, J.P. 2008. Exploring the full spectrum of macrophage activation. *Nat Rev Immunol* 8:958-969.

73. Ashkar, S., Weber, G.F., Panoutsakopoulou, V., Sanchirico, M.E., Jansson, M., Zawaideh, S., Rittling, S.R., Denhardt, D.T., Glimcher, M.J., and Cantor, H. 2000. Eta-1

(osteopontin): an early component of type-1 (cell-mediated) immunity. *Science* 287:860-864.

74. Isoda, K., Nishikawa, K., Kamezawa, Y., Yoshida, M., Kusuhara, M., Moroi, M., Tada, N., and Ohsuzu, F. 2002. Osteopontin plays an important role in the development of medial thickening and neointimal formation. *Circ Res* 91:77-82.

75. Weber, G.F., Zawaideh, S., Hikita, S., Kumar, V.A., Cantor, H., and Ashkar, S. 2002. Phosphorylation-dependent interaction of osteopontin with its receptors regulates macrophage migration and activation. *J Leukoc Biol* 72:752-761.

76. Smith, L.L., Cheung, H.K., Ling, L.E., Chen, J., Sheppard, D., Pytela, R., and Giachelli, C.M. 1996. Osteopontin N-terminal domain contains a cryptic adhesive sequence recognized by alpha9beta1 integrin. *J Biol Chem* 271:28485-28491.

77. Rajachar, R., Truong, A., and Giachelli, C. 2008. The influence of surface mineral and osteopontin on the formation and function of murine bone marrow-derived osteoclasts. *J Mater Sci Mater Med* 19:3279-3285.

78. Beckstead, B.L., Tung, J.C., Liang, K.J., Tavakkol, Z., Usui, M.L., Olerud, J.E., and Giachelli, C.M. 2009. Methods to promote Notch signaling at the biomaterial interface and evaluation in a rafted organ culture model. *J Biomed Mater Res A* 91:436-446.

79. Hermanson, G. 1996. *Bioconjugate Techniques*. San Diego: Academic Press.

80. Scatena, M., Almeida, M., Chaisson, M.L., Fausto, N., Nicosia, R.F., and Giachelli, C.M. 1998. NF-kappaB mediates alphavbeta3 integrin-induced endothelial cell survival. *J Cell Biol* 141:1083-1093.

81. Martin, S.M., Ganapathy, R., Kim, T.K., Leach-Scampavia, D., Giachelli, C.M., and Ratner, B.D. 2003. Characterization and analysis of osteopontin-immobilized poly(2-hydroxyethyl methacrylate) surfaces. *J Biomed Mater Res A* 67:334-343.

82. Konno, S., Hoshi, T., Taira, T., Plunkett, B., and Huang, S.K. 2005. Endotoxin contamination contributes to the in vitro cytokine-inducing activity of osteopontin preparations. *J Interferon Cytokine Res* 25:277-282.

83. Koguchi, Y., Kawakami, K., Kon, S., Segawa, T., Maeda, M., Uede, T., and Saito, A. 2002. Penicillium marneffei causes osteopontin-mediated production of interleukin-12 by peripheral blood mononuclear cells. *Infect Immun* 70:1042-1048.

84. Abel, B., Freigang, S., Bachmann, M.F., Boschert, U., and Kopf, M. 2005. Osteopontin is not required for the development of Th1 responses and viral immunity. *J Immunol* 175:6006-6013.

85. Potter, M.R., Rittling, S.R., Denhardt, D.T., Roper, R.J., Weis, J.H., Teuscher, C., and Weis, J.J. 2002. Role of osteopontin in murine Lyme arthritis and host defense against Borrelia burgdorferi. *Infect Immun* 70:1372-1381.

86. O'Regan, A.W., Hayden, J.M., and Berman, J.S. 2000. Osteopontin augments CD3-mediated interferon-gamma and CD40 ligand expression by T cells, which results in IL-12 production from peripheral blood mononuclear cells. *J Leukoc Biol* 68:495-502.

87. Sharma, R., and Li, D.Z. 2006. Role of dendritic cells in atherosclerosis. *Asian Cardiovasc Thorac Ann* 14:166-169.

88. Renkl, A.C., Wussler, J., Ahrens, T., Thoma, K., Kon, S., Uede, T., Martin, S.F., Simon, J.C., and Weiss, J.M. 2005. Osteopontin functionally activates dendritic cells and induces their differentiation toward a Th1-polarizing phenotype. *Blood* 106:946-955.

89. Schulz, G., Renkl, A.C., Seier, A., Liaw, L., and Weiss, J.M. 2008. Regulated osteopontin expression by dendritic cells decisively affects their migratory capacity. *J Invest Dermatol* 128:2541-2544.

90. Ridley, A.J., Schwartz, M.A., Burridge, K., Firtel, R.A., Ginsberg, M.H., Borisy, G., Parsons, J.T., and Horwitz, A.R. 2003. Cell migration: integrating signals from front to back. *Science* 302:1704-1709.

91. Abram, C.L., and Lowell, C.A. 2009. The ins and outs of leukocyte integrin signaling. *Annu Rev Immunol* 27:339-362.

92. Harburger, D.S., and Calderwood, D.A. 2009. Integrin signalling at a glance. *J Cell Sci* 122:159-163.

93. Etienne-Manneville, S., and Hall, A. 2001. Integrin-mediated activation of Cdc42 controls cell polarity in migrating astrocytes through PKCzeta. *Cell* 106:489-498.

94. Marcondes, M.C., Poling, M., Watry, D.D., Hall, D., and Fox, H.S. 2008. In vivo osteopontin-induced macrophage accumulation is dependent on CD44 expression. *Cell Immunol* 254:56-62.

95. Steitz, S.A., Speer, M.Y., McKee, M.D., Liaw, L., Almeida, M., Yang, H., and Giachelli, C.M. 2002. Osteopontin inhibits mineral deposition and promotes regression of ectopic calcification. *Am J Pathol* 161:2035-2046.

96. Duvall, C., Weiss, D., Robinson, S., Alameddine, F., Guldberg, R., and Taylor, W. 2008. The role of osteopontin in recovery from hind limb ischemia. *Arterioscler Thromb Vasc Biol* 28:290-295.

97. Nomiyama, T., Perez-Tilve, D., Ogawa, D., Gizard, F., Zhao, Y., Heywood, E.B., Jones, K.L., Kawamori, R., Cassis, L.A., Tschop, M.H., et al. 2007. Osteopontin mediates

obesity-induced adipose tissue macrophage infiltration and insulin resistance in mice. *J Clin Invest* 117:2877-2888.

98. Kanayama, M., Kurotaki, D., Morimoto, J., Asano, T., Matsui, Y., Nakayama, Y., Saito, Y., Ito, K., Kimura, C., Iwasaki, N., et al. 2009. Alpha9 integrin and its ligands constitute critical joint microenvironments for development of autoimmune arthritis. *J Immunol* 182:8015-8025.

99. Kummer, C., and Ginsberg, M.H. 2006. New approaches to blockade of alpha4-integrins, proven therapeutic targets in chronic inflammation. *Biochem Pharmacol* 72:1460-1468.

100. Cantor, J.M., Ginsberg, M.H., and Rose, D.M. 2008. Integrin-associated proteins as potential therapeutic targets. *Immunol Rev* 223:236-251.

101. Kanayama, M., Morimoto, J., Matsui, Y., Ikesue, M., Danzaki, K., Kurotaki, D., Ito, K., Yoshida, T., and Uede, T. 2011. α9β1 integrin-mediated signaling serves as an intrinsic regulator of pathogenic Th17 cell generation. *J Immunol* 187:5851-5864.

102. Shima, M., Teitelbaum, S.L., Holers, V.M., Ruzicka, C., Osmack, P., and Ross, F.P. 1995. Macrophage-colony-stimulating factor regulates expression of the integrins alpha 4 beta 1 and alpha 5 beta 1 by murine bone marrow macrophages. *Proc Natl Acad Sci U S A* 92:5179-5183.

103. Razzouk, S., Brunn, J.C., Qin, C., Tye, C.E., Goldberg, H.A., and Butler, W.T. 2002. Osteopontin posttranslational modifications, possibly phosphorylation, are required for in vitro bone resorption but not osteoclast adhesion. *Bone* 30:40-47.

104. Kazanecki, C.C., Uzwiak, D.J., and Denhardt, D.T. 2007. Control of osteopontin signaling and function by post-translational phosphorylation and protein folding. *J Cell Biochem* 102:912-924.

105. Christensen, B., Kazanecki, C.C., Petersen, T.E., Rittling, S.R., Denhardt, D.T., and Sorensen, E.S. 2007. Cell type-specific post-translational modifications of mouse osteopontin are associated with different adhesive properties. *J Biol Chem* 282:19463-19472.

106. Ek-Rylander, B., and Andersson, G. 2010. Osteoclast migration on phosphorylated osteopontin is regulated by endogenous tartrate-resistant acid phosphatase. *Exp Cell Res* 316:443-451.

107. Nathan, C. 2006. Neutrophils and immunity: challenges and opportunities. *Nat Rev Immunol* 6:173-182.

108. Liddiard, K., Rosas, M., Davies, L.C., Jones, S.A., and Taylor, P.R. 2011. Macrophage heterogeneity and acute inflammation. *Eur J Immunol* 41:2503-2508.

109. Patel, S.S., Thiagarajan, R., Willerson, J.T., and Yeh, E.T. 1998. Inhibition of alpha4 integrin and ICAM-1 markedly attenuate macrophage homing to atherosclerotic plaques in ApoE-deficient mice. *Circulation* 97:75-81.

110. Bellingan, G.J., Caldwell, H., Howie, S.E., Dransfield, I., and Haslett, C. 1996. In vivo fate of the inflammatory macrophage during the resolution of inflammation: inflammatory macrophages do not die locally, but emigrate to the draining lymph nodes. *J Immunol* 157:2577-2585.

111. Ghosn, E.E., Cassado, A.A., Govoni, G.R., Fukuhara, T., Yang, Y., Monack, D.M., Bortoluci, K.R., Almeida, S.R., and Herzenberg, L.A. 2010. Two physically, functionally, and developmentally distinct peritoneal macrophage subsets. *Proc Natl Acad Sci U S A* 107:2568-2573.

112. Barth, M.W., Hendrzak, J.A., Melnicoff, M.J., and Morahan, P.S. 1995. Review of the macrophage disappearance reaction. *J Leukoc Biol* 57:361-367.

113. Wu, Q., Feng, Y., Yang, Y., Jingliu, Zhou, W., He, P., Zhou, R., Li, X., and Zou, J. 2004. Kinetics of the phenotype and function of murine peritoneal macrophages following acute inflammation. *Cell Mol Immunol* 1:57-62.

114. Ploplis, V.A., French, E.L., Carmeliet, P., Collen, D., and Plow, E.F. 1998. Plasminogen deficiency differentially affects recruitment of inflammatory cell populations in mice. *Blood* 91:2005-2009.

115. Anderson, J.M. 2001. Biological responses to materials. *Annual Review of Materials Research* 31:81-110.

116. Darby, I.A., and Hewitson, T.D. 2007. Fibroblast differentiation in wound healing and fibrosis. *Int Rev Cytol* 257:143-179.

117. Ratner, B.D., and Bryant, S.J. 2004. Biomaterials: Where we have been and where we are going. *Annual Review of Biomedical Engineering* 6:41-75.

118. Luttikhuizen, D.T., Harmsen, M.C., and Van Luyn, M.J.A. 2006. Cellular and molecular dynamics in the foreign body reaction. *Tissue Engineering* 12:1955-1970.

119. Ward, W.K., Quinn, M.J., Wood, M.D., Tiekotter, K.L., Pidikiti, S., and Gallagher, J.A. 2003. Vascularizing the tissue surrounding a model biosensor: how localized is the effect of a subcutaneous infusion of vascular endothelial growth factor (VEGF)? *Biosens Bioelectron* 19:155-163.

120. Takeda, Y., Tachibana, I., Miyado, K., Kobayashi, M., Miyazaki, T., Funakoshi, T., Kimura, H., Yamane, H., Saito, Y., Goto, H., et al. 2003. Tetraspanins CD9 and CD81 function to prevent the fusion of mononuclear phagocytes. *J Cell Biol* 161:945-956.

121. Sterling, H., Saginario, C., and Vignery, A. 1998. CD44 occupancy prevents macrophage multinucleation. *J Cell Biol* 143:837-847.

122. Speer, M.Y., Chien, Y.C., Quan, M., Yang, H.Y., Vali, H., McKee, M.D., and Giachelli, C.M. 2005. Smooth muscle cells deficient in osteopontin have enhanced susceptibility to calcification in vitro. *Cardiovasc Res* 66:324-333.

123. Gough, P.J., and Raines, E.W. 2003. Gene therapy of apolipoprotein E-deficient mice using a novel macrophage-specific retroviral vector. *Blood* 101:485-491.

124. Taylor, P.R., Martinez-Pomares, L., Stacey, M., Lin, H.H., Brown, G.D., and Gordon, S. 2005. Macrophage receptors and immune recognition. *Annu Rev Immunol* 23:901-944.

125. Ghosn, E.E., Yang, Y., Tung, J., and Herzenberg, L.A. 2008. CD11b expression distinguishes sequential stages of peritoneal B-1 development. *Proc Natl Acad Sci U S A* 105:5195-5200.

126. van Gisbergen, K.P., Sanchez-Hernandez, M., Geijtenbeek, T.B., and van Kooyk, Y. 2005. Neutrophils mediate immune modulation of dendritic cells through glycosylation-dependent interactions between Mac-1 and DC-SIGN. *J Exp Med* 201:1281-1292.

127. Kim, S., Iizuka, K., Kang, H.S., Dokun, A., French, A.R., Greco, S., and Yokoyama, W.M. 2002. In vivo developmental stages in murine natural killer cell maturation. *Nat Immunol* 3:523-528.

128. Sasmono, R.T., Oceandy, D., Pollard, J.W., Tong, W., Pavli, P., Wainwright, B.J., Ostrowski, M.C., Himes, S.R., and Hume, D.A. 2003. A macrophage colony-stimulating factor receptor-green fluorescent protein transgene is expressed throughout the mononuclear phagocyte system of the mouse. *Blood* 101:1155-1163.

129. MacDonald, K.P., Rowe, V., Bofinger, H.M., Thomas, R., Sasmono, T., Hume, D.A., and Hill, G.R. 2005. The colony-stimulating factor 1 receptor is expressed on dendritic cells during differentiation and regulates their expansion. *J Immunol* 175:1399-1405.

130. Zheng, W., Li, R., Pan, H., He, D., Xu, R., Guo, T.B., Guo, Y., and Zhang, J.Z. 2009. Role of osteopontin in induction of monocyte chemoattractant protein 1 and macrophage inflammatory protein 1beta through the NF-kappaB and MAPK pathways in rheumatoid arthritis. *Arthritis Rheum* 60:1957-1965.

131. Henderson, R.B., Hobbs, J.A., Mathies, M., and Hogg, N. 2003. Rapid recruitment of inflammatory monocytes is independent of neutrophil migration. *Blood* 102:328-335.

132. Boring, L., Gosling, J., Chensue, S.W., Kunkel, S.L., Farese, R.V., Broxmeyer, H.E., and Charo, I.F. 1997. Impaired monocyte migration and reduced type 1 (Th1) cytokine responses in C-C chemokine receptor 2 knockout mice. *J Clin Invest* 100:2552-2561.

133. Lu, B., Rutledge, B.J., Gu, L., Fiorillo, J., Lukacs, N.W., Kunkel, S.L., North, R., Gerard, C., and Rollins, B.J. 1998. Abnormalities in monocyte recruitment and cytokine expression in monocyte chemoattractant protein 1-deficient mice. *J Exp Med* 187:601-608.

134. Koh, A., da Silva, A.P., Bansal, A.K., Bansal, M., Sun, C., Lee, H., Glogauer, M., Sodek, J., and Zohar, R. 2007. Role of osteopontin in neutrophil function. *Immunology* 122:466-475.

135. Nishimichi, N., Higashikawa, F., Kinoh, H.H., Tateishi, Y., Matsuda, H., and Yokosaki, Y. 2009. Polymeric osteopontin employs integrin alpha 9beta 1 as a receptor and attracts neutrophils by presenting a de novo binding site. *J Biol Chem*.

136. Beckwith, J., Cong, Y., Sundberg, J.P., Elson, C.O., and Leiter, E.H. 2005. Cdcs1, a major colitogenic locus in mice, regulates innate and adaptive immune response to enteric bacterial antigens. *Gastroenterology* 129:1473-1484.

137. Champy, M.F., Selloum, M., Zeitler, V., Caradec, C., Jung, B., Rousseau, S., Pouilly, L., Sorg, T., and Auwerx, J. 2008. Genetic background determines metabolic phenotypes in the mouse. *Mamm Genome* 19:318-331.

138. Mori, R., Shaw, T., and Martin, P. 2008. Molecular mechanisms linking wound inflammation and fibrosis: knockdown of osteopontin leads to rapid repair and reduced scarring. *J Exp Med* 205:43-51.

139. Roger, V.L., Go, A.S., Lloyd-Jones, D.M., Benjamin, E.J., Berry, J.D., Borden, W.B., Bravata, D.M., Dai, S., Ford, E.S., Fox, C.S., et al. 2012. Executive summary: heart disease and stroke statistics--2012 update: a report from the American Heart Association. *Circulation* 125:188-197.

140. Libby, P. 2002. Inflammation in atherosclerosis. *Nature* 420:868-874.

141. Schalkwijk, C.G., and Stehouwer, C.D. 2005. Vascular complications in diabetes mellitus: the role of endothelial dysfunction. *Clin Sci (Lond)* 109:143-159.

142. Stapleton, P.A., Goodwill, A.G., James, M.E., Brock, R.W., and Frisbee, J.C. 2010. Hypercholesterolemia and microvascular dysfunction: interventional strategies. *J Inflamm (Lond)* 7:54.

143. Hadi, H.A., Carr, C.S., and Al Suwaidi, J. 2005. Endothelial dysfunction: cardiovascular risk factors, therapy, and outcome. *Vasc Health Risk Manag* 1:183-198.

144. Giachelli, C.M., Liaw, L., Murry, C.E., Schwartz, S.M., and Almeida, M. 1995. Osteopontin expression in cardiovascular diseases. *Ann N Y Acad Sci* 760:109-126.

145. Kwon, H.M., Hong, B.K., Kang, T.S., Kwon, K., Kim, H.K., Jang, Y., Choi, D., Park, H.Y., Kang, S.M., Cho, S.Y., et al. 2000. Expression of osteopontin in calcified coronary atherosclerotic plaques. *J Korean Med Sci* 15:485-493.

146. Momiyama, Y., Ohmori, R., Fayad, Z.A., Kihara, T., Tanaka, N., Kato, R., Taniguchi, H., Nagata, M., Nakamura, H., and Ohsuzu, F. 2010. Associations between plasma osteopontin levels and the severities of coronary and aortic atherosclerosis. *Atherosclerosis* 210:668-670.

147. Strom, A., Franzen, A., Wangnerud, C., Knutsson, A.K., Heinegard, D., and Hultgardh-Nilsson, A. 2004. Altered vascular remodeling in osteopontin-deficient atherosclerotic mice. *J Vasc Res* 41:314-322.

148. Panda, D., Kundu, G.C., Lee, B.I., Peri, A., Fohl, D., Chackalaparampil, I., Mukherjee, B.B., Li, X.D., Mukherjee, D.C., Seides, S., et al. 1997. Potential roles of osteopontin and alphaVbeta3 integrin in the development of coronary artery restenosis after angioplasty. *Proc Natl Acad Sci U S A* 94:9308-9313.

149. Giachelli, C.M., Bae, N., Almeida, M., Denhardt, D.T., Alpers, C.E., and Schwartz, S.M. 1993. Osteopontin is elevated during neointima formation in rat arteries and is a novel component of human atherosclerotic plaques. *J Clin Invest* 92:1686-1696.

150. Plump, A.S., Smith, J.D., Hayek, T., Aalto-Setälä, K., Walsh, A., Verstuyft, J.G., Rubin, E.M., and Breslow, J.L. 1992. Severe hypercholesterolemia and atherosclerosis in apolipoprotein E-deficient mice created by homologous recombination in ES cells. *Cell* 71:343-353.

151. Zaragoza, C., Gomez-Guerrero, C., Martin-Ventura, J.L., Blanco-Colio, L., Lavin, B., Mallavia, B., Tarin, C., Mas, S., Ortiz, A., and Egido, J. 2011. Animal models of cardiovascular diseases. *J Biomed Biotechnol* 2011:497841.

152. Pendse, A.A., Arbones-Mainar, J.M., Johnson, L.A., Altenburg, M.K., and Maeda, N. 2009. Apolipoprotein E knock-out and knock-in mice: atherosclerosis, metabolic syndrome, and beyond. *J Lipid Res* 50 Suppl:S178-182.

153. Senger, D.R., Perruzzi, C.A., Papadopoulos-Sergiou, A., and Van de Water, L. 1994. Adhesive properties of osteopontin: regulation by a naturally occurring thrombin-cleavage in close proximity to the GRGDS cell-binding domain. *Mol Biol Cell* 5:565-574.

Vita

Susan Amanda Lund was born in Santa Rosa, California in 1981. She graduated with honors from Analy High School in 1999. Afterwards, she went on to attend Oregon State University where she graduated with a Bachelors of Science in Bioengineering. She then joined Siga Technologies and became a research assistant developing novel vaccine vectors to treat infectious diseases and under the mentorship of Dr. Travis Warren became inspired to pursue graduate studies.

She then moved to Seattle, Washington to pursue her Ph.D. in Bioengineering at the University of Washington. There she joined the lab of Dr. Cecilia Giachell and Dr. Marta Scatena. In June of 2012, she completed her Ph.D. dissertation titled "The role of osteopontin in macrophage-mediated inflammation".